PONTIFICIA UNIVERSIDAD CATÓLICA DE CHILE
ESCUELA DE INGENIERÍA

FULLY SOLAR POWERED ELECTRIC VEHICLE FOR HARVESTING FRESH MARKETS FRUITS

GIOVANNI ALEJANDRO MEDRANO RÍOS

Thesis submitted to the Office of Research and Graduate Studies in partial fulfillment of the requirements for the Degree of Master of Science in Engineering

Advisor:
LUCIANO E. CHIANG

Santiago de Chile, December 2017

PONTIFICIA UNIVERSIDAD CATÓLICA DE CHILE
ESCUELA DE INGENIERÍA

FULLY SOLAR POWERED ELECTRIC VEHICLE FOR HARVESTING FRESH MARKETS FRUITS

GIOVANNI ALEJANDRO MEDRANO RÍOS

Members of the Committee:

LUCIANO CHIANG SÁNCHEZ

JULIO VERGARA AIMONE

MARLENE AYALA ZAPATA

JUAN CARLOS FERRER ORTIZ

Thesis submitted to the Office of Research and Graduate Studies in partial fulfillment of the requirements for the Degree of Master of Science in Engineering

Santiago de Chile, December 2017

To my parents, Alejandro and Karina, to my siblings, and to Paula, who have given me their unconditional support, strength, and always have been there.

ACKNOWLEDGEMENTS

I would like to thank my supervisor Luciano Chiang for their support during all the years of study and research, professor Marlene Ayala for her valuable contribution in the agronomy field, and Members of the Committee who provide valuable comments to improve this work. I also want to thank Fernando Martínez, Sergio Cortez, Francisco Chiang, Jorge Aising, Hector, and all the people in the Mecatrónix team who helped in this project.

Also, I would like to thanks to my parents, who gave me the confidence, the support and the strength in the moments of difficulty, to my siblings for their unconditional support, to Paula for her help, space, listening and valuable comments, and to my friends.

The authors of the article would like to thank producers Agrícola Vergara, Agrícola Miguel Vial, and Agrícola Garcés for allowing to test the harvesting platform in their orchards.

The solar vehicle proposal design was financed partially by the program *Fondo de Innovación a la Competitividad Regional* (FIC-R) of the O'Higgins region in Chile, project code IDI 30343725-0.

CONTENTS

Page

LIST OF TABLES

Page

LIST OF FIGURES

Page

ABSTRACT

A fully solar-powered vehicle was designed, built and tested to assess feasibility for harvesting fresh fruit in Chile, particularly stone fruits, which are exported in large quantities to far away markets. Energy self-reliance, productivity, ergonomics, and environmental benefits are some of the advantages of the vehicle. Fruit damage is observed during harvest, and hand picking must be carried with extreme care generating low harvest efficiency and strenuous physical effort for workers. Therefore, the proposed solar vehicle is a means to increase hand labor productivity while preserving fruit quality for export. Solar energy is collected from 6 m^2 of photovoltaic panels, and stored in a bank of deep discharge batteries. A 5 kW BLDC motor with dynamic braking capability provides mechanical power for traction. A 4-wheel steering system allows maneuvering in tight spaces in the orchard. The harvesting work cycle consists in moving forward the length of the vehicle using energy from the batteries. Then with the vehicle stopped, the crew on board handpicks the fruit. This gives enough time to recover energy spent on the solar panels. The bank of batteries can thus recover charge for the next cycle and operate this way indefinitely. This vehicle helps increase productivity because hand pickers get less tired and do not waste time setting a ladder or walking to deliver fruit buckets. The vehicle can be operated by remote control, and in the future, degrees of autonomous navigation would be attempted. Field energy consumption and productivity results are reported here after testing two harvesting seasons on sweet cherry and nectarine high-density orchards.

Keywords: solar energy agricultural vehicle, fresh fruit harvesting, sustainable agriculture research, energy saving agricultural machinery.

RESUMEN

Se diseñó, construyó y probó un vehículo completamente solar para evaluar la factibilidad de cosechar fruta fresca en Chile, particularmente frutas de cuesco, que se exportan en grandes cantidades a mercados de larga distancia. La autosuficiencia energética, la mejora en productividad, ergonomía y los beneficios ambientales adicionales son algunas de las ventajas del vehículo. Existe un daño en la fruta que se observa durante la cosecha, por ende, la recolección manual debe llevarse a cabo con extremo cuidado, generando una baja eficiencia en la cosecha y un esfuerzo físico extenuante para los trabajadores. El vehículo solar propuesto es un medio para aumentar la productividad del trabajo manual mientras se preserva la calidad de la fruta para la exportación. La energía solar se obtiene de 6 m^2 de paneles fotovoltaicos y se almacena en un banco de baterías de descarga profunda. Un motor eléctrico BLDC de 5 kW con capacidad de frenado dinámico proporciona potencia mecánica para la tracción. Un sistema de rotación independiente de las 4 ruedas permite maniobrar en espacios reducidos en el huerto. El ciclo de trabajo de recolección consiste en avanzar la longitud del vehículo utilizando la energía de las baterías. Luego, con el vehículo detenido, la tripulación a bordo recoge la fruta. Esto le da tiempo suficiente para recuperar la energía consumida en un avance, la cual pasa a través de los paneles solares. De este modo, el banco de baterías puede recuperar la carga para el siguiente ciclo y operar de manera indefinida mientras halla sol. Este vehículo ayuda a aumentar la productividad porque los recolectores se cansan menos y no pierden el tiempo colocando una escalera o caminando para entregar cubetas de fruta. El vehículo puede ser operado por control remoto y en el futuro, se intentarán grados de navegación autónoma. Los resultados de productividad y consumo de energía de campo se informan aquí después de probar dos temporadas de cosecha en huertos de cereza dulce y nectarina de alta densidad.

Palabras Claves: vehículo agrícola de energía solar, cosecha de fruta fresca, investigación de agricultura sostenible, maquinaria agrícola de ahorro de energía.

1. ARTICLE BACKGROUND

Hurricanes Irma and Harvey have been classified as one of the strongest and devastating Atlantic hurricanes in recorded history. Collective estimates for the damage caused by both are upwards of US$200 billion, which in comparison to other hurricanes means half the total cost of damage caused by all together over the past 50 years (Corsentino, 2017; Donnelly, 2017). Recent studies show that the increase in the strength and destructiveness of these hurricanes could be directly related to climate change effects, such as rising sea levels and warmer oceans, making these issues a global concern (Drash, 2017; Sun et al., 2017).

Nowadays, it is difficult to establish direct relationships between climate change and what are the possible causes. In general, when it comes to phenomena of such a large scale, the variables involved are so many that it begins to be defined as a chaotic system, where the prediction of future states becomes practically impossible with current technology. In fact, the consensus about the causes of global warming is still an issue with active research, but rising temperatures, melting glaciers, and rising sea levels are facts that cannot be denied. Furthermore, if some fundamental points about recent changes in the world begin to be analyzed, certain conjectures can be established with sufficient certainty to concern about the need of regulations.

By the year 1800 CE, human population reached 1 billion in over 200,000 years, but according to United Nations data, only 200 years later that number increased dramatically to more than 7 billion of people living in the world (Roser & Ortiz-Ospina, 2017). This incredible recent growth of our species has many causes, among them the industrial revolution, the development of medicine, the level of technology achieved (Kremer, 1993), and others that can be widely discussed. However, the situation becomes interesting and alarming at the same time when the consequences of this tremendous change begin to be analyzed. The increase of the world population is highly relevant for humanity's impact on the earth and the use of natural resources. A high number of people with high levels of interconnectivity, technology, and continuous development requires

huge amounts of food, resources, and energy, producing a high volume of waste in the social metabolic process. Projection from data shows that, although the growth rate is going down, by the year 2100 the world population is expected to reach over 11 billion (Roser & Ortiz-Ospina, 2017). The growing demographic volume demands a better management of natural resources, raises the importance of agriculture with a particular interest in food supply methods and requires new economic models with greater sustainability over time.

1.1 Motivation

The motivation of this work can be organized in three different aspects mentioned in the previous background, which complement each other and are closely related in a particular way. These are; natural resources, agriculture, and economy.

1.1.1 Natural Resources

One of the primary natural resources that have driven the growth of the population through the recent centuries is oil and their vast amount of applications discovered since the industrial revolution. The development of interconnected electrical systems with generation plants regarding energy, the invention of individual, collective and load transport vehicles, among other advances, have allowed the development of world economies and the impulse of technology. However, at the same time that everything has grown and advanced, so has done the direct and indirect waste. Many cities have experienced air pollution with high hydrocarbons levels resulting in increased respiratory diseases of the population, having to drive regulatory programs such as vehicular restraint, and technological advances such as catalytic converter, as well as new energy generation technologies.

On the other hand of pollution, the world's oil reserves are moving closer to depletion as oil runs out, which can be observed around the world through the increase in the price of the fuels. The same reactive effect that has made us advance as a society requires us to face these environmental concerns. It is not surprising

then that leading automobile manufacturers in the world are announcing the development of new models of hybrid vehicles and fully electric cars. Mercedes-Benz recently announced electrification of all its models for 2022 (Reuters, 2017), and Renault, Nissan, and Mitsubishi announced an alliance to launch 12 new models of electric cars and 40 autonomous driving vehicles for the same year (Lippert, Ma, & Nussbaum, 2017).

One of the main components in electric vehicles are batteries, and although there are many models with different technologies, features, costs, and capacities, one of the most relevant with greater acceptance and performance are lithium batteries, including all their different versions.

The main economic engine in Chile is copper mining, but as is happening with oil, copper is a natural resource that has a deadline, and eventually, it will become increasingly expensive in extraction. In the same line, significant lithium reserves have been found in the national territory that is expected to be exploited, meeting in the close future the growing demand for lithium batteries.

It is a world tendency to support the change from energy matrix, and Chile, as a developing country, is up to date with this trend, leading investment in renewable energy with US$3.2 billion, and achieving the first place in South America and the Caribbean region (Ministerio de Energía, 2016). These results are the consequence of the government interest in positioning the country as a leader in innovation in the area. Due to its particular geography, the national territory has substantial advantages concerning solar photovoltaic and wind energy. The longitudinal features, with enormous mountains to the east and higher-pressure levels to the west, propitiate the generation of high winds in those transverse valleys, making each of them an essential potential candidate for the installation of wind turbines. On the other hand, in the first quarter of the northern national territory, that includes the Atacama Desert, the annual average solar radiation exceeds the 7 $kWh/m^2/day$ (Ministerio de Energia & Departamento de Geofísica Universidad de Chile, 2017). These are high levels compared to other places in the world, mainly due to an annual

average frequency of clear cloudless sky days of the year close to 95%. This characteristic has attracted the manufacture of the world's leading astronomical observational telescopes with important projects as ALMA and LSST, as well as important renewable energy projects.

1.1.2 Agriculture

There are many global efforts involved in reducing greenhouse gases in hopes of slowing climate change and improve sustainability. Perhaps one of the most known is the establishment of the concept of carbon footprint and its increasing interest to influence in the decisions of purchase of people and companies. According to Carbon Trust definition (2009), it tries to represent the total set of greenhouse gas emissions caused by an individual, event, organization, or product, expressed as carbon dioxide equivalent. Virtually, any process whether human or productive involves emissions, and the food is not the exception.

The increase in world population has driven the development of improvements in food production systems, making them more profitable and scalable. Many solutions have been designed to partially or fully automate food production and harvesting processes, but many of the existing mechanical solutions are based on internal combustion engines (Li, Lee, & Hsu, 2011; Shepardson, Markwardt, Millier, & Rehkugler, 1970). These increase carbon footprint of the food and requiring the use of chemicals to facilitate automated harvesting process. The development, for one hand, of potent compounds to keep crops, and for the other, of genetically modified (GM) food has enabled the creation of more resistant plant species to pests and more durable fruits for resisting mechanical harvest and long shipping trips. However, there is an active research trying to demonstrate the advantages and safety of these new biotechnology products (Dias & Ortiz, 2013; Ehlert, Moreano, Busch, & Engel, 2008) and clear the concerns about human diseases development, like cancer.

The countries that lead the world's Gross Domestic Product (GDP), as they have grown, have changed their economic matrix, focusing mostly on the development of

technology and services production, but reducing the participation of the agriculture. This is a phenomenon that can also be observed in the evolution of the structure of the Chilean GDP since 1980 onwards (World Bank, 2017), but that does not necessarily indicate a lack of interest of these countries by the agricultural activity. Despite this, it is essential to consider the increasing demand for food in the world, which can be profoundly potentiated as an economic activity with vast opportunities for innovation.

The primary geographic characteristics that give Chile an important potential in renewable energies also provides a natural barrier against pests and other biological hazards that could affect both plant and animal crops. The Cordillera de Los Andes in the east, the Atacama Desert in the north, the Pacific Ocean in the west and the low temperatures of the Antarctic in the south, place the country in a privileged environment conducive to agriculture and animal farming. It is not surprising then that two of the country's most important economic activities are agriculture and salmon farming. Chile is the second largest exporter of salmons in the world after Norway (SalmonChile.cl, 2017) and one of the largest exporters of fresh fruit in the southern hemisphere (Alcaino, Müller, Betinyani, & Brito, 2014). This last activity, called horticulture, is one of the leading responsible of employing outside the capital, which has a centralized structure for organization and economical to maintains the 90% of the population located in the middle third of the country's capital of Santiago (CIA, 2017). For those residents outside the central region employment opportunities are scarce, and it is common to see older adults doing work of considerable physical effort. National horticulture is one of the best examples, where harvesting mechanisms are still traditional with ladders, mostly performed by older women who have to endure 12 kg mats crossed on their chests during a full working day under full sun conditions. Many of these workers, called *"temporeras,"* are single mothers who have to feed and educate their children and the harvest is practically one of their only work options. Besides this, the population in Chile as in the world is undergoing a demographic transition, which can be observed in Figure

1-1. This means that the number of older people is increasing while that of younger is decreasing. This is the reflection of changes in fertility, mortality, and international migration. Chile could benefit from its favorable new age structure, but it will need to keep its sizeable working-age population productively employed, removing the physical effort component of some jobs through the use of technology and innovation, and preparing to provide for the needs of its growing proportion of older adults (CIA, 2017).

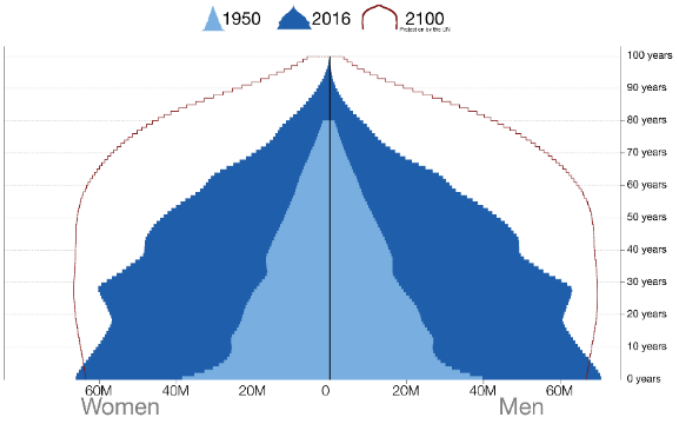

a) World population pyramid for 1950, 2016 and 2100[1]

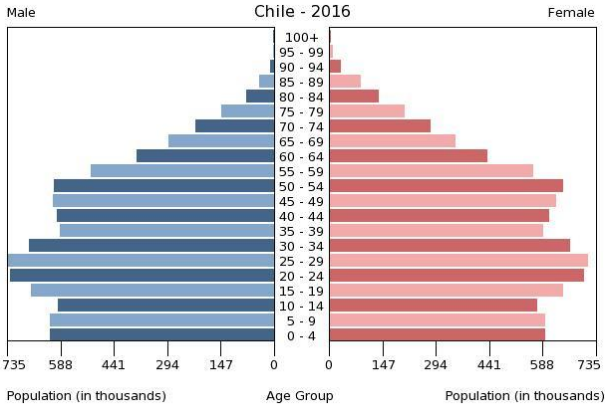

b) Chile population pyramid for 2016[2]

Figure 1-1: Population pyramid comparison between Chile and the World.

[1] Source: https://ourworldindata.org/world-population-growth/
[2] Source: https://www.cia.gov/library/publications/the-world-factbook/geos/ci.html

The automation of agriculture is an imminent event that will come sooner or later due to economies of scale and cost reduction. Moreover, the recent shortage of unskilled labor that has been experienced in different industrial sectors, as a result of the increase in the educational levels of the population, dictates the need for a change. However, due to economic stability and other agents, has begun a steady Latin American immigration to the national territory, which is stopping the unskilled labor shortages but is also accelerating the process of demographic transition.

1.1.3 Economy

The automation of unskilled labor and the continuous development of new technology is almost a certainty. These advances are one of the leading precursors of the increase in world population as of their well-being, but the actual economic processing model is reaching limitations concerning sources for resource inputs and sinks for waste. The use of natural resources and the development of products from a linear economy model is producing an adverse effect on the environment. This process begins with the extraction and refinement of resources, then through the manufacture and assembly of parts, these are transformed into products that will be acquired and used by consumers for a specified period, but eventually, these refined resources that were solutions one will end up as waste in some landfill.

In the European Union, there is a novel concept defined as the circular economy (CE) that is gaining strength, w. The CE is a simple, but convincing, strategy, which aims at reducing both inputs of raw materials and output of wastes by closing economic and ecological loops of resource flows (Haas, Krausmann, Wiedenhofer, & Heinz, 2015). Estimation from this study shows that while globally roughly four gigatons per year (Gt/yr.) of waste materials are recycled, this flow is of moderate size compared to 62 Gt/yr of processed materials and outputs of 41 Gt/yr. The authors state that the low degree of circularity of the linear model has two main reasons: First, 44% of processed materials are used to provide energy and are thus

not available for recycling. Second, socioeconomic stocks are still growing at a high rate with net additions to inventories of 17 Gt/yr.

From the foundation words, a strategy is a multi-R approach; rethink, redesign, re-manufacture, repair, redistribute, reduce, reuse, recycle and recover energy. Trash is a design error that can be corrected by changing the way we think about product design, making them upgradeable, not only in software. The different materials and mechanisms that form a product can be thousands. Each of these components has different failure rates, service life, and programmed obsolescence. Better thinking about product design and manufacturing process can reduce the costs, price, and resources needed to innovate and attract the purchase of new technologies, without starting from scratch. Besides this, one of the leading challenges that face CE is to become attractive to both companies and customers, and perhaps the solution could be rooted in the concept of leasing. Chile as a based and known mining country needs to move out from the main economic engine of resource extraction to ensure sustainable growth. The development of this work can be considered, in a certain way, as a proof of CE concept application, developing industrial machinery with recycled components.

1.2 Objectives

This central thesis objective is to design and determine the feasibility of an electric harvesting vehicle exclusively powered by photovoltaic solar energy, to continuously harvest fruit orchards of nectarines and sweet cherries, transporting up to eight harvesters and three bins[3] of 500 kg each.

Among the specific objectives are the following:

[3] A cubic container for fruit transport of 1200x1000x760 mm.

- Design an electric traction system that allows the vehicle to be mobilized on the rough terrain of orchards without complications or lack of power.
- Design an electric steering system that allows maneuvering the vehicle easy and efficiently on the narrow rows of the orchards without demanding special driving skills.
- Complement the vehicle with an efficient loading and discharge of Bins system to facilitate and improve the harvesting process, reducing downtimes.
- Design a power system (solar photovoltaic panels, batteries, and charge controllers) for the continuous operation of all electromechanical systems.
- Design an ergonomic and adaptable platform to meet most of the dimensions of Chilean sweat cherry and nectarine orchards.
- Implement a protocol for the measurement and analysis of current and voltage to determine the consumptions and loads of the systems separately.
- Determine, from the results, the rates of charge and discharge of batteries.

This thesis addresses these objectives by designing, fabricating, and testing a solar harvesting vehicle with an academic purpose.

1.3 Hypothesis

The hypothesis of this work is that solar photovoltaic energy, with a catchment area reduced to the available space in the vehicle's roof, is sufficient to feed by itself the systems of traction, direction, and operation of a heavy load electric harvesting vehicle for selection fruit.

1.4 Background

Since the industrial revolution, many machines have been created in the framework of human tasks automation. The image of the first mass-production factories, where people located in the assembly lines repetitively performing a strictly defined work during all

day, have been falling quickly in the past. This is being replaced by hundreds of robotic arms that exceed in precision, strength, and speed to the human skills to perform repetitive movements, but now predefined by a code and without the necessity of individual extended training.

1.4.1 Harvesting Machines

In the case of harvest in agriculture, fully robotic automation is a standard that is not yet possible to achieve due to geometrical complexities of plants and delicacy required in handling the fruit. Almost 50 years ago, Shepardson et al. (1970) performed a review of the existing harvesting machines to that date (see Figure 1-2). Most of the reviewed current mechanisms in those years are still actively used today, intending from the beginning to reduce the high costs of harvesting in the fruit production process.

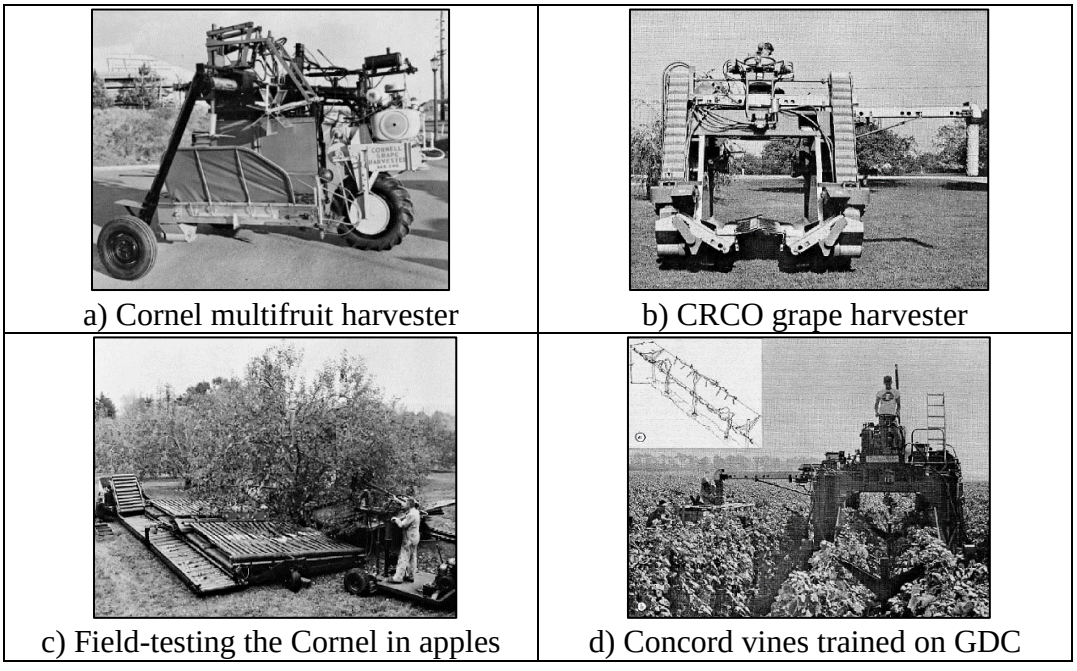

a) Cornel multifruit harvester

b) CRCO grape harvester

c) Field-testing the Cornel in apples

d) Concord vines trained on GDC

Figure 1-2: Experimental mechanical harvest machines in the early 1960s.[4]

[4] Source: See reference Shepardson et al. (1970).

One of the main reasons for the early success of these mechanisms was the cooperative work of agronomists and engineers in the co-design of orchards and harvesting machines. This practice ensures complete adaptability of booths, orchards, and machines, as well of an optimized production (Larbi & Karkee, 2014), but it requires essential investment into research and development, to implement, test and validate the new designs.

There are different levels of achievable harvest automation, which have been identified with the research and are shown as a progression in Figure 1-3. This thesis focuses on the second level. The engine behind the automation progression in harvesting techniques is the need to send clean fruit to customers without brushes and with a high degree of selectivity. These requirements are merged with the production interest to maintain the business profitably, then the stage of a company can be determined according to the size and technological disposition of the producers.

Different national efforts have been made to move forward from traditional manual harvest. New ladder designs and lightweight materials such as aluminum have been used to release physical effort and improve labor efficiency, maintaining the current harvest process and reducing the complexity of the implementation. From words of the managers, working conditions have been improved, but not higher efficiency has been found.

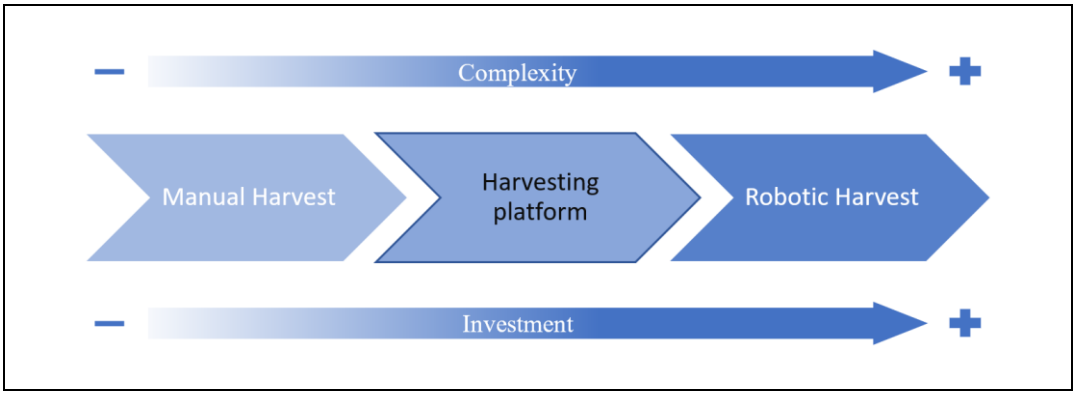

Figure 1-3: Levels of harvest automation.

Harvesting platforms are the best solution up to date that keeps using human skills to select and to pick-up carefully the fruit maintaining competitiveness efficiency at low cost. There are many alternatives based on the same concept but with modifications between them (see Figure 1-4).

a) Fratelli Festi Bins 2[5]

b) Pulcinelli PSRF 2.4[6]

c) Automated Ag Bandit Xpress[7]

d) Billo Big 2000[8]

Figure 1-4: State of the art in harvesting platforms.

[5] Source: http://www.fratellifesti.it/bins_2.php#
[6] Source: https://www.pulcinellicosmec.com/produzione/macchina-per-raccolta-frutta-mod-psrf-2-4.html
[7] Source: https://www.automatedag.com/banditxpressgallery
[8] Source: http://www.billosrl.it/es/big-2000.php

The main characteristics of these are summarized next:

- Edges with high horizontal three-bar railings, at mid stomach, mid-leg and near the feet for safety, ergonomic and productive reasons
- Double extensible platforms by the sides, independent and hydraulic powered
- Independent wheel improvement
- Height and base level adjustable hydraulically
- Diesel powered

The differences between the solutions are features like electric powered, hybrid equipped, leveling of the platform, individual height adjusting, hydraulic steering, steering wheel, joystick, the inclination of bar railing, among others.

Many of the harvesting machinery (including platforms, mechanic and robotic solutions) that has been designed in a specific region is unlikely to function with equal performance in a different one. This is principally due to differences in geographic, environment, plant species, culture, and social conditions, where most of the original requirements change, not being the same with which the machine was initially designed. That is why the direct use of foreign machinery, without the implementation of the necessary changes, is destined to fail, as has been the case of some national producer's investments. They reported that the platforms were too wide or too short for their orchards, the trees were not conditioned (very long branches), jams on large slopes and thick grooves, and lack of location for the baskets without a processing system. Also, they affirm that people are still more skillful with ladders, and one of the main disadvantages of the platforms is workers focusing too much on productivity, leaving aside the selectivity. In sum, implementing machinery in the harvest requires the redesign of the processes, the organizational form of the workers, and also of their payment systems.

Chile is a developing country that has begun to make its way in the industrial automation race, but there is still a significant road to travel to equate the investments in scientific research of developed countries. In the particular case of fruits harvest,

there are some national solutions designed to semi-automate the processes which are slowly starting to be attractive to producers. The MC01 is the perfect example of a domestic machine created by *Cosecha Mecanizada* (COMEC) in response to the specific requirements of the Chilean vines (see Figure 1-5). The downside of the mechanical harvest, besides what has already been exposed regarding fruit handling, is the post-selective management that is no longer carried out by people. Harvesting machines like MC01 remove all the fruit at once without pre-selecting it, increasing the complexity of the packaging lines adding automated sorting process.

There are several studies focused on fully automating crop processes, with millions of dollars invested in research. Li et al. (2011) make a review of the harvesting methods up to date and their potential use in automated systems. The results show that some automatic systems have been practiced to a trade-off between the conventional harvesters and mechanical harvesters. Still, none of those methods match the capability of the human labor faultlessly, especially in the vision and the recognition capability.

Figure 1-5: MC01 grapes harvesting machine made in Chile by COMEC.[9]

[9] Source: https://www.cosechasmecanizadas.cl/cosechadora-uvas

1.4.2 PV Electric Vehicles (EV)

EVs have recently begun to replace those with internal combustion (IC) engines, but it is essential to consider that both were invented only with a couple of years of difference between them. At the beginning of the industrial revolution, the main characteristic that prevailed those years was the range of autonomy and the easy of refueling acquisition of ICs. Nowadays, thanks to technological advances, the autonomy of EVs has been dramatically improved, achieving results that exceed the traditional ones. Despite this, there is still no robust and distributed network of chargers, making it familiar to see the owners parked and inside their vehicles waiting for one of the few existing chargers per station to be vacated. Some projects are trying to solve this issue where the proposal is to change the entire bank of batteries, so customers do need to wait for the whole recharge process, but there are still some details to solve as is the difference in the useful life of used batteries and their ownership.

On the other hand, the real environmental impact of electric vehicles is mostly obtained when the energy comes from non-conventional renewable sources or non-fossil sources. This is because if the electrical power is produced by gas or coal plants, the final efficiency of the electric vehicle is maintained in similar numbers to the internal combustion vehicles.

Several studies have analyzed solar energy as a fuel for electric vehicles, but all agree that the current efficiency of photovoltaic cells is not enough to feed a commercial vehicle exclusively, and commonly is used only in an ultra-light competition car, or just to auxiliary power systems.

1.5 Methodology

The design of the solution was achieved from research to test in 4 months starting in September 2016. The principal methods used were scrum and design thinking. Scrum is a process focused on the results and the agility of a project. The use is extensive from

software to product development and is especially suitable for complex environments where the requirements are not fixed or are customizable, meaning that they could change as the project progresses. For the other hand, design thinking is a methodology that uses anthropological studies and techniques such as short ethnographies with semi-structured interviews, or card sorting, to allow the identification of a list with fundamental requirements that must meet any solution to the problem or opportunity discovered. The process (see Figure 1-6) ensures that having the technical knowledge and experience to develop a technologically robust solution, this last is going to be relevant to the "problem" or "need" identified from the beginning, after the implementation of the solution. Also, the proposed methodology introduces a preliminary step to the traditional design process, forcing to question the problem submitted by a third party and using anthropological research to identify the root of the problem through the identification of its requirements.

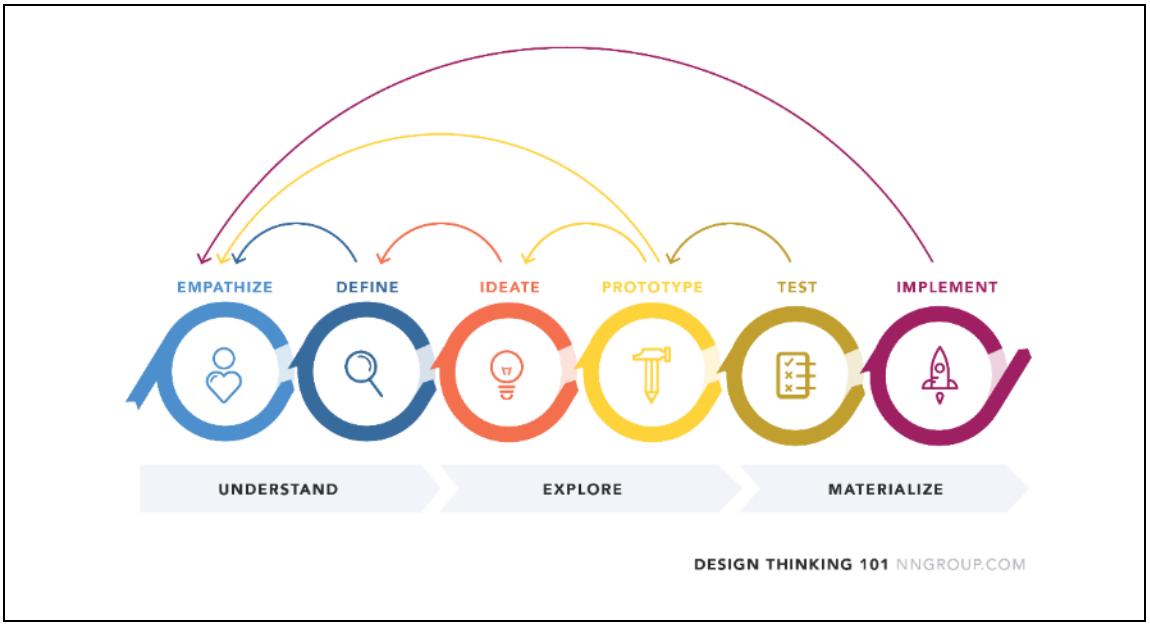

Figure 1-6: Design Thinking iterative process.[10]

[10] Source: https://www.nngroup.com/articles/design-thinking/

The “empathize” phase was addressed with field research into the standard characteristics of orchards to identify the requirements of workers and producers. For this, more than 4 hours of videos, interviews with the workers, harvesting process and short interviews with the workshop manager about their field experience were realized and analyzed. Later, during one of the tests implementing the prototype, the traditional harvesting process was experienced side by side with the workers, giving valuable data by breaking the barriers with them and earning their trust. Also, a review of state of the art regarding technology, products, and academic research was conducted to “define” and complete the “understand” phase, leading to the situation requirements. From the result of this investigation, a structured and defined list was obtained which is presented in a section later. The “ideate” phase was carried out with the individual addressing of each requirement, preparing an experimental modular design based on the mentioned list and on the benchmarking of the solutions that try to solve the problem of low productivity and high physical demand of fruit harvest, especially those focused on platforms concept. The improvements developed focused on vehicle steering, traction, dimensional platform flexibility, and ultimately the robustness of the overall design.

1.5.1 Chassis & Steering

The vehicle was required to move at low speed with high-level steering control in off-road terrain. Once within the orchard, an exceptional performance demand in the steering system had to be considered when changing rows and while driving within the confined space to avoid damaging the branches of the trees. In consequence, the proposal consisted in a 4-wheel steering (4WS) system, independent axes, and electrically powered each one. According to the academic literature, a 4WS allows a two-wheel steering vehicle to reduce its turning radius by half (Lohith, Shankapal, & Monish Gowda, 2013). The problem then was in the specifications, the implementation, and the control design. Figure 1-7 shows the particular capabilities of an electric 4WS independent system.

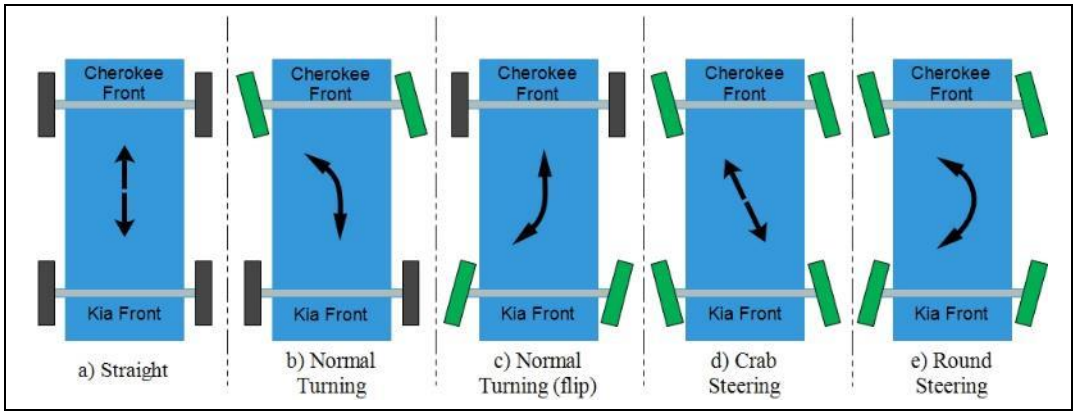

Figure 1-7: 4-Wheel Steering movements capabilities.

It is electric because if the axes were mechanically connected, a design only could cover crab steering (d) or round steering (e), but not both together. To make a mechanical system able to switch between these two states, a highly sophisticated design need to be conceived, including the disadvantage of the enormous additional mechanical effort to turn both axes at the same time.

The proposal then, was to use two front chassis of vehicles and joining them, electrically powering the steerable axis of each one, leaving both independent, and allowing to perform all the movements from Figure 1-7. It is important to mention that the vehicle is never going to get stuck when the moves are mixed, or in the transition from one to another state, or in partial movements. This is because when the vehicle starts from (a) state, and one of the axes is moved in any direction, the vehicle change immediately to (b) or (c) state. If both axes are driven at the same time, the vehicle will enter to (d) or (e) state immediately. Depending on the direction where each axis was run, the axes are returned to the neutral position (collective or individually) the vehicle would pass through (b) or (c) but eventually will back to (a) always in a fluid process. All these features mean a unique utility when the vehicle is closer to a wall of trees, uneven, with the front more distant than the tail, i.e., then the driver can quickly level it by turning the rear axis and moving forward only a couple of meter, without wasting time neither compromising the

harvest. Another example could be when the vehicle is harvesting a double wall of trees, but closer to one of them, then the driver only need to move both axes in the same direction, entering to crab state (d), and moving forward to be even without losing the parallelism with the row in the process. A particular case occurs when the vehicle finishes an end row. Orchards space is optimized to get as much as trees as possible in the field, then at the borders of the terrain, it becomes difficult to enter to a row with a large vehicle and even harder to change from one row to the next. Then the round steering state (e) is highly required to optimize the length of the vehicle and orchards.

In order to facilitate the design, a chassis of a previous prototype vehicle was used and the second was acquired in a junkyard instead of designing an entirely new 4WS system. The decision was based in the use of recycled vehicle components that still have a much useful life, reducing costs, manufacture resources, time, and promoting the concept of the applied CE (Fundación Economía Circular, 2017). As this is a research prototype, there is no issue in using old components that still work. Besides, the concept can also be expanded to final product designs, but renting it under leasing modality or similar instead of selling it, and does not jeopardize the customer's quality appreciation of the product.

One of the axes needs to come from a 4x4 vehicle. The reason is that at least one of them was necessary to give traction to the vehicle and being steerable at the same time, but front wheel drive vehicles do not have a fixed axis, either differential because usually the gearbox is coupled directly, and the suspension axes are independent. For this reason, the chosen 4x4 chassis was a Jeep Grand Cherokee 98. After checking the blueprints of the two chassis, a Computer Aided Design (CAD) was developed using the software Autodesk Inventor Professional 2017 (see Figure 1-8) to replicate both frame on 3D in order to design the intersection structure and ensure that there was no interference or structural weakness in the final merge of the chassis. The main difficulty in the union process was the gap in height and width between both frames, including also the original wheel size difference that had to be

considered to maintain the chassis at a horizontal level in the subsequent standardization with traction wheels.

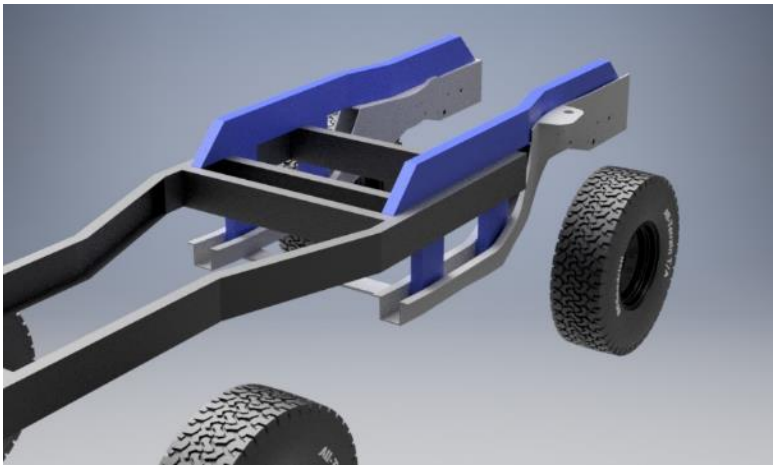

Figure 1-8: CAD chassis. Front Kia Besta (black), front Cherokee (grey), and joint structure (blue).

Figure 1-9: Fabrication of the chassis.

An essential reference used during the design of the solar vehicle was the book " The Automotive Chassis Engineering" by Reimpell, Stoll, & Betzler (2001), which is considered a masterpiece in vehicle design. In there was inspired the chassis structure, reviewed the Ackerman geometry concept, checked the suspension, and based the main calculations for the mechanical systems design.

Between the different researched alternatives of power steering systems (BOSCH, 2015; Seminarsonly.com, 2016), electric linear actuators were found to be the most suitable option according to the requirements, especially considering the high required force to turn the wheels of a heavy load vehicle, which is calculated below. Each axis was carefully measured and calculated to have a maximum steering angle β of 25° for Besta Front (BF), and 18° for Cherokee Front (CF), equal to left or right (see Figure 1-10.a). The length of the steering arm a (1) on each axis (2) is 0.15 m, the linear actuator (3) is fixed to the axis allowing to turn the wheel (4) when it extends or contracts by pushing the steering arm and converting linear movement into rotational on the wheel (see mechanism in Figure 1-11). As the tail of the actuator is going to be fixed to the axis after a ball joint, the calculation of the real maximum travel distance should consider the variation angle between the actuator and the axis $\Delta\theta$, but as the length of the arm is far smaller than the length of the actuator, that variation can be approximate to zero:

$$a \ll l_{actuator} \xrightarrow{yields} \Delta\theta \cong 0 \tag{1.1}$$

In addition, the objective is to determine the maximum variation in travel length of the actuator, where it comes from full left angle $-\beta$ to full rigth $+\beta$, making the beginning of θ angle almost equal to the end (see Figure 1-11):

$$\theta_{left(-\beta)} \approx \theta_{right(+\beta)} \tag{1.2}$$

Then, the maximum distance that the linear actuator should be able to travel (see Figure 1-10.b), from one side to the other is given by D, where it is equal to:

$$D = 2a \sin\beta \tag{1.3}$$

Then, for each axis the travel distances are:

$$D_{BF} = 2 \times 0.15 \sin 25 = 0.13 \text{ m}$$

$$D_{CF} = 2 \times 0.15 \sin 18 = 0.093 \text{ m}$$

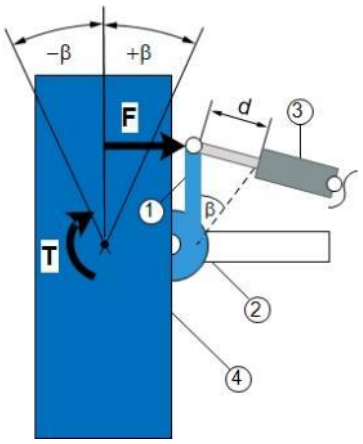

a) Steering top view detail

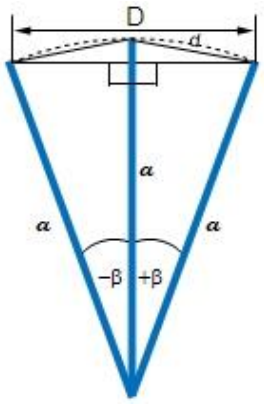

b) Arm geometry

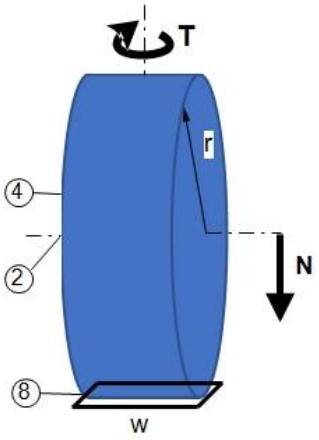

c) Wheel front view

Figure 1-10: Diagrams of the steering system.

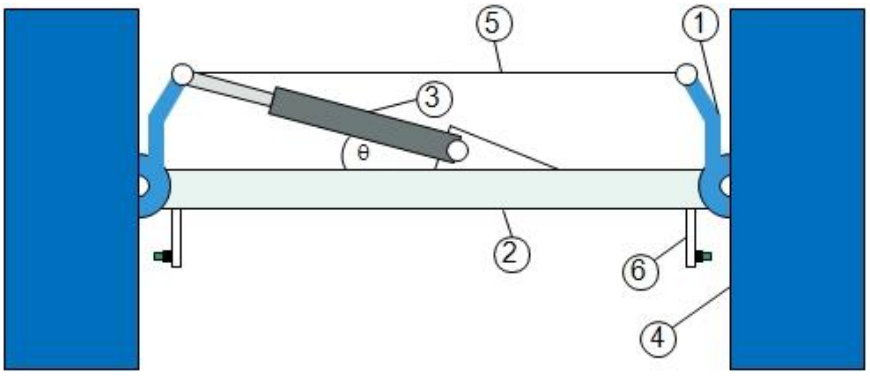

Figure 1-11: Full axis top view steering system.

Using a 1.5 factor of safety with the most significant value to clearance the limits and to not damage the linear actuator's mechanism, it should have then a maximum travel length of:

$$D = 1.5 \times 0.13 = 0.20 \text{ m}$$

It is necessary also to know the force F needed to characterize the linear actuator that turns both wheels of each axis from one side to the other, as is shown in Figure 1-11. The steering arms (1) of each wheel are connected through a link bar (5) and both push-pull together with the linear actuator (3) that is connected to the axis (2) with a ball joint as a rear support. The travel limit is established by sensors (6) at the end of each angle rotation. The force F then is the double of the required torque T to rotate each wheel individually, but divided by the steering arm length:

$$F = 2\frac{T}{a} \tag{1.4}$$

To obtain the torque, first, it is necessary to know the load force N on each wheel. The total mass of the vehicle, including 8 people on board (80 kg each) and 3 bins (500 kg each) is 2,940 kg. Then the load in each wheel is given by N, where mg is the total weight (mass by gravity constant):

$$N = \frac{mg}{4} \tag{1.5}$$

$$N = \frac{2940 \times 9.8}{4} = 7{,}203 \text{ N}$$

To calculate the torque, it is necessary also to know the pressure of the tire including the parameters shown in Figure 1-10.c. The tires used were Goodyear model wrangler 31x10.50 R15 LT. Each one has a maximum load capacity of 1,020 kg at 50 psi (350 kPa), a diameter of 31 inches (787.4 mm) which means a radius r of 0.3937 m, and width w of 0.267 m. The pressure used P_a was 40 psi (276 kPa) considering the total weight estimated before.

In equilibrium, the area of the contact surface (8) of the wheel is given by:

$$A = \frac{N}{P_a} \tag{1.6}$$

Because the force applied to the tire to not go down is equal to the pressure inside the tire by the area in touch with the ground. Then, using the Equation 1.6, the area is:

$$\text{A}= \frac{7203}{276\times10^3} = \ 0.0261 \text{ m}^2$$

Then, the torque is given by the integration of the differential torque function (see Figure 1-12 and Equation 1.7) where μ is the coefficient of friction from the terrain.

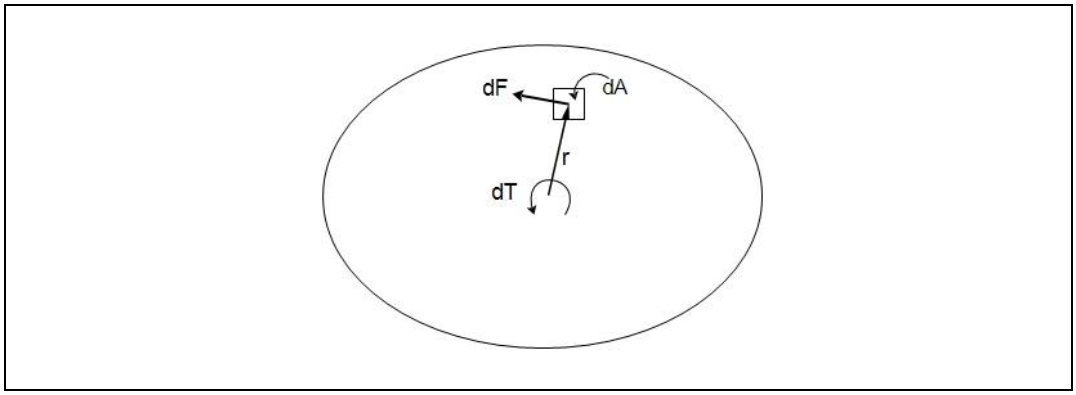

Figure 1-12: Contact surface of the wheel with the ground.

$$T = \int dT \tag{1.7}$$

$$dT = rdF \tag{1.8}$$

$$dF = \mu P_a dA \tag{1.9}$$

In this case, the highest coefficient of friction in which the tire is going to be submitted with full load is from loose gravel terrain condition; then the coefficient μ is 0.5 (Reimpell et al., 2001). The contact surface area is assumed to be circular shape for practical reason, then the parameters of this surface are:

$$A = \ \pi R^2 \tag{1.10a}$$

However, from Equation 1.6 the area was already calculated, the parameters are then:

$$R = \sqrt{\frac{A}{\pi}} \tag{1.10b}$$

$$R = \sqrt{0.0261/\pi} = 0.091 \text{ m}$$

This allows to solve the integral and calculate the torque using Equations 1.7 to 1.9. Considering dA as a complete circle double differential using polar coordinates:

$$dA = rd\theta dr \tag{1.11}$$

$$T = \iint r\mu P_a r d\theta dr \tag{1.12a}$$

$$T = 2\pi \int r\mu P_a r dr \tag{1.12b}$$

$$T = 2\pi\mu P_a \int_0^R r^2 dr \tag{1.12c}$$

$$T = 2\pi\mu P_a \, R^3/3 \tag{1.12d}$$

$$T = 2\pi \times 0.5 \times 276 \times 10^3 \times 0.091^3/3$$

$$T = 217.8 \text{ Nm}$$

Then, using Equation 1.4, the force required by the actuator is obtained:

$$F = 2\frac{217.8}{0.15} = 2{,}904 \text{ N}$$

Using a 1.5 factor of safety so as not overload the actuator, the final required force is:

$$F = 1.5 \times 2{,}904 = 4{,}356 \text{ N}$$

With this both parameter (length travel and force) it was possible to find the right linear actuator to fit the requirements. Between all the options, the fastest was the SKF CAHB-21 (see Table 1-1). The speed was an additional but important

parameter because the response from moving the wheels from one to another side should be comparable to the time of the steering wheel, which is about 4 seconds at normal speed. The reason of this is to make the vehicle easy to drive, without the necessity of special training, and using the experience acquired driving a normal vehicle.

The longest axis has a travel length of 0.094 m. Hence the required speed needs to be at least:

$$S = D/t \tag{1.13}$$

$$S = 0.094/4 = 0.024 \text{ m} \cdot \text{s}^{-1}$$

Table 1-1: Technical specification of linear actuator SKF CAHB-21[11]

Parameter	Value
Voltage	24 V
Ultimate push-pull static load	4500 N
Speed at full load	up to 0.045 $m \cdot s^{-1}$
Stroke	0.20 m
Operating temperature	-40 to +85°C

The control of the steering system was designed with two joysticks (each for one axis) as a user interface, and a Siemens PLC as a receptor of the input signal from the limit sensor and the joystick, sending an output signal to relays connected in parallel to the actuators.

In addition, it was going to be necessary to drive the vehicle on asphalt sometime, but rarely carrying the same amount of weight. This is why additional calculations were made in the same way before to determine the load on the linear actuators, with eight people on board, but without the bins. Considering the μ coefficient of dry

[11] Source: http://www.skf.com/cl/products/actuation-systems/linear-actuators/cahb-series/cahb-21e/index.html

asphalt equal to 1, and a total mass load of 1,440 kg, the result shown a required force F of 3,000 N on the actuator after safety factor of 1.5. The selected actuators then should work fine.

Figure 1-13: Linear actuator (black) installed in the chassis upside down.

1.5.2 Traction system

The traction is one of the most current demanding electrical systems in EVs. In this work, as the objective is to rely only on photovoltaic energy, the design of the traction is one of the most crucial steps. On the harvesting process, the forward movements of the proposed concept vehicle need to be precise, short and consistent. The traction needs to be reliable enough considering the total load, and sometimes it needs to be able to increase the maximum speed limit to move vast distances faster, i.e., from the storage warehouse to the field. In addition, as some stuck in deep groves where mentioned by managers during the interviews, the vehicle required a high torque traction system and a clean space under the chassis to bypass these issues.

The proposal of solar photovoltaic energy as exclusive power source dictates the use of efficient electric motors. The benefits of using these over the traditional diesel engines are many, being the first quietest, do not pollute, do not consume oxygen, have a fast start, are easily reversible in directional rotation, reversible in power, have a more straightforward manufacture, lower cost, higher performance, higher efficiency, regenerative brake capabilities, and are very controllable in speed. The main drawback of EVs is the energy storage capability, where still besides the technological advances nothing can be compared with the specific energy (Wh/kg) found in gasoline, which is around 10,000 Wh/kg in comparison to the 150-300 Wh/kg found in the state of the art of Li-ion batteries (Dixon, 2010; Kimura, Seki, Shin, Takahashi, & Makino, 2016). However, the idea of this heavy-duty EV concept is to maintain always the energy on the bank of batteries, considering an intermittent use and a continuous charge with photovoltaic energy on the field, thus never running out of power. In addition, the weight of the batteries is not an issue because of the overall loads, which is higher.

The electric vehicle (EV) industry is currently dominated by two types of electric motors, brushless DC (BLDC) and induction motors. Both have similar stators, work with a current inverter, and have regenerative braking capability, but they present differences in the rotor and its drive principle. An electric induction motor works with a squirrel cage rotor, which is magnetically induced by a rotary field of the three-phase current in the stator. This allows the motor to have torque from the start at any current frequency and it can be easily controllable in speed through the simple variation of the frequency of the current, without the need for an absolute positioning sensor, only from speed. On the other hand, a BLDC motor works with a rotor of permanent magnets, which allows it to follow the stator by adjusting the frequency of the field, but in order to start from zero, the frequency needs to do so. In addition, it requires an absolute position sensor to be able to have speed control, usually a hall effect sensor. Both types of motors do not have significant differences until here, besides the specific kind of control code. The most important differences lie in the

greater complexity of the induction motors, but the lower cost due to the absence of permanent magnets, and the higher temperature generated in the induction stators, but their ability to modify the magnetic flux of the stator into different speeds. Despite this, there are no substantial distinctions that position one over the other, and just as there are different types of internal combustion engines for various applications, the same happens with electric motors (Wally Rippel, 2007).

Then, following the same approach of recycled components mentioned in the past section, the electric motor used was a BLDC 5 kW Golden Motor obtained from a previous version prototype of harvesting vehicle. It was attached to a reduction box of 10:1 and the axis used, mentioned before from the Cherokee chassis, comes with a differential that has an internal reduction as well. The proposal consisted then in connecting all these components in series, but with the goal of obtaining high torque at low speed efficiently. The main characteristics of the motor are summarized in Table 1-2. The motor controller used was from the same manufacturer, and its main features are outlined next in Table 1-3.

Table 1-2: Technical specification of BLDC Motor HPM5000B[12]

Parameter	Value
Rated voltage	48 V
Rated power	5,000 W
Rated current	120 A
Rated speed	3500 rpm
Maximum efficiency	91%

The primary objective in the design of the traction was to achieve the torque requirements, ideally with the less current consumption possible. Hence, the system needs to work on the highest torque point, which is 24.12 Nm raised at 2,389 rpm as

[12] Source: https://www.goldenmotor.ca/HPM48-5000.pdf

shown in Figure 1-14 and Table 1-4, where the efficiency at that point is 72.1% with a peak current consumption of 176.4 A.

Table 1-3: Key features of BLDC Motor Controller HPC300H48360[13]

Features
Regenerative braking
Brake control
Slope holding control
Cruise speed control
FWD/REV control
Overheat protection for both motor and controller
Programmable via USB PC/Laptops
DSP control
Dual controller synchronous drive

[13] Source: https://www.goldenmotor.com/HPC%20Series%20Controller%20User%20Guide.pdf

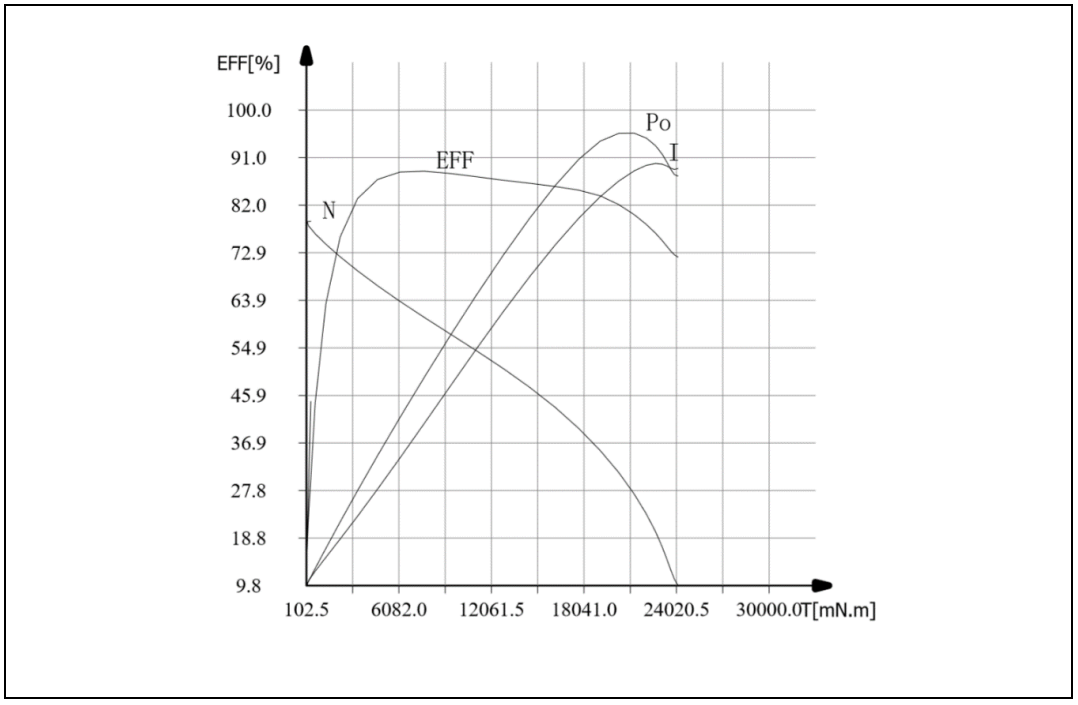

Figure 1-14: Test curve Golden Motor HPM5000.[14]

Table 1-4: Test data Golden Motor HPM5000[14]

Description	Current/A	Torque/Nm	Speed/rpm	Efficiency
Upload point	8.18	0.36	4389	42.2%
Efficient point	73.69	7.73	3861	88.4%
Max. power point	175.4	21.28	2892	80.2%
Max. torque point	176.4	24.12	2389	72.1%
Rated rotate point	132.9	14.54	3476	86.1%

Now, to determine the ideal gear ratios to keep the electric motor working efficiently, it is necessary to calculate the required torque to move the vehicle, which

[14] Source: https://www.goldenmotor.ca/HPM48-5000Curve.pdf

can be obtained as follow, where T_w is the torque at the traction wheels, r_w is the radius of the wheels and F_t is the tractive force:

$$T_w = F_T r_w \tag{1.14}$$

The tractive force is composed of four main forces; the tire rolling resistance force F_r, the slope gravity force F_g, the aerodynamics drag force F_d, and the acceleration force F_a.

$$F_T = F_r + F_g + F_d + F_a \tag{1.15}$$

$$F_r = k_r mg \tag{1.16}$$

$$F_g = mg \sin \alpha \tag{1.17}$$

$$F_d = \frac{1}{2} \rho v^2 C_d A \tag{1.18}$$

$$F_a = ma \tag{1.19}$$

The rolling resistance force is the result of energy loss in the tire explained by the generation of heat coming from the deformation of the tire area in contact because of the spring properties of the rubber (Reimpell et al., 2001). The parameter k_r is called the rolling resistance factor, which depends on the tire pressure and on the vertical reaction force N. Between the asphalt and the orchard, the highest k_r value is presented in dirt/mud terrain, with a factor of 0.037 (Chauhan, 2015). The slope gravity force is the action of pulling or pushing the vehicle when it is climbing or descending an inclined surface. The hardest case scenario to consider in this work is the vehicle ascending on a platform with an angle α of 10° in order to be transported. The total weight in this case is going to be only the vehicle carrying the driver. For a second case scenario, the inclination of the orchard considered is an angle α of 1° but carrying the full load. The aerodynamics drag force dependent from the geometry C_d of the vehicle, the cross-sectional area A, and the density of the air, because a bad combination could create turbulences in the fluid and vacuum effect

at the back when the shape is short and squared. But it is more dependent on the speed of the vehicle, which is quadratic. Considering that the vehicle is not designed to move at high speed, this force is assumed to be marginal, and its order can be observed in Figure 1-15. Last but not least, in this work the acceleration force is one of the main components of the total traction force because of the heavy weight, and it depend from the total mass and the desired acceleration of the vehicle, which is programmed to be 0.5 m/s^2.

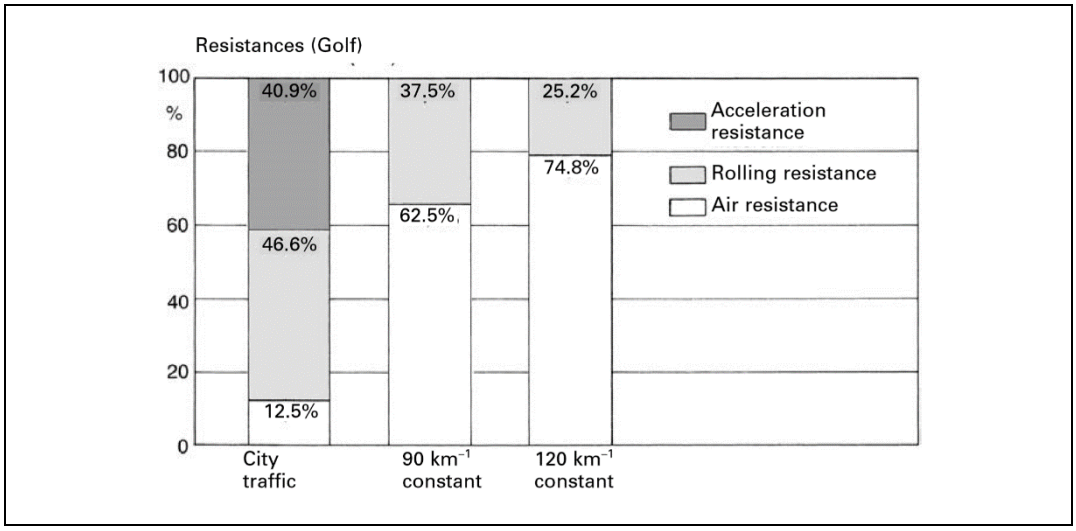

Figure 1-15: Ranges of participation in total tractive force at different speeds of a Volkswagen Golf.[15]

For the technical purpose, the first calculation is going to be the orchard case. Using Equations 1.15 to 1.19, and with the parameters obtained from the literature, the tractive force is:

$$F_r = 0.037 \times 2{,}940 \times 9.81 = 1{,}067 \text{ N}$$

$$F_g = 2{,}940 \times 9.81 \sin 1° = 503 \text{ N}$$

[15] Source: See reference (Reimpell et al., 2001)

$$F_a = 2{,}940 \times 0.5 = 1{,}470 \text{ N}$$

To demonstrate the marginal order of the aerodynamic force, it is calculated this time:

$$F_d = \frac{1}{2} 1.225 \times 3^2 \times 0.8 \times 2 = 18 \text{ N}$$

It is important to consider that the forces are applied in different space-time frames, i.e., the aerodynamic only apply when the vehicle is achieving speed incrementally, while acceleration force decrease as the vehicle raises the speed limit desired. The total tractive force calculated next consider all the forces as a maximum peak current demand when the vehicle starts from the rest:

$$F_T = 1{,}067 + 503 + 1470 + 18 = 3{,}058 \text{ N}$$

Then, with a radius of 0.39 m, the required torque at the wheels is:

$$T_w = 3{,}058 \times 0.39 = 1{,}193 \text{ Nm}$$

Using a safety factor of 1,5 to include the friction losses and the inertia of internal components:

$$T_W = 1.5 T_w \tag{1.20}$$

$$T_W = 1.5 \times 1193 = 1{,}790 \text{ Nm}$$

Finally, the minimum ratio necessary for the traction system is given by:

$$Ratio_m = T_m : T_w \tag{1.21}$$

$$Ratio_m = 24.12 : 1{,}790$$

$$Ratio_m = 1 : 74$$

Also, the same calculations for the second case scenario, ascending a platform or a steep road of 10°, with a curb weight of 1,000 kg by gravity, resulting in a second minimum ratio of:

$$Ratio_{m,2} = 1:26$$

The design then needs to be contingent on the highest ratio. The selected components of the traction system are summarized next in Table 1-5. Following the circular economy concept of this work, the gearbox was acquired in the same junkyard than the chassis, in *La Pintana*. The reduction box was extracted from another project together with the motor, and the gearbox was from a Chevrolet LUV. The universal shaft was fabricated, and the differential comes with the chassis. A particular piece was necessary to design and to manufacture in order to connect the reduction box with the gearbox.

Table 1-5: Traction system component list with ratios

Component	ratio
BLDC motor	1:1
Reduction box	1:10
4-speed gearbox	1st gear 1:3.8
	2nd gear 1:2
	3rd gear 1:1.5
	4th gear 1:1
Universal shaft	1:1
Differential	1:3

The total system ratio of all the components connected in series depends on the gear selected on the gearbox, then the minimum and maximum values are:

$$Ratio_{S,min} = 1:30$$

$$Ratio_{S,max} = 1:114$$

This ratio allows fulfilling the torque requirements. On the other hand, the motor was tested and was not possible to achieve a higher motor speed than $\omega_m =$

2,000 rpm because of software limitations. Then, the maximum allowed speeds for the vehicle are given by:

$$V_{max} = 2\omega_m \pi r_w Ratio/60 \tag{1.22}$$

$$V_{max;S,min} = 2 \times 2{,}000\pi 0.39 \frac{1}{30}\frac{1}{60} = 2.7 \text{ m/s}$$

$$V_{max;S,max} = 2 \times 2{,}000\pi 0.39 \frac{1}{114}\frac{1}{60} = 0.7 \text{ m/s}$$

Summarizing, the final design of the vehicle has a traction system with a minimum speed limit of 0.7 m/s (2.52 km/h) and a maximum of 2.7 m/s (9.72 km/h), where the maximum torque at the wheel is of 2,750 Nm, and the minimum is 723.6 respectively. The only drawback with the design is that because of the high reduction to achieve maximum torque requirements; the maximum speed was lower than the desired.

$$0.7\ m/s\ < 3\ m/s$$

Besides, the length to move the vehicle forward is about 5 meters per cycle, and the resulted time to achieve the next sector is given by the acceleration time up to top speed t_1, and the constant speed time t_2:

$$t = t_1 + t_2 \tag{1.23}$$

$$v_f = v_o + at_1 \tag{1.24a}$$

$$t_1 = \frac{v_f - v_o}{a} \tag{1.24b}$$

$$t_1 = \frac{0.7-0}{0.5} = 1.4 \text{ s}$$

$$d_1 = v_o t_1 + \frac{1}{2} a {t_1}^2 \tag{1.25}$$

$$d_1 = 0 \times 1.4 + \frac{1}{2} 1 \times 1.4^2 = 0.98 \text{ m}$$

$$d_2 = \frac{1}{2}(v_f + v_o)t_2 \quad (1.26a)$$

$$t_2 = \frac{2d}{v_f + v_o} \quad (1.26b)$$

$$t_2 = \frac{2(5 - 0.98)}{0.7 + 0.7} = 5.74 \text{ s}$$

$$t = t_1 + t_2 = 1.4 + 5.74 = 7{,}14\ s$$

The resulted time is not ideal, but it is acceptable to move between the sectors giving space to react with the direction system.

a) Motor BLDC with reduction box

b) Gearbox Chevrolet LUV

c) Cherokee's differential

d) Universal shaft

Figure 1-16: Components of the traction system.

Figure 1-17: Complete traction system installed on the chassis upside down.

1.5.3 Platform

Stone fruit orchards in Chile have a wide variety of parameters and configurations. Also, as was mentioned above in the motivation, to facilitate optimum performance of a semi-automated harvesting machine, it is necessary that both orchards and machine be designed on the whole. A project of this type requires many resources to be able to be carried out, considering that an entire sector of an orchard should be worked experimentally, jeopardizing the profitability of the owners but may generate substantial long-term benefits. In the case of this work, neither the resources nor the possibility of designing a whole orchard sector in conjunction with the harvesting machine was feasible, so it was finally decided to focus the design of the platform on obtaining the most considerable flexibility with the available resources. The orchards accessible to test the vehicle were two (see Figure 1-18),

one of the sweet cherries and other of nectarines, both with similar parameters shown in Table 2-1, later in the article section.

a) Sweet cherries orchard border

b) Nectarines orchard row

Figure 1-18: Accessible fruit orchards overview.

The requirements include then the need to be extensible in width to adapt to these two orchards. Also, support the weight of 4 people per side without danger of overturning, allow workers to reach the highest fruit in the trees from the middle, or from the point where the walk team does not reach to harvest, interchangeable for multipurpose, adjustable in height, and with the central part with the width enough to enter two bins from the lift system.

The proposal includes a removable platform with four anchorage points in the chassis, two manual retractable side platforms, a small step to increase the reach of the stretched hand, an automated fixation system of lateral platforms by weight, retractable safety rails in line with the design of the platforms, and central support for photovoltaic module structure.

The measures of the orchards dictate the parameters of the platform, especially regarding width range and height. This was required to variate from 2 m to 3 m in width, considering that the sweet cherries orchard has a separation of 3.5 m between threes row, while the nectarines orchard has a 3-m separation. The extension of the

worker's arm outside the border of the side platforms should be enough to complete the 0.25 m left per side, while the minimum value allows to compact the structure and test the platform in more adjusted orchards. The width of the orchards was quite similar, between 3.0 m to 3.2 m. Considering a typical height of 1.6 m in the workers, the platform should be at 1.4 m from the ground. The addition of a 0.5 m step at the border of the orchard should allow them to reach the totality of the fruit by the majority of workers. The width of the central platform should be at least of 1.2 m in order to fit a bin inside, including the support structure for the photovoltaic panels, the final value was 1.3 m. The design of the system considers the central platform as a sandwich structure, including inside the two lateral platforms in different heights to be able to have an extension width higher than half of the central value per side (Figure 1-19), achieving at the same time the requirement of the load. The automated fixation system was implemented with a support guide, which reduces its width if it is subjected to a vertical load. This piece was acquired in an elevators store, and the main advantage is that when people stand up over the platform, the part closes itself avoiding the platform to move freely. Figure 1-20 shown the guide support and the fabrication of the platform.

a) Platform orthogonal bottom view

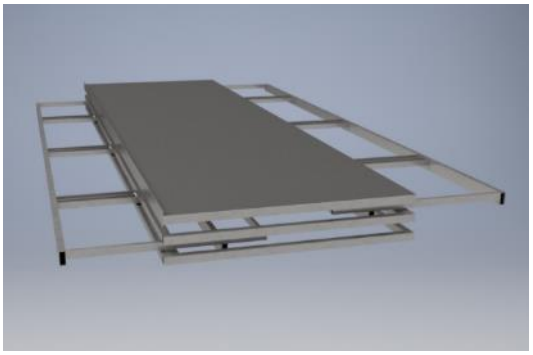

b) Platform orthogonal top view

Figure 1-19 CAD platform assembly.

To ensure the structural stability of the side platforms, which remain cantilever supporting four people at the edge, a structural finite element analysis was performed in Autodesk Inventor 2017 to determine the maximum stresses and deformations of the structure. The results are shown in Figure 1-21 and Figure 1-22. The maximum Von Mises stress σ_{vM} is less than the yield strength σ_Y, reaching 246.8 MPa. The maximum deformation does not exceed 9 mm. Then, the safety factor is 1.25 for the 2 mm steel used. Its properties are summarized next in Table 1-6.

Table 1-6: Technical specification of Steel SAE1010[16]

Parameter	value
Material	Steel SAE1010
Young's modulus	200 GPa
Yield strength	305 MPa
Tensile strength	365 MPa

a) Rail support guide and brake system

b) Platform structure with guides

Figure 1-20: Components and fabrication of the platform.

[16] Source: https://www.azom.com/article.aspx?ArticleID=6539

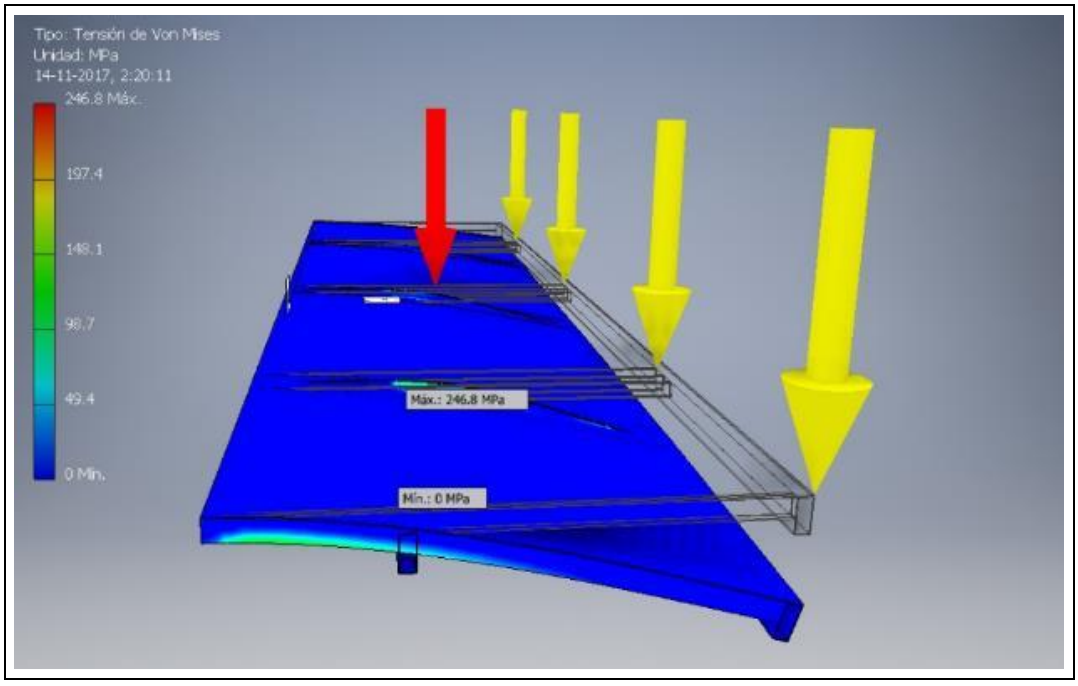

Figure 1-21: Von Mises stress for side platform full extended. Máx: 246.8 Mpa.

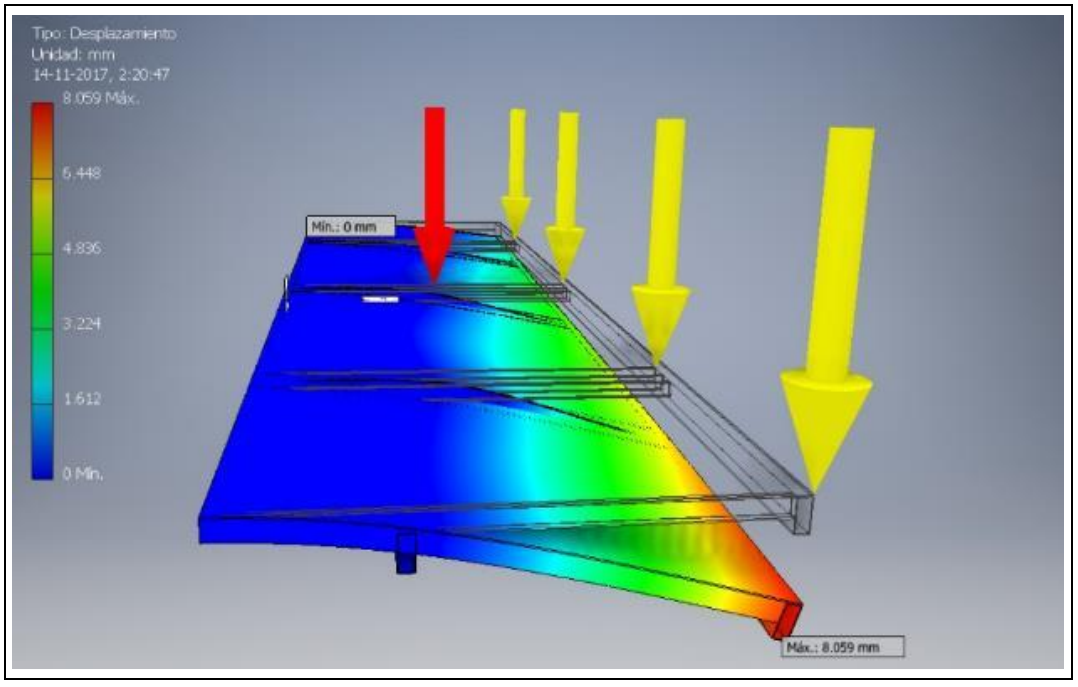

Figure 1-22: Deformation for side platform full extended. Máx: 8.059 mm.

Figure 1-23: The final platform with steep and safety rails.

1.5.4 Overall design

In this section, the electrical calculation and the global design aspect of the vehicle will be addressed. The requirement can be divided into two aspects, for the electrical terms, this needs to be self-sustaining, i.e., the energy consumed must be less than the available power or the supply energy for the photovoltaic panels. The general aspects of the design need to be complemented with the rest of the systems to achieve continuous harvesting of the orchards without any problem.

The electric systems are divided in three according to their working voltage, the 48 V traction system, the 24 V steering system, and the 12 V lift system. First, the primary electrical system and the most demanding regarding energy is traction. The current consumption of the harvesting movements in this system can be estimated from Table 1-4 and Equations 1.23 to 1.26. The maximum rated torque will draw a maximum current of 176 A at 24.12 Nm in the motor. The current consumption in a

BLDC electric motor is linearly proportional to the torque, where k_t is a constant, I is the current, and T_M is the torque at the motor:

$$T_M = k_t I \quad (1.27)$$

The estimated maximum required torque at the wheel obtained from Equation 1.14 without safety factor is 1,193 Nm, which divided by the total reduction ratio of 114 gives a required maximum torque at the motor of 10.46 Nm. The current can be estimated as follows by the proportional behavior:

$$I_{req} = T_{M,req} \frac{I_{max}}{T_{M,max}} \quad (1.28)$$

$$I_{req} = 10.46 \frac{176}{24.12} = 76.33\ A$$

However, this will only happen when the vehicle is fully loaded (the three full bins), and just for 1.4 s of the total 7.14 s movement (6.2%). That is the time of the vehicle's acceleration up to maximum speed. After this, the consumption will drop off because the acceleration force will be close to zero and the motor will only have to fight against the rolling resistance and the gravity to keep the speed in the small slope of the orchard. Then, considering an average load of 1.5 bins during the whole day, the required torque for constant speed can be re-estimated using Equation 1.14, giving a needed torque value of 899 Nm, which will draw an average current of 57 A at full speed during around 3 s, were the rest is supposed to be addressed by inertia in between and slowing down during the rest 2 seconds at the end of the movement. The photovoltaic available energy in Coltauco at the VI Region in Chile, in the location of San Fernando, where the orchard is located (34.24, -71.04), and specifically in the months of December and January, when the harvest is taking place, is around 8.4 kWh/m^2/day (Ministerio de Energia & Departamento de Geofísica Universidad de Chile, 2017; Molina Monje & Rondanelli Rojas, 2012).

This available energy means that during the day, in 12 solar working hours, the average radiation is around 700 W/ m^2, which can be observed graphically in Figure 1-24. The photovoltaic panel used were ET-M53685 modules of monocrystalline silicon cells of 0.125 m x 0.125 m. The electrical characteristics of this module are summarized in Table 1-7 and Figure 1-25.

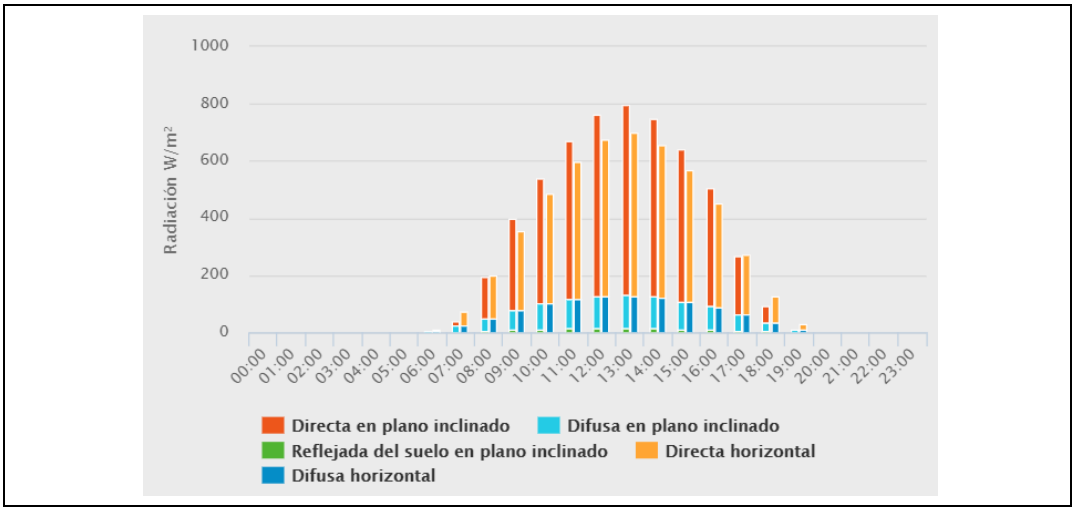

Figure 1-24: Daily radiation cycle in San Fernando, Chile (-34.24, -71.04).[17]

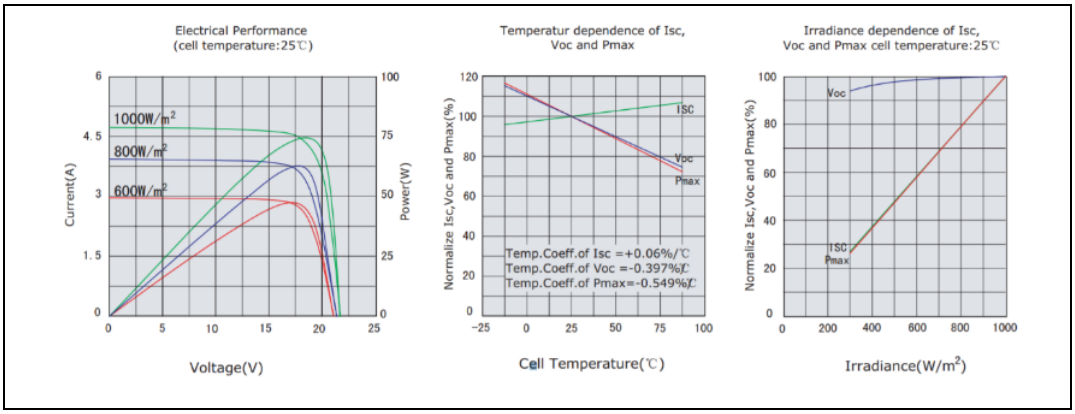

Figure 1-25: Electric performance, temperature dependence and irradiance dependence of module ET-M53685.[18]

[17] Source: http://www.minenergia.cl/exploradorsolar/

Table 1-7: Technical specification of PV module ET-M53685[18]

Parameter	value
Cell type	Monocrystalline Silicon 125x125 mm
Peak power	85 W
Number of cells	36 cells in series
Maximum power voltage (Vmp)	18.05 V
Maximum power current (Imp)	4.71 A
Open circuit voltage (Voc)	21.94 V
Short circuit current (Isc)	5.29 A
Maximum system voltage	DC 1,000 V

If the information of the available energy on the location and the characteristics of the cells is crossed, the current available per module should be between 2.5 to 4 A, depending strongly on the time of day. The expected time to be harvesting is at least of 60 s, then the energy delivered during that period by the PV system should be at least between 0.04-0.07Ah, variable depending on the cloudiness conditions. For the other hand, the consumed energy after the current and time mentioned before should be around 0.05Ah. Hence the balance should be positive in good conditions (without clouds), the case presented between the 92-95% of the time on the location during the harvest months[17]. The other electric systems are less used than the traction or require less energy. The steering only consumes 6 A as maximum current drawn, and it is supposed to be used only at the same time that the traction. For the other hand, the lift system has a peak drawn current of 200 A, but it is expected to be used only three to four times during the whole day, for no more than 10 seconds per location. This gives enough time to recover the energy. Also, the lift system would include two PV modules in parallel, increasing the charging energy at the double. Then all the electrical system should be positives in energy balance as well.

[18] Source: http://www.etsolar.com.ar/folletos/ET-M536(70-85w).pdf

The entire photovoltaic modules installed were eight, where four in series are for the traction system, two in series for the steering system, and two in parallel for the lift system. One of the main problems of the PV modules is that they get dirty very quickly, lowering their performance and the charging current. This is why a quick cleaning system was designed to facilitate the task, which can be seen in Figure 1-26.

Figure 1-26: Quick cleaning system for PV modules with hinge and door lock.

As the weight it is not a problem in this design, the batteries selected were 12 V deep cycle lead acid of 90Ah. Due to the available current of 4 A, these are suitable due to a perfect match in current charging specifications of the manufacturer. Then, following the photovoltaic design, eight batteries were installed, 4 in series for the traction, 2 in series for the steering, and 2 in parallel for the bin (see Figure 1-27).

Figure 1-27: a) Batteries installed and connected under the chassis. b) Specifications for Gonher battery G-27 DC.

The other design aspects were solved with a hydraulic brake, a pool ladder type to get on the platform, a lift system to get the bins on the platform, a dashboard to drive the vehicle, and a distribution board to centralize the electronics. Some of them are shown in the following Figures.

Figure 1-28: Driver dashboard with front axis at left and rear lever axis right

Figure 1-29: Electric distribution board with 3 MPPT in blue and black at left, PLC Siemens at the center, distribution lines at the top, and relays on the bottom.

Figure 1-30: Overall view of the vehicle with lift system and quick cleaning PV.

1.5.5 Measurement system

To validate the hypothesis of this thesis, a method to measure the electrical variables in situ for the harvesting tests was required. The two main parameters to monitor were the current and voltage for each operation. The equipment used was a battery monitor BMV-702 from Blue Solar, the same manufacturer of the two main MPPT installed. The Blue Solar battery monitor system record four essential parameters; SOC (%), Voltage(V), Current(A), and Consumed Energy(Ah). In addition, DAQ hardware and software from Measurement Computing (MC) was used for data logging backup and to monitor the auxiliary systems. The MC board only read voltage from 0-10 V. So, in order to read current, two types of sensors were used to convert current into voltage. For low current consumption and charge monitoring, the ACS712 current hall effect sensor was used. For high current monitoring, LEM

AC/DC current transducer DHR-C5 was used. The data acquired with these sensors was later normalized according to Equations shown in Figure 1-31.

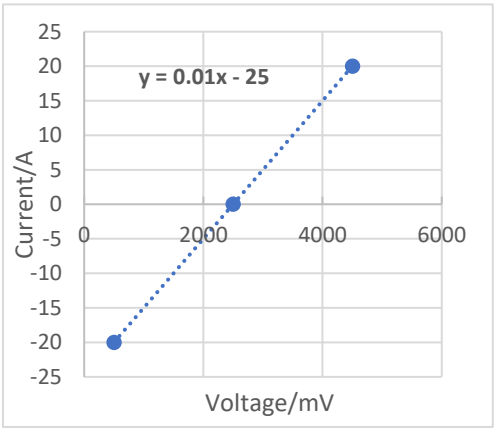

a) Current sensor ACS712

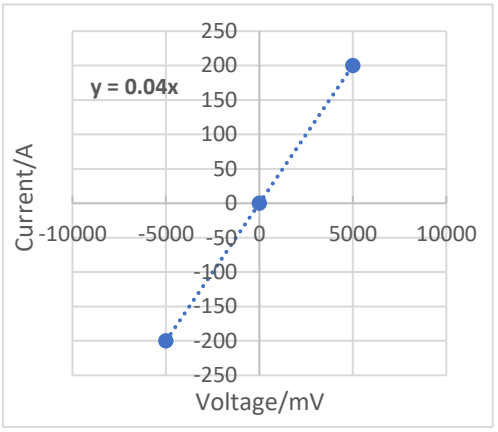

b) Current LEM sensor DHR-C5

Figure 1-31: Characterization of the current sensors.

For the other hand, regarding voltage lead-acid batteries can be estimated in SOC (%). Figure 1-32 shows the characterization of Gonher 90Ah batteries.

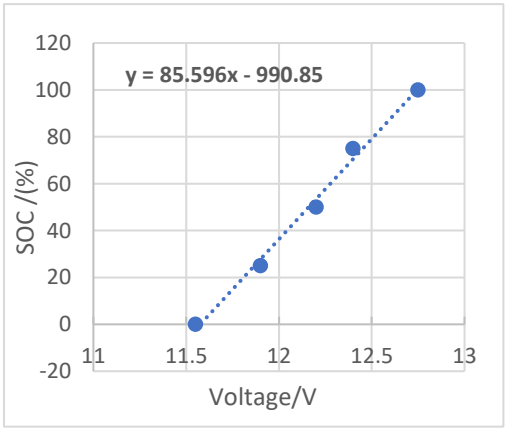

a) SOC of 12 V battery system

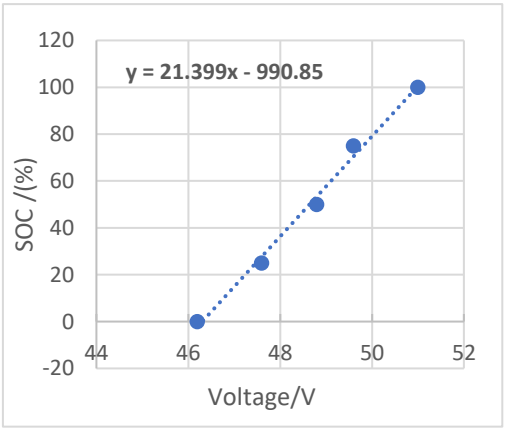

b) SOC of 48 V battery system

Figure 1-32: Characterization of the Gonher battery system.

To validate the working behavior of the electric components used, these were monitored in isolation to corroborate the values delivered by the manufacturers in the datasheets.

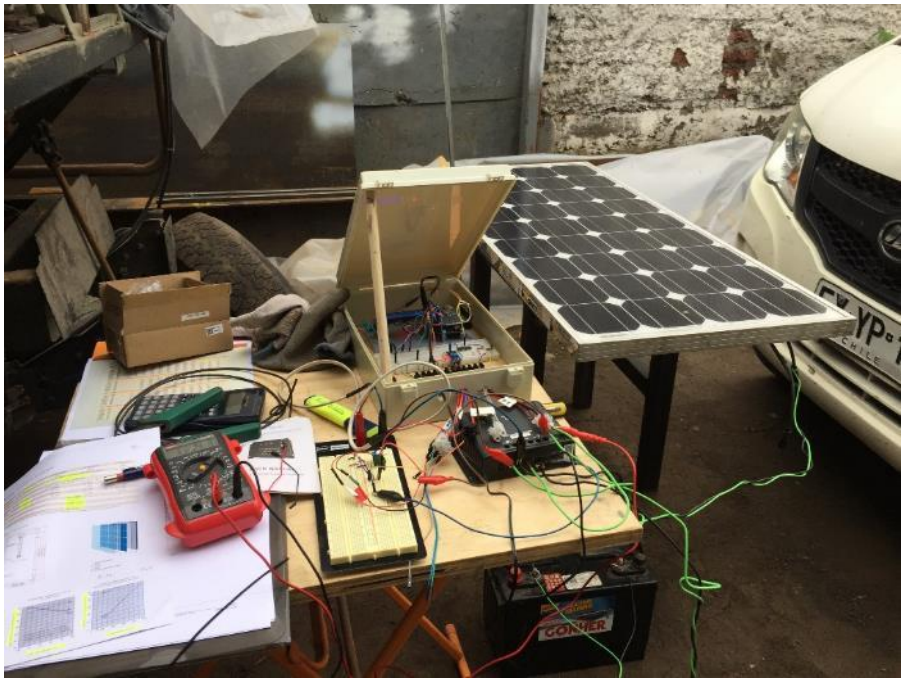

Figure 1-33: Testing PV module, battery, MPPT, data logging, and components.

The results shown that the values of the components were accurate enough, then to validate the theoretical calculation and the working behavior of the systems installed in the vehicle, mainly of the 48 V traction system, a particular set of simulation harvesting test were designed where voltage and current were measured at 1 S/s (sample per second) from the battery systems.

The machine was designed to arrive at the orchard towed by a tractor and in fully charged state. Then the operator should position it at the beginning of the first row of trees to start harvesting with all the workers on board. The harvesting movements would be performed after all the workers finish picking the fruit, then the machine should try to move 5 m approx. (length of the vehicle) to achieve next sector with

fruit, then stop, lock the brake, and restart the harvest process, charging the battery systems with photovoltaic energy while the workers are picking the fruit.

The purpose of the first experiment was to identify the minimum time required to recover the energy used in the displacement, expecting this time to be minor to the required harvest time of the slowest worker, so as not to compromise productivity with the new semi-automated process. The experiment was performed on street Los Orfebres, which has an orientation North-South with an inclination of 1° going up in north direction. The street was paved, with 135 m length and the samples were divided into four different series of sub-experiments.

a) Harvesting vehicle prototype testing

b) DAQ system onboard

Figure 1-34: Testing on street Los Orfebres.

The result of the first complete experiment shown that the energy used in each displacement was minimum, in many cases the SOC didn't change from 100%, and in the worst case, it dropped just until 98.8% (see Figure 2-7). For this reason, it was necessary to analyze different parameters to identify the behavior.

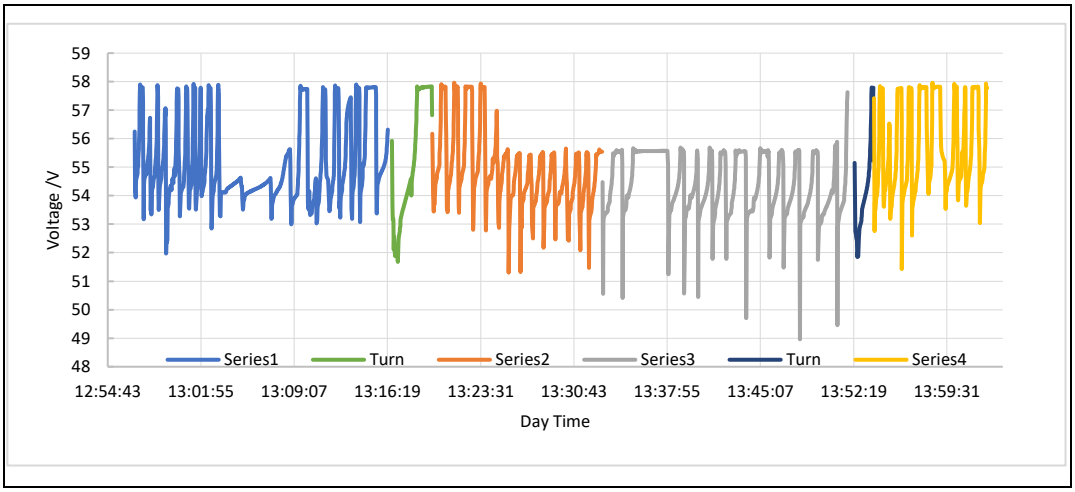

Figure 1-35: Traction 48 V battery voltage.

The voltage of the battery neither is a proper parameter because when each displacement was performed the voltage dropped down more than the real SOC (see Figure 1-35), presenting a delay to recover itself after discharge and reach finally the actual voltage level where it was left. For this reason, when the MPPT was charging the batteries was almost impossible to know the exact charged state of the system.

For the other hand, the current through the battery (see Figure 1-36) and the consumed energy (see Figure 2-8) showed consistent information of each series, level of charging, current, energy used, and energy recovered in all the experiment. Despite this, all the series were mixed and so the groups, turning challenging to identify the timing and series characteristics. Also, the main energy drops observed as down peaks in the consumed energy graph correspond to 180° turning movement performed to change orientation in the street.

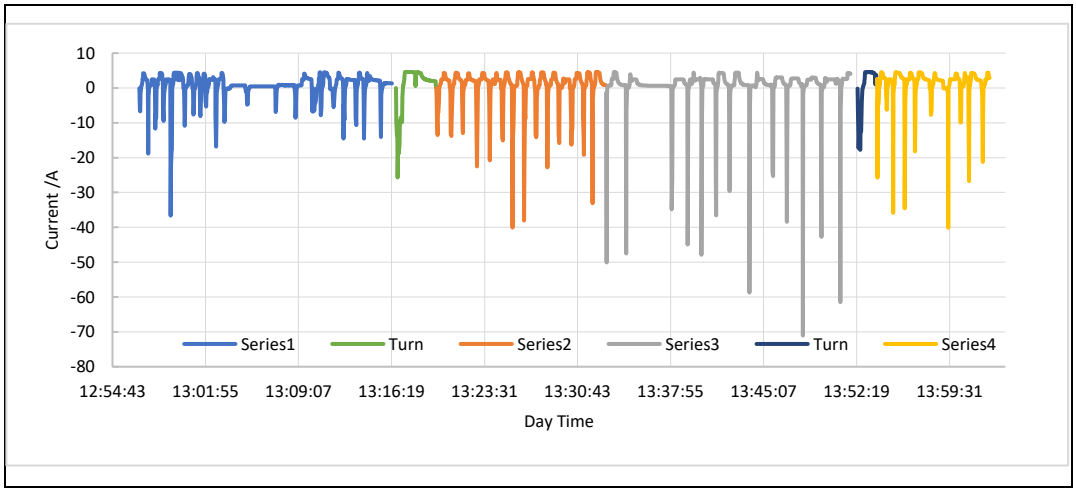

Figure 1-36: Traction 48 V battery current.

In order to have a zoomed view per simulated harvesting movement, a set of macros were created to split data individually (See Appendix). The results are shown in Figure 1-37.

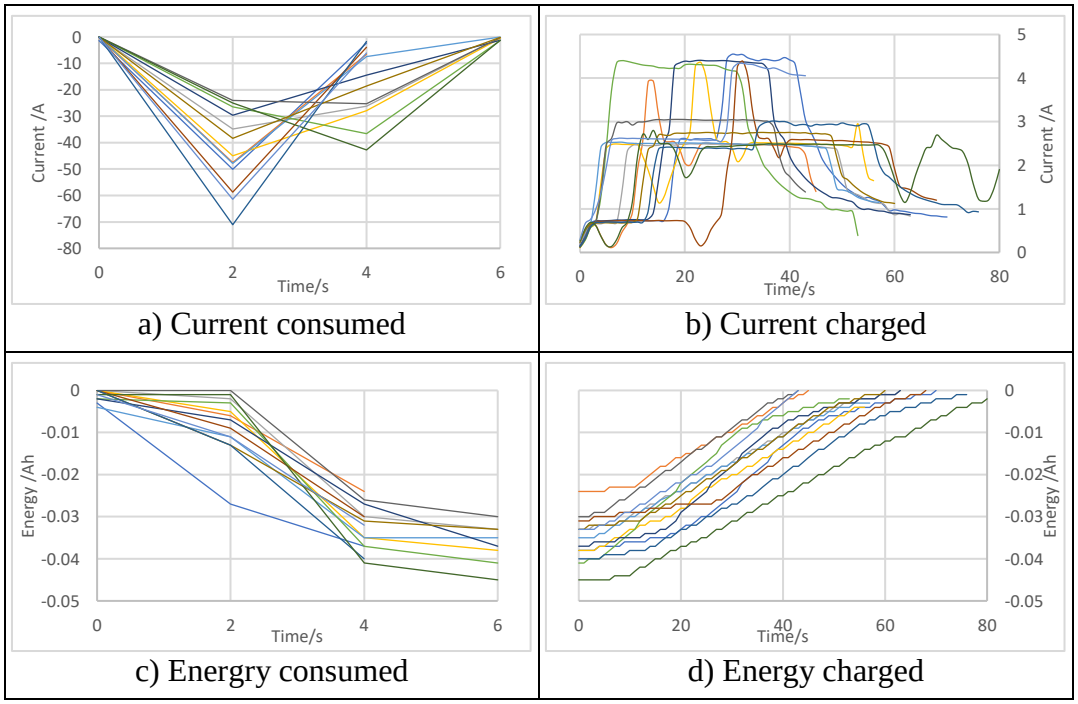

Figure 1-37: Samples isolation from series 3 in simulated harvesting movements.

The graphs showed that the results are consistent with the series. The first graph up-left (a) shows the peak current in the motor due to the fast movement from rest. The differences in the series are because to the different levels of quick acceleration (foot accuracy), and the short duration of the movements in combination with the low sample rate produce a low resolution in the observation process. These results are contrasted with the theoretical being the necessary displacement time less than the one calculated (7.14 s). The second graph up-right (b) shows the current supplied from the MPPT to the batteries. The significant differences in the consistency are because of the alternating modes in the MPPT, the cloud conditions and the better resolution due to the longer time of the charging process, what means more data points. The difference observed between the series are explained because when the machine is in motion, the MPPT is in float mode, disconnected from the batteries and avoiding the risk of overcurrent itself. Then, when the battery is connected again, it takes some time to get out from float mode and enter into bulk charging mode. That is the reason why current levels are so marked in steps. Technically, batteries should be able to charge faster than 60 seconds, because current available with actual solar condition of the region and technical features of the PVs used is 4.5A, as the peaks in the graph show, but configuration of reaction time of the MPPT makes it deliver an average current of 2.19A, which is less than the half available. The third graph down-left (c) shows energy consumed after the forward movement, and the differences in the slopes are because of the different level of fast acceleration mentioned before. The values are entirely consistent and validate the theoretical results (0.05Ah). The fourth and last graph down-right (d) shows the energy recharged and the time needed for the battery to be recovered. The slope is consistent in all the cases, and this is because of the notorious configuration time and current from the MPPT.

The rest of the main findings are shown in the respective section of the article.

1.6 Contribution

It was expected that, as the workers harvest in their sector, the batteries would be able to fully recover the energy consumed during the forward movement to the next fruit sector. An equilibrium between energy consumed and power returned was expected, less than the necessary time to harvest the available fruit in the assigned area. The results were higher energy charge curves than discharge ones only constrained to the worker's picking fruit time.

The scientific contribution of this thesis is as the concept of heavy-load transport vehicle working exclusively with photovoltaic solar energy was probed, further innovations in new vehicles can start to integrate photovoltaic panels in their designs to power traction and other high demanding energy systems instead of only auxiliary systems, reducing its carbon footprint.

In addition, here was probed the feasibility of a semi-automated harvesting machine to perform primary functions of the fruit picking process, having desirables harvest production in nectarines and sweet cherry orchards.

Additional contributions include:

- Improving working conditions in the harvesting processes reducing the demand for physical effort.
- Empowering people's selectivity skills and delicate handling of fruit in the harvesting process, reducing the amount of work and distraction associated, allowing higher incomes due to increases in productivity.
- Reducing the labor gender gap between men and women in jobs of high physical exigency, specifically in the fruit picking processes of selection.
- Increasing the limit age of labor usefulness for women and men in jobs of high physical exigency, specifically in the fruit picking process of selection.

- Reducing the carbon footprint of Chilean exported fruit to improve competitiveness in international markets through the replacement of internal combustion machinery in the harvesting processes by solar charging electric machinery.
- Reducing of chemicals needs in harvesting automated process by offering an alternative to better profitability than the manual harvesting process.
- Reducing of the need for genetically modified characteristics in the fruit to make it more resistant to damages caused by the automated harvesting processes.
- Proof of applied circular economy product design.

1.7 Further Research

The traction and electric steering characteristics of the harvesting vehicle give it the ability to be controlled remotely. Even with the remote installation of position sensors, accelerometers, distance sensors or stereo cameras, it is possible to develop an autonomous harvesting vehicle with the proper software design. The importance of this upgrade is highly desired since during the working trials it was identified a positive correlation between productivity and the pressure of a limited harvesting stop time. This dictates the steps to be taken with crop optimization software that allows the vehicle to know the harvest rate in real time and determine the optimal stopping times automatically for further productivity research.

During the test performed it was identified the necessity of a new harvesting process design. The actual one is based on the payment for productivity, where the advantages are the increase of production but at the expense of higher control cost, management, and more complexity. It works individually, means that productivity of each worker depends on personal motivation and physical resistance. Whit the new harvesting vehicle, the paradigm change because when one of the fastest workers finishes harvesting his assigned sector in the platform, he has to wait until the rest of his colleague end in order the platform can move to the next section of trees, or in the meantime begin harvesting in a sector that is assigned to another person. This dictates the change, maybe to a team productivity

payment or something mixed, that overpass the externalities of workers that take advantages of the team.

On the other hand, being a fully electric vehicle, it is possible to install an inverter to the battery system and use all kinds of tools or devices, so it is expected that in the following research will develop this type of improvements and test its influence in performance and productivity.

Furthermore, the redesign of the orchards in conjunction with the vehicles is highly conducive to increased productivity.

For the other hand, the contribution of this works leads to validate the concept of industrial electrical machinery in agriculture, opening the road to designing further solutions in agriculture reducing carbon footprint. The concept even can be expanded to other industries, making use of the photovoltaic solar energy in vehicles of heavy load transport used for outdoor intermittently, as mining trucks and others.

2. FULLY SOLAR POWERED ELECTRIC VEHICLE FOR HARVESTING FRESH MARKET FRUITS

2.1 Introduction

Chile is one of the largest exporters of fresh fruit in the southern hemisphere with species such as nectarines (Prunus Persica L.) and sweet cherry (Prunus Avium L.) (Alcaino et al., 2014; "Precios, comercio exterior y fichas de fruta frescas exportada," 2017). Nominal exports of fresh fruit have grown steadily in the last two decades, especially to Asia, which now comprises the most important markets for Chilean fruit (Schmidt-Hebbel, 2015). Fresh fruit must reach distant export markets in good condition to ensure customer acceptance. In the case of sweet cherry, most postharvest defects are consequence of bruising so that harvest must be carried out by hand with extreme care and diligence (Param & Zoffoli, 2016).

Between 25% and 29% of regional employment in Chile is associated to agriculture, being the third largest national economic sector in terms of jobs occupation ("Mejora el mercado laboral y crece el empleo agrícola," 2016). However, reduced harvest efficiency, shortage of labor, carbon footprint, and inadequate manipulation in harvesting fresh market fruits produced in Chile and exported to far away markets are current limitations to maintain its competitiveness.

Sweet cherry fruit is harvested mainly by "hand picking" because of careful handling requirements to preserve quality until reaching export markets. In most commercial orchards, ladders exceeding 3 meters in height are used, as shown in Figure 2-1. As a consequence, fruit removal is highly inefficient and physically demanding due to ladder climbing, repositioning, and bucket delivery along and between rows. Hand picking represents 46% of the total cost of the complete production process of cherries ("Ficha técnica de cerezo lapins," 2015; Shepardson et al., 1970; Shiigi et al., 2008).

Several systems have been proposed to increase labor efficiency in commercial orchards (Li et al., 2011; Smith & Whiting, 2007) including shaker solutions (Peterson, Whiting, & Wolford, 2003; Shepardson et al., 1970), fully automated solutions (Qingchun, Xiu,

Wengang, Quan, & Kai, 2012; Shiigi et al., 2008), and moving platforms. Shakers tend to induce bruises that become visible in long distant travels before reaching destination markets. To increase harvesting rates, some chemicals (e.g., growth regulators) are commonly used to reduce the fruit retention force (Larbi & Karkee, 2014; Peterson et al., 2003). The productivity of shakers is still less than that of humans (Li et al., 2011; Peterson et al., 2003; Peterson & Wolford, 2001; Qingchun et al., 2012) and in many cases cause significant damage to the tree (Snell, 2008).

Figure 2-1: Conventional sweet cherry harvesting process in Coltauco, Chile.

Robotic solutions are not yet fully developed in Chile. To date, there is no fully automated process combining the human selectivity capacity and productivity for stone fruit harvest,

considering fully automated solutions as a combination of state of the art sensing technology (Bechar & Vigneault, 2016; Fernández, Salinas, Montes, & Sarria, 2014). However this is a promising field, and significant advances in terms of navigation of mobile platforms in irregular terrain has been achieved to foresee applications in the future (Howard & Kelly, 2005; Rogers-Marcovitz, Seegmiller, & and A. Kelly, 2012; Seegmiller & Kelly, 2013). Some growers have attempted to use imported semi-automated harvesting machinery (e.g., platforms), which reduce physical effort and inefficiency, but the investment is high, and the designs are not optimally suited to Chilean orchards. Generally, in platforms, the primary source of energy comes from internal combustion engines. Mechanical limb shaker systems in sweet cherry harvest have shown a wide range of harvesting rates, from 12 trees/h in a 55° Y-trellis configuration of Skeena variety without chemical treatment, to 158 trees/h in a 45°-60° Y-trellis configuration of Bing variety with an abscission chemical compound (Larbi & Karkee, 2014). Orchard characteristics, such as the training system, tree spacing on the row, space between rows and row length, play a special role in mechanical cherries harvesting rate. In consequence, orchards must be designed with a specific harvesting machine technology in mind to achieve maximum labor efficiency.

Most of current agricultural machines still rely in fossil fuel consumption. Fuel expenditures are high and induce undesired environmental and health effects. However, considering electric vehicles (EV) as a more ecological alternative, the overall efficiency of a traditional grid-based EV, including the 33% efficiency of an average thermoelectric power plant (original source of energy), ends up in a final efficiency of 23%, which is not meaningfully higher than the approximate 20% efficiency of an internal combustion engine (Kim, Baek, Hong, & Chang, 2014). Hence, the environmental impact of EVs is strongly related to the source of the electricity, improving considerably when the primary source is renewable energy (Bhatti, Salam, Aziz, & Yee, 2016).

The most promising alternative in terms of cost and efficiency is photovoltaic (PV). The two most feasible approaches up to date on charging techniques for EVs are the combination of PV-grid, and/or PV-standalone charging stations (Bhatti et al., 2016),

which are better than PV panels on the roof. There are EV such as solar competition vehicles, that are highly aerodynamic, light, and efficient that can run solely on PV energy, but their industrial use is very limited (Kim et al., 2014; Letendre, 2009). In normal cities or commuter use, even the lightest EVs need a charging station for adequate energy management (Azidin & Hannan, 2012; Louie, 2015). The main problem for EV with autonomous recharging is the reduced surface of the vehicles (Bhatti et al., 2016; Nguyen, Kim, Lee, & Choi, 2013). Heavy load EVs, exclusively powered by PV arrays have not been used for agricultural applications as far as our knowledge.

Considering all the above, the objective of this research was to validate the hypothesis that a fully solar powered vehicle for harvesting hand-picked fresh fruit can operate adequately in terms of energy self-reliance and, at the same time, improve labor efficiency by reducing physical effort and decreasing downtimes. To achieve this, a design of the vehicle and its main systems is proposed, built, and tested in real harvesting conditions. A protocol for measurement and analysis of current and voltage is implemented for testing purpose. Since fossil fuels are not used, the carbon footprint of the fruit is reduced. Initially, the vehicle was designed for sweet cherry harvesting, but it was also validated in a nectarine orchard with minor adjustments.

2.2 Materials and Methods

Stone fruit orchards in Chile have a wide variety of configurations. These differences are mainly because of phenotype variation between different fruit tree species used, but also between orchards of the same specie due to tree design, where owners try to optimize the productive space and the harvest process itself with different techniques. Hence, the flexibility of the vehicle for working in different orchards is a design issue, as it needs to adapt to different types of fruit in order to be a wide general solution.

Listed in Table 2-1 are two types of fruit orchards where the platform was tested, which were selected due to their similarities in dimensions, as well as for the conventional picking process using ladders and individual baskets.

Table 2-1: Characteristics of tested orchards in Chile

Characteristic	Cherries Orchard Value	Nectarines Orchard Value
Width of aisles w/m	3.5	3.0
Height of trees h/m	3.0	3.2
Tree configuration	V-trellis	Central axis
Length of Aisles l/m	150	200

Both types of orchards were quite similar in terms of width and height of the trees. The differences were mainly in the tree configuration, where sweet cherry trees had a more triangular shape leaving significant fruit voids between trees, while nectarines had a more squared shape leaving a denser harvesting wall with fruit. Traditional harvesting process of both species have different efficiency in terms of hand labor productivity, due to different concentration of fruit per tree, delicacy in handling, and fruit size, which makes the comparison between the species qualitatively different.

2.2.1 Solar Vehicle Design

The vehicle uses solar panels to capture enough energy to sustain consumption, thus preserving the charge in a bank of batteries. The intermittent harvest cycle lends very favorably to this purpose, as will be explained. The batteries feed power to a traction BLDC electric motor, steering actuators, and as well as automated mechanisms to handle the fruit on the platform. Efficiency is further enhanced by using BLDC motors with dynamic braking, so that braking energy is returned to the batteries instead of being dissipated as heat. A PLC coordinates all internal systems. Table 2 2 summarizes design requirements and specifications, defined after extensive interviews with workers and growers, including field observation during harvesting process. These requirements lead a design solution proposal whose main features are shown in Table 2 3.

Table 2-2: List of requirements for a cherry/nectarine harvesting vehicle.

Module	Requirements
Chassis	• At least 2500 kg total weight capacity • Trade-off between chassis length and turning capability • Ability to make small radius turns • Possibility of mounting different platform designs
Traction and Steering	• Slow speed and high torque • 4-wheel steering • Adjustable speed and power • Strong and safe braking
Platform	• Adjustable in width • Adjustable in height reach • Comfortable for workers • Safe • Easy access to electronics components • Interchangeable
Electronics	• Well organized cabling • Easy monitoring and diagnostics
Photovoltaic Panels	• Easy to remove • Easy to clean • Adjustable in height • Easy to connect/disconnect
Safety	• Adjustable safety rails for workers • Foods, water, and personal belonging carrying capacity • Ergonomic

Table 2-3: Main characteristics of solar harvesting vehicle

Item	Value
Weight w/kg	975
Platform Length L_0/mm	4,026
Platform Length with lift L_e/mm	6,068
Adjustable Platform Width P_l/mm	2,010-3,500
Platform base height P_b/mm	1,220
Traction	Electric
Primary Energy Source	Solar Photovoltaic
Electric motor	BLDC 5 kW
Solar Panels	8×PVs, 750 W total
Batteries	8×deep cycle flooded, 12 V, 90 Ah
Wheel size diameter W/in	31
Maximum Velocity V_{max}/km·h^{-1}	9.66
Working autonomy in fruit harvesting	Unlimited
Continuous trajectory autonomy A/km	10.16

a) Main System: Drivetrain

The traction requirements were solved by a 5 kW BLDC motor, a 1:10 helicoidal gear reduction, and a light truck gearbox, all connected in series to the axle differential, as shown in Figure 2-2. This kinematic chain gives a range of reduction from 1:44 in third gear to 1:117 in first gear, with a range of speeds from 9.66 km/h to 2.52 km/h respectively. Final torque in the wheels ranges from of 1,056 Nm to 2,808 Nm at 2000 rpm, with an estimated efficiency of 72% ("Motor HPM48 5000W curve of power," 2016).

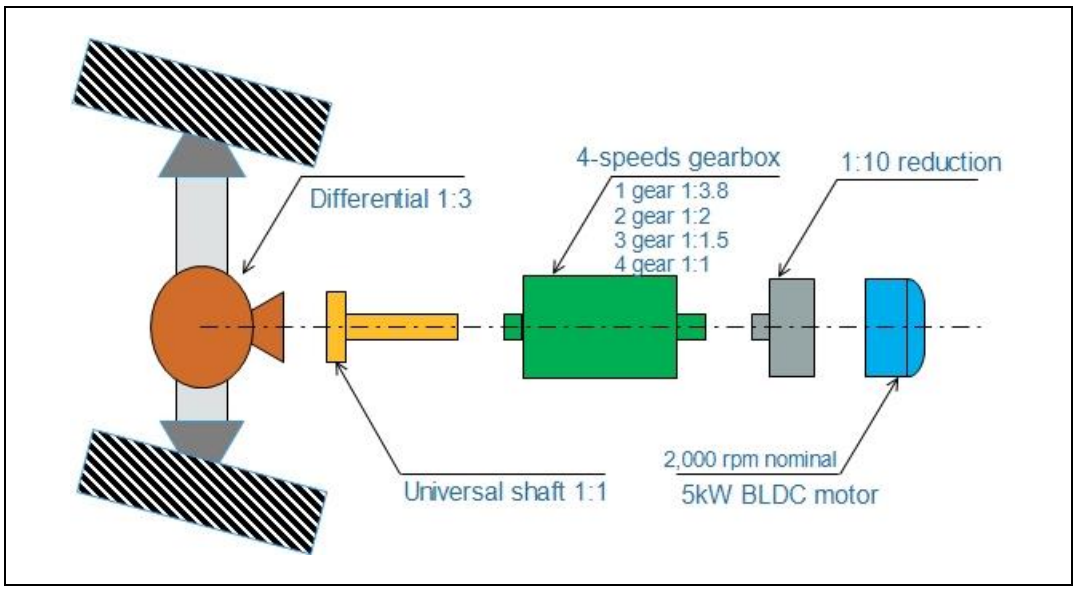

Figure 2-2: Details of 48V traction system components connected in series.

b) Steering System

The vehicle had a 4-wheel steering (4WS) drive system that was crucial for turning in short spaces, as shown in Figure 2-3. Authors have reported that a 4WS vehicle allows reducing a normal turning radius to about half of a 2 wheel steering (2WS) (Lohith et al., 2013). Passing from the end of a row to the beginning of a parallel one is a complicated maneuver, considering that the separation between orchard rows is narrow varying between 3.5 m to 5.0 m so little space is left unused at the orchard borders, given the high prices of the premium orchard land.

Linear electric actuators commanded by joystick via PLC were used to steer the vehicle. This facilitated control and simultaneous coordination of front and rear axle in terms of both traction as well as steering. The maximum steering force required for orchard maneuvers was estimated in 4.2 kN. The chosen linear actuators had a nominal speed of 17 mm/s, which is adequate to safely complete turns at the maximum speed of the vehicle (10 km/h).

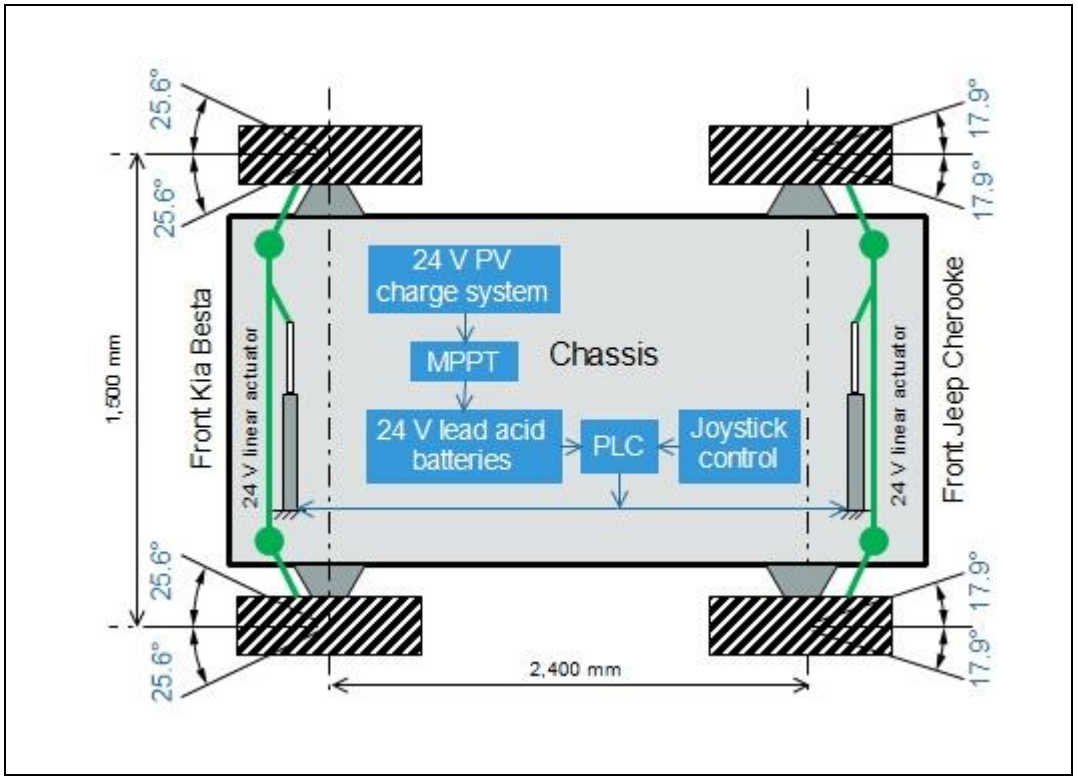

Figure 2-3: Details of 24V steering system components connected.

c) Energy System

The battery bank for energy storage consisted in 8 batteries of 12 V and 90 Ah each. One group of 4 batteries connected in series was used for the traction system that worked nominally at 48 V. Two batteries were used in the 24 V steering system. The two remaining batteries were used for PLC, sensors, data acquisition, alarms, and other miscellaneous tasks.

An array of 8 solar panels was mounted on the vehicle as shown in Figure 2-4. The surface of each panel was 1.2 m x 0.55 m, delivering 85 Watts at 12 V nominally. Four solar panels in series deliver energy to the 48 V traction system, two panels in serie are for powering the 24 V steering system with the PLC, and two panels in parallel deliver energy to the bin 12 V lifting system and miscellaneous auxiliary systems. Each system was managed by an MPPT to optimize battery charge.

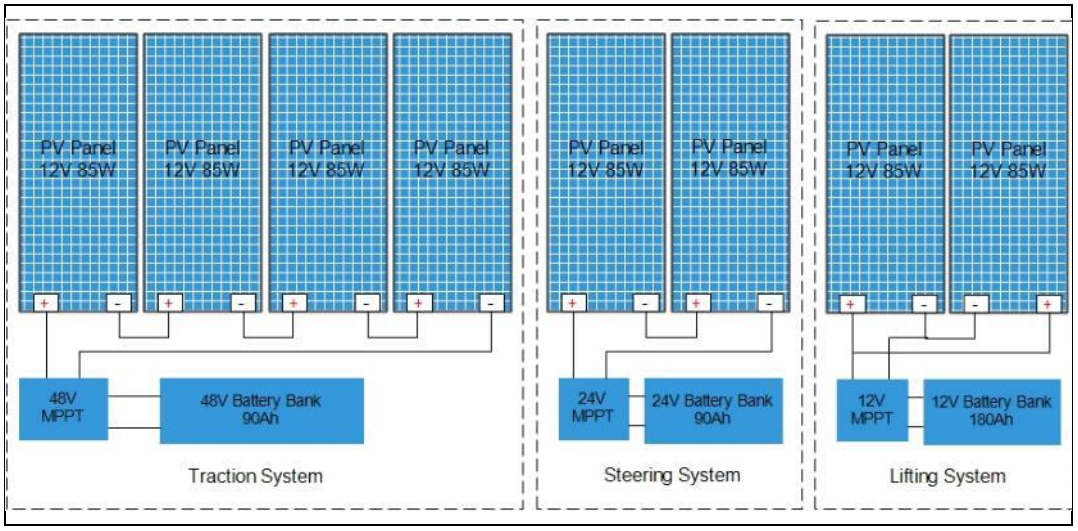

Figure 2-4: Diagram of the 8 PV solar panels mounted on the vehicle's roof.

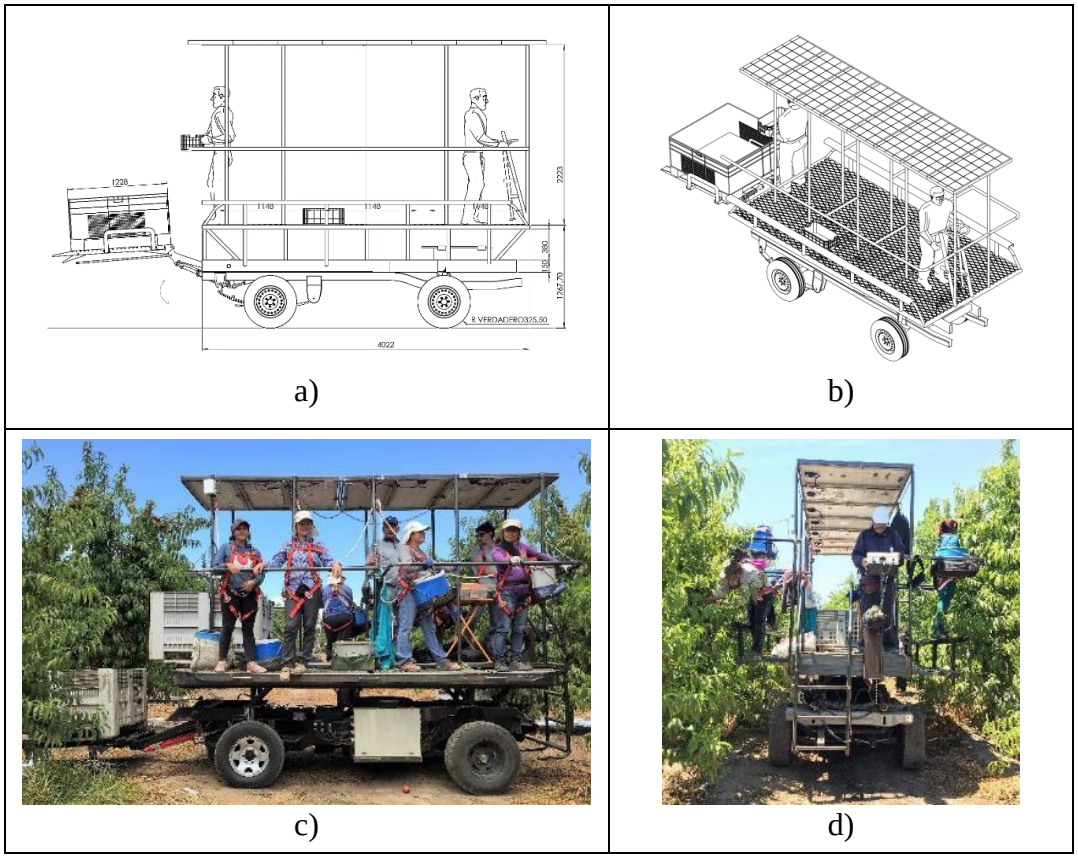

Figure 2-5: Schematics and images of the solar powered harvesting vehicle.

2.2.2 Test Descriptions

A set of four experiments was designed to ascertain the viability of the vehicle to operate exclusively on solar energy with an adequate harvesting productivity. Descriptions are given in Table 2-4 and Table 2-5.

Table 2-4: Set of experiments, abbreviation and description

Measurement Type	Description
Work Cycles Normal Operation (WCNO)	Harvesting unit cycles were carried out with battery charging
Continuous Trajectory Without Recharging (CTWR)	Measurement of maximum travel distance on batteries alone
Static Battery Recharging (SBR)	Charge of batteries while the vehicle is at rest without use
Work Cycle Without Recharging (WCWR)	Measurement of discharge rate and maximum battery duration

Results of complete sets of experiments in three different occasions (see Table 2-5) are presented in this article.

Table 2-5: Test Days Reported

Test	Date	Location
Harvesting Simulation on Street (HSS)	September 2016	Street Los Orfebres, La Reina, Santiago de Chile
Field Harvesting Day 1 (HD1)	January 9, 2017	Nectarines Orchard in Coltauco, Rancagua, Chile
Field Harvesting Day 2 (HD2)	January 16, 2017	Nectarines Orchard in Coltauco, Rancagua, Chile

A battery monitoring system (Blue Solar Battery Monitor Model 702) was used to register 4 main variables in the Traction, Steering, and Lift system: State of Charge (SOC%), Voltage (V), Current (A), and Consumed Energy (Ah). Measurements were done at a frequency of 1 Sample/second (S/s). GPS data was also collected to measure distances and slopes. By convention, negative values correspond to batteries in consumption mode while positive values correspond to batteries in charging mode.

Previous to actual harvesting, HSS tests were carried out on a selected road emulating working conditions in the orchard, taking samples in a more controlled way to assess energy consumption system performance. Experiments were more comprehensive in terms of system performance in lieu of measuring fruit harvesting productivity.

2.2.3 HSS Special Aspects

a) Working Cycle Normal Operation (HSS_WCNO)

The purpose here was to measure the minimum time required to recover the energy used in the displacement phase of the work cycle, expecting this time to be much less than the harvesting time interval at that position, thus not compromising productivity. The measurements were performed on a short street in Santiago with a North-South orientation with an inclination of 2.62% in the north direction. Energy consumption and battery capacity were measured in working cycles emulating actual harvesting, where the vehicle moved forward 5 meters, and then stayed 2-3 minutes at rest, while workers were supposed to be harvesting. A paved street stretch of 135 m in length was used. The experiment was divided in 4 groups of cycles, where each of them had different characteristics shown in Table 2-6 and Table 2-7. Each cycle begins with a forward displacement, followed by a stop during which the batteries can be recharged, but with different characteristic between them Figure 2 6 shows a graphical spatial orientation of this cycles.

Table 2-6: HSS_WCNO experiment series of measurements

Series	Begin	End	Time	Cycles
1	12:56	13:16	0:19	16
2	13:19	13:32	0:13	14
3	13:32	13:51	0:18	13
4	13:53	14:02	0:08	10

Table 2-7: HSS_WCNO experiment description

Series	Total dist./m	Dist. sample/m	Direction	Pace
1	75	5 ±0.5	South (down)	Normal
2	75	5 ±0.5	North (up)	Normal
3	60	5 ±1.0	North (up)	As fast as possible
4	60	5 ±1.0	South (down)	As fast as possible

Figure 2-6: Aerial view of street Los Orfebres, 135 m length (North is represented by the compass's red arrow).

b) Continuous Trajectories Without Recharging (HSS_CTWR)

The purpose here was to determine the maximum distance the vehicle would be able to run without recharging. Consumption and discharge rate were measured in continuous trajectories from 100% SOC to 80% SOC, with 7 people on board and running around a large block in the industrial park of street Los Orfebres until reaching 80% SOC, always making a right at the end of each street end. The people on board amounted to a weight load of 500 kg.

c) Static Battery Recharging (HSS_SBR)

The purpose was to get an estimation of the required time to charge the batteries from 80% to full SOC, in cloudy conditions and early in the day, both unfavorable circumstances representing a worst-case scenario at the orchard. The measurement was performed at the middle of street Los Orfebres with the vehicle parked at rest, charging the battery from 80% up to 100% SOC.

2.3 Results and Discussion

2.3.1 Harvesting Simulation Street Test (HSS)

a) Working Cycles (HSS_WCNO) Evaluation

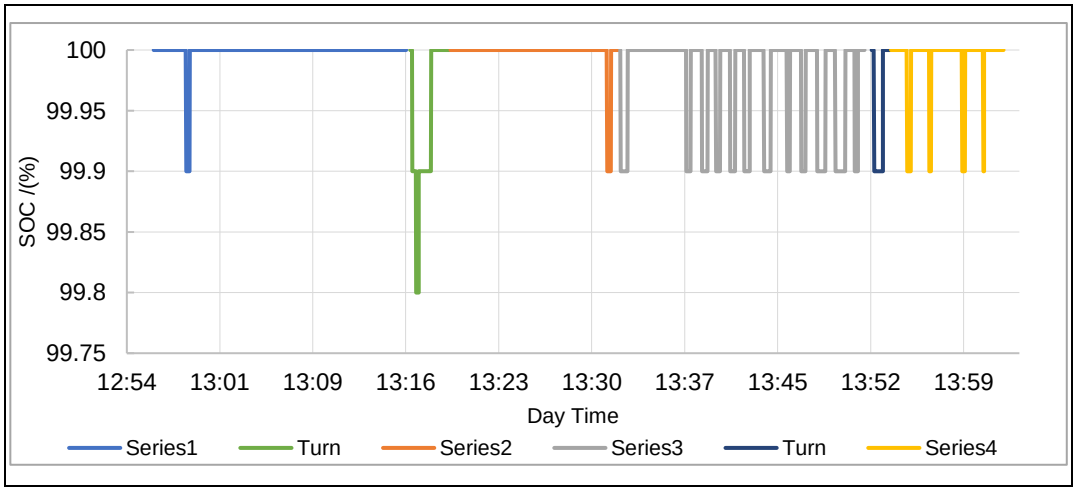

Figure 2-7: SOC in the 48 V, 90 Ah battery banks in experiment HSS_WCNO.

This experiment was conducted during the morning on September 27, 2016. As expected, energy expenditure in each displacement was small as seen in Figure 2-7. At most, in a single cycle, the SOC dropped only to 98.80%. Lead acid battery need to be charged in bulk mode at 2.47 Volts-per-cell (VPC). Then, a 12 V battery in bulk mode is charged at 14.80 V, which in our 48 V system means a charging voltage of 59.20 V ("Trojan battery user's guide," 2012).

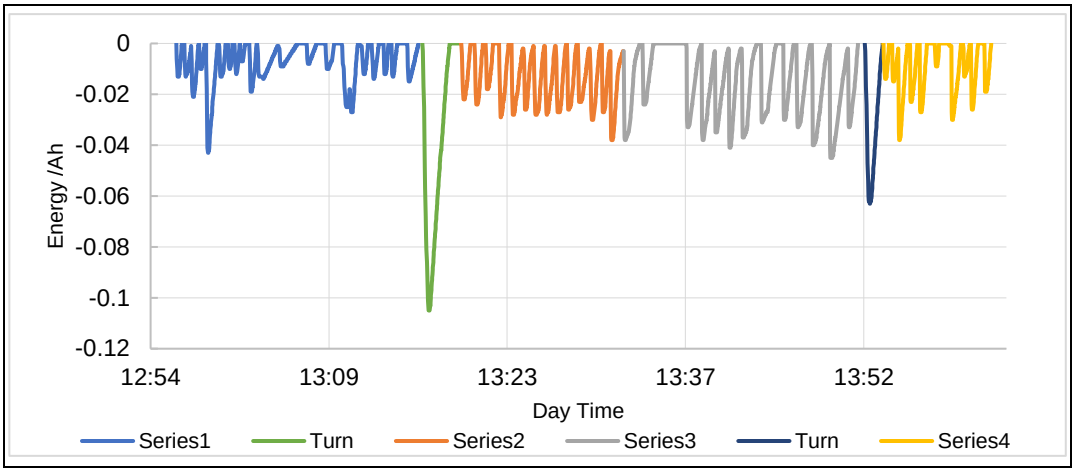

Figure 2-8: Energy Consumption (Ah) in traction system in HSS_WCNO.

Figure 2-8 shows the same motions than Figure 2-7 but in energy terms. The highest consumption occurs in 180 degrees U turns. The results in energy consumption mode are shown in Table 2-8 and in recharging mode in Table 2-9.

Table 2-8: Forward motion mode averages in experiment HSS_WCNO

Series Consumption Data	Avg time/s	I mean/A	Ipeak mean/A	ΔCE mean/Ah
1	8	-4.31	-10.70	-0.012
2	9	-8.60	-21.29	-0.024
3	5	-17.14	-45.32	-0.030
4	6	-7.31	-22.65	-0.020

Table 2-9: Charging mode averages in experiment HSS_WCNO

Series Charge Data	Avg time/s	I mean/A	Ipeak mean/A	ΔCE mean/Ah
1	22	2.33	3.56	0.014
2	37	2.58	4.29	0.026
3	60	2.19	3.6	0.034
4	28	2.79	4.18	0.021

The most demanding experiment series was group 3 (Table 2-8) because the 5 m forward motions were carried out in an upward slope and as fast as possible as shown in Table 2-5. In this case, the forward displacement took only 5 s on average, and the mean current was -17.14 A, with a peak of -45.32 A. In these most demanding load conditions, the required recharging recovery time was only 60 seconds on average, with a mean charge current of 2.19A (Table 2-9). The energy consumption in each cycle was between 0.030-0.034 Ah on average. Hence under the solar conditions of the day and at maximum load condition (i.e., worst case scenario), if the picking time interval in the orchard is longer than 60 seconds in average, it can be expected that the moving platform can preserve the battery bank charged indefinitely.

b) Continuous Trajectories Without Recharging (HSS_CTWR)

This experiment was conducted during the afternoon on September 27, 2016. The vehicle completed over 2.5 loops around the block before reaching 80% SOC. The results are shown in Table 2-10.

Table 2-10: Result of experiment HSS_CTWR

Parameter	Value measured	Extrapolation to ΔSOC 80%
ΔSOC	20%	80%
ΔEnergy/Ah	10.293	41.172
Time	20:44	1:22:56
Total distance covered/km	2.54	10.16

The results show that at maximum speed in a road of mild slope characteristics, the vehicle would run 12.7 km using 80% of its SOC, in less than 1.5 h at an average speed of 7.35 km/h. This is possible because deep cycle flooded batteries can be discharged down to 20% SOC without suffering permanent damage ("Trojan battery user's guide," 2012) allowing the vehicle to use almost all of its battery capacity.

Different levels of current consumption were observed during this test. In streets with negative downward slope, average current consumption was -10.81 A, while in streets with positive upward slope, average current increased to -50.13 A. In straight flat terrain, the autonomy range distance should increase substantially.

One of the main disadvantages of a solar machine is that the photovoltaic energy availability is weather dependent. A cloudy day renders less energy and thus more charging time is required than in a sunny day. In this experiment, a distance up to 12.7 km could be covered without recharging. The normal distance covered daily by the vehicle during actual harvesting would be in the order of 1-2 km at most, as the global positioning system (GPS) data showed during the tests.

c) Static Charging (HSS_SBR) Evaluation

This experiment was conducted on September 29, 2016. The day started with a cloudy morning but cleared around 13:50 as shown in Figure 2-9.

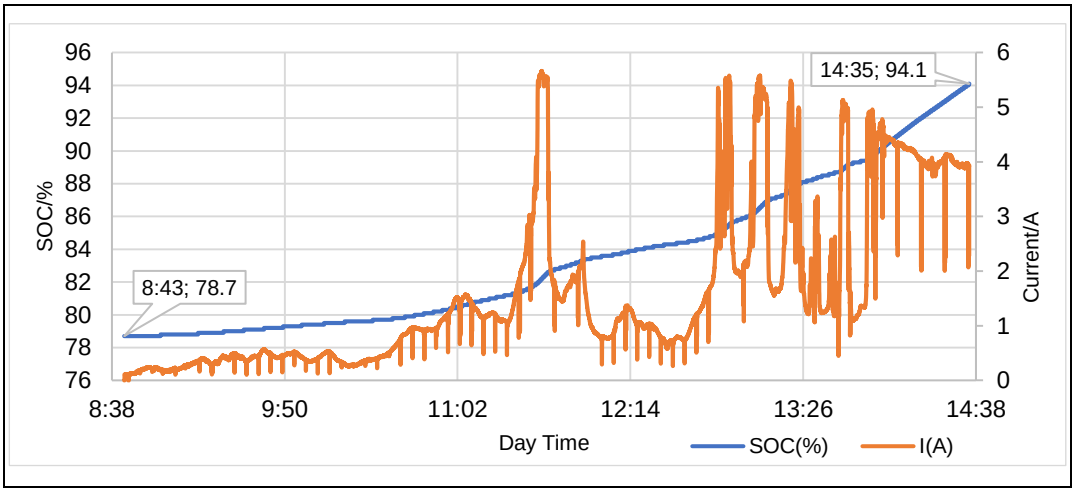

Figure 2-9: Energy recovery and charging current in the 48 V, 90 Ah system in a cloudy morning day in Santiago, Chile. Experiment HSS_SBR.

The available solar energy peaked around 11:37, time coinciding with the sky clearing up. The charging current then reached 5.6 A. When clouds covered the sky again; the charging current dropped abruptly to less than 2 A. That day the sky was not completely clear until 13:53. Under these conditions, the battery bank charged from 78.7% to 94.1% SOC in 6 h (Fig 9).

Clear days are expected in summer during the harvesting season in the geographic area with high density sweet cherry and nectarine orchards located in the surroundings of Coltauco, Rancagua, Chile (Latitude -34.248556°, Longitude -71.047878°). Previous test results showed that a charging current of at least 4-5 A can be expected, allowing to charge the batteries from 80% to 100% in less than 3 h. Charging conditions achievable with a full clear sky during this tests in La Reina, Santiago, in a spring day, are shown in Figure 2-10.

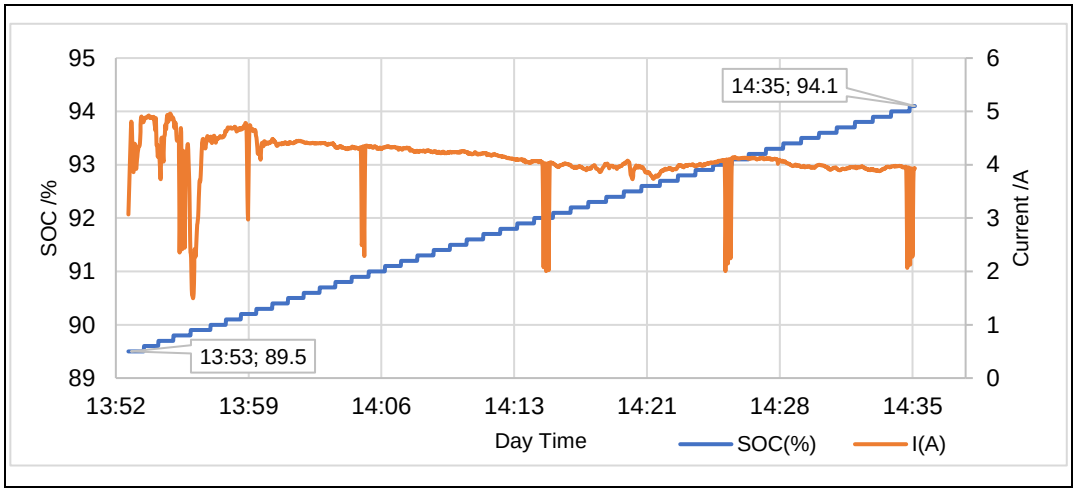

Figure 2-10: Energy recovery and charging current for the 48 V, 90 Ah system in fully sunny conditions in Santiago, Chile (September 2016). Experiment HSS_SBR

Table 2-11: Estimation of charging time in a fully sunny day. Experiment HSS_SBR.

Parameter	Start value	End value	Difference
Data time	13:53:08	14:35:39	42:31
Data SOC	89.5%	94.1%	4.6%
Estimation time	00:00:00	3:04:51	3:04:51
Estimation SOC	80%	100%	80%

2.3.2 Field Harvesting Day Tests

The vehicle worked properly under controlled conditions on a street, and the hypothesis in actual harvesting conditions was tested next in the field. Data collected in two different days of nectarines harvest in Coltauco were selected for reporting here and are reviewed next. The conventional working day started at 8:00 and finished around 17:00, with 1-hour break for lunch, thus totaling an 8-hour working.

a) Preliminary Test in Harvest Day 1

Harvesting without charging the batteries for 50 minutes was first carried out (Experiment HD1_WCWR). Current consumption and SOC are shown Figure 2-11.

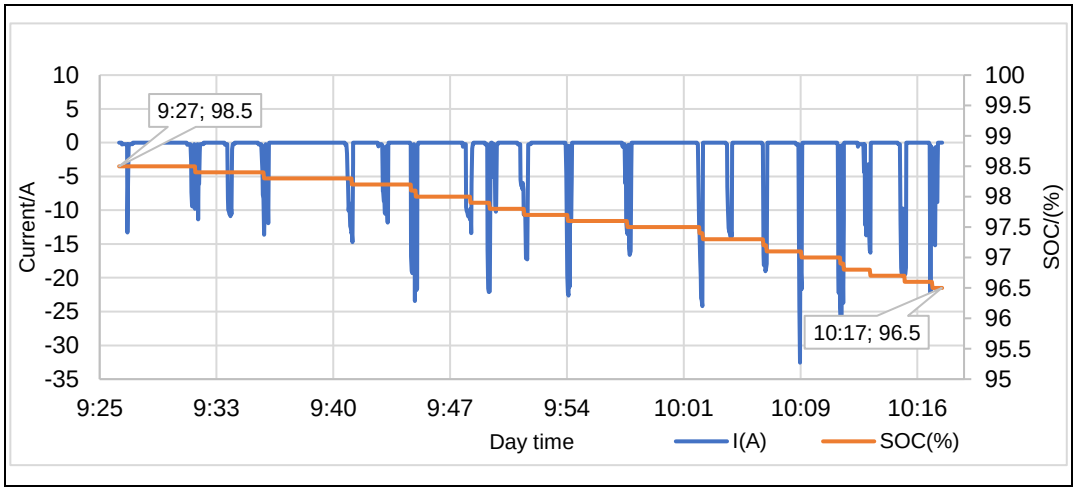

Figure 2-11: Current and SOC for the traction system in experiment HD1_ WCWR.

SOC consumption rate was -2.4%/h, and **Δ**Capacity rate was -1.66 Ah/h, which at 48 V gives a **Δ**Energy rate of -79.49 Wh/h as shown in Table 2-12.

Table 2-12: ΔEnergy during harvest. Experiment HD1_WCWR

ΔTime/min	ΔSOC	ΔCapacity/Ah	ΔEnergy/Wh
50	-2.0%	-1.38	-66.24
60	-2.4%	-1.66	-79.49

Extrapolating the results of Table 2 10 to a complete 8 h working day gives an energy consumption of 635.92 Wh, thus using 19.2% SOC. This means that the vehicle would operate an entire working day without recharging, using less than 20% of its SOC.

During the worker's lunch hour, the batteries were charged without moving the vehicle (Experiment HD1_SBR), recreating the static charging experiment described in section 3.1.3 (HSS_SBR).

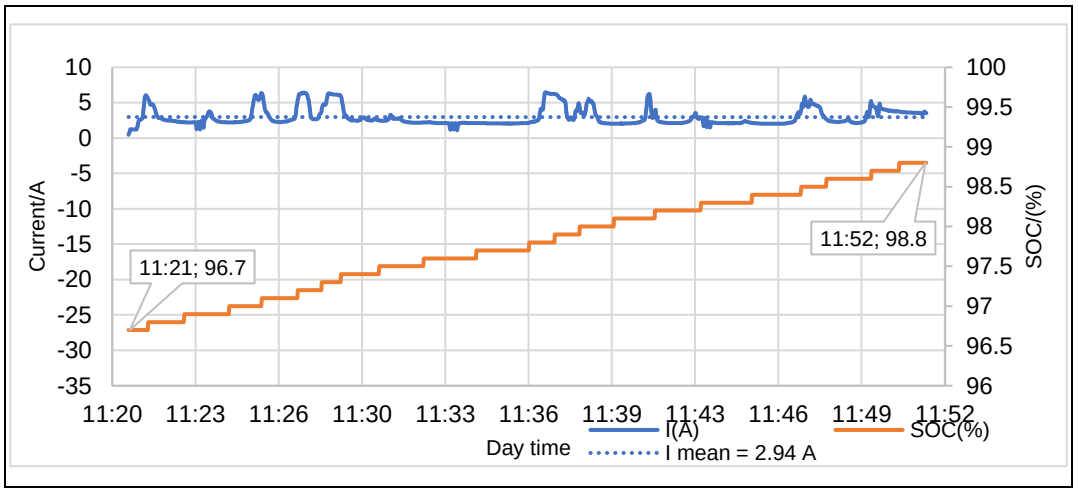

Figure 2-12: HD1_SBR Charge validation experiment for the traction system.

SOC charge rate was 4.1%/h, and ΔCapacity recovery rate was 2.79 Ah/h (Figure 2-12), which at 48V gives a ΔEnergy rate of 133.97 Wh/h, as shown Table 2-13. Interestingly and promising was that energy charge rate was higher than energy consumption (i.e., 133.97 Wh/h versus 79.49 Wh/h). Projecting the values shown in Table 2-13, the expected time to recover from 80% to 100% SOC, would be 4 h and 53 min.

Table 2-13: Estimation of ΔEnergy recovery rate. Experiment HD1_SBR

ΔTime/min	ΔSOC	ΔCapacity/Ah	ΔEnergy/Wh
31	2.1%	1.44	69.22
60	4.1%	2.79	133.97

b) Harvest Day 1 Work Cycles in Normal Operation Experiments (HD1_WCNO)

HD1 testing day started at 9:00 and finished at 14:30, with a one hour lunch break in between, which gave a production harvesting time interval of 4.5 h. However, the effective harvesting time was actually only 3 h, because of adjustments, configuration, and other small problems during this period. In these 3 h, the distance covered was 396 m, and the number of individual harvesting cycles was 90 (including tests described in section 3.2.1), which means 4.4 m forward distance on average.

The rest of the day, experiment HD1_WCNO was carried out in 3 separate groups, and the results are given in Table 2-14, Table 2-15, and Table 2-16.

Table 2-14: Log data of cycle series in experiment HD1_WCNO

Group Series	Begin	End	Time	N samples(S)
1	10:40	11:11	0:30	16
2	13:14	13:39	0:25	16
3	14:01	14:23	0:22	14

Table 2-15: Forward motion cycle averages in experiment HD1_WCNO

Group Motions	Avg time/s	I mean/A	Ipeak mean/A	ΔCE mean/Ah
Series 1	24	-11.48	-21.34	-0.072
Series 2	27	-11.56	-26.32	-0.075
Series 3	23	-8.22	-17.91	-0.049

Table 2-16: Charge cycle averages in experiment HD1_WCNO

Group Charges	Avg time/s	I mean/A	Ipeak mean/A	ΔCE mean/Ah
Series 1	86	2.71	3.89	0.063
Series 2	65	2.89	5.51	0.051
Series 3	72	2.01	3.08	0.044

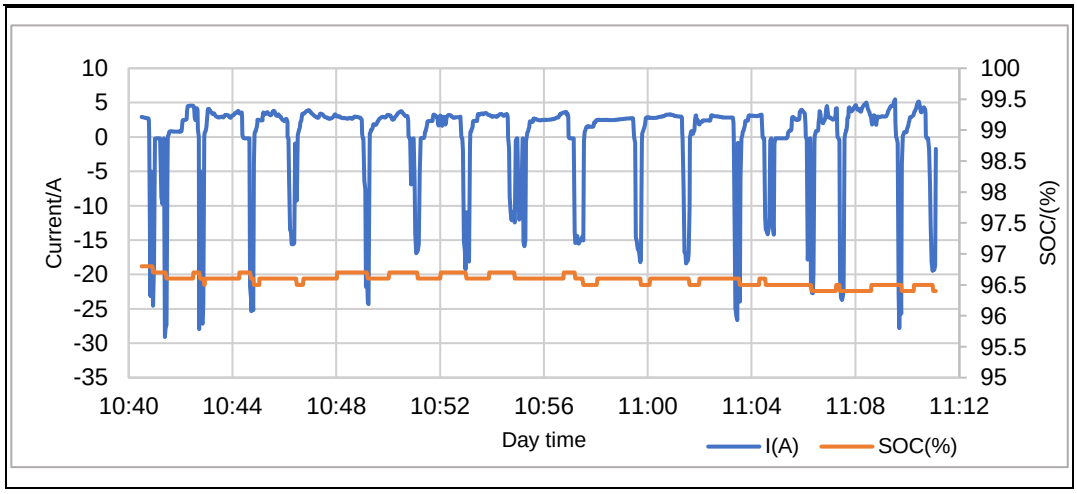

Figure 2-13: Current and SOC in traction system in experiment HD1_WCNO Series1

In Figure 2-13, the SOC is practically constant, which means that energy consumed is completely recovered on every harvesting cycle. Data in Table 2-14, Table 2-15, and Table 2 16 show that average harvesting time (charging mode) per cycle of 4.4 m long was 74.4 s, with an average charging current of 2.6 A, while average forward moving time per cycle (consumption mode) was 24.7 s with an average current consumption of -10.5 A.

The 24 V Steering System was monitored in paralell. Figure 2 14 shows the recorded voltage.

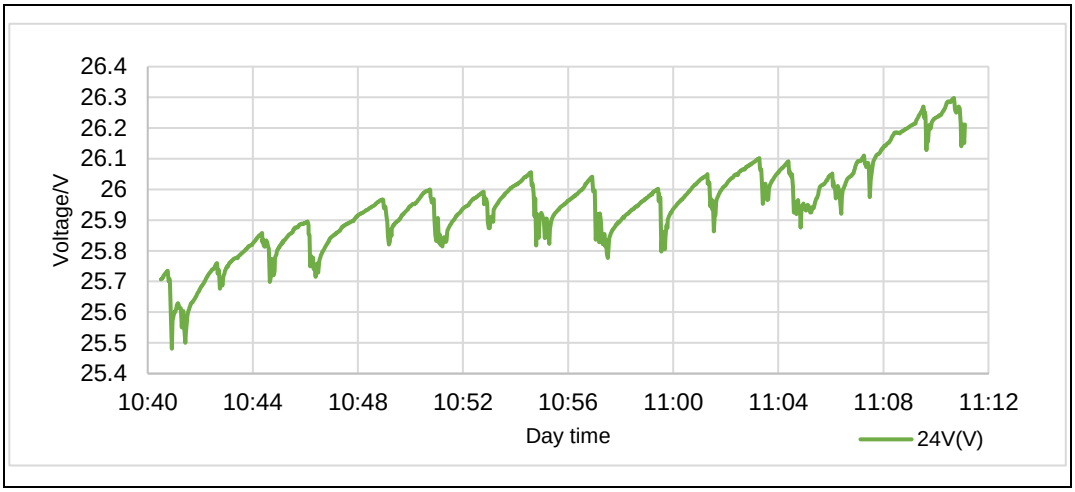

Figure 2-14: Voltage and SOC for steering system in HD1_WCNO Series1 cycles.

Voltage, in general, is not a good variable to monitor SOC because of a time delay in reflecting the real state after a work cycle. However, in this case, since data from Figure 2-14 shows that voltage is always increasing, this is enough to prove that energy consumed is less than energy recovered. The 12 V auxiliary system used for control purposes and the Bin Lift System behaves similarly.

c) Harvest Day 2 (HD2)

This testing day started at 8:50 and finished at 14:30 on January 16, 2017, with a one hour lunch break from 11:30 to 12:30, resulting a work interval of 4 ½ h. The harvesting crew was reduced to 4 people on board plus 2 on foot. The working distance covered this day was 750 m, and the number of individual cycles was 213, which gives 3.52 m on forward motion average. Results this day are divided in 3 main groups of data: morning, mid-day, and afternoon, which are represented as groups 1, 2, and 3 respectively in Table 2 17.

Table 2-17: Log data of cycles in experiment HD2_WCNO

Group Series	Begin	Fin	Time	N samples(S)
1	8:50	11:25	2:34	91
2	12:36	13:10	0:33	30
3	13:16	14:30	1:14	92

Table 2-18: Forward motion cycle averages in experiment HD2_WCNO

Group Motions	Avg time/s	I mean/A	Ipeak mean/A	ΔCE mean/Ah
Series1	21	-9.76	-17.11	-0.053
Series2	28	-5.62	-14.76	-0.040
Series3	16	-6.52	-12.68	-0.028

Table 2-19: Charge cycle averages in experiment HD2_WCNO

Group Charges	Avg time/s	I mean/A	Ipeak mean/A	ΔCE mean/Ah
Series1	78	2.32	2.82	0.050
Series2	37	1.92	2.95	0.023
Series3	30	2.07	3.40	0.022

Table 2-18 and Table 2-19 indicate that as the day progressed, average cycle-times shortened because the crew kept improving the work pace. Series3 by the end of the day achieved the fastest pace.

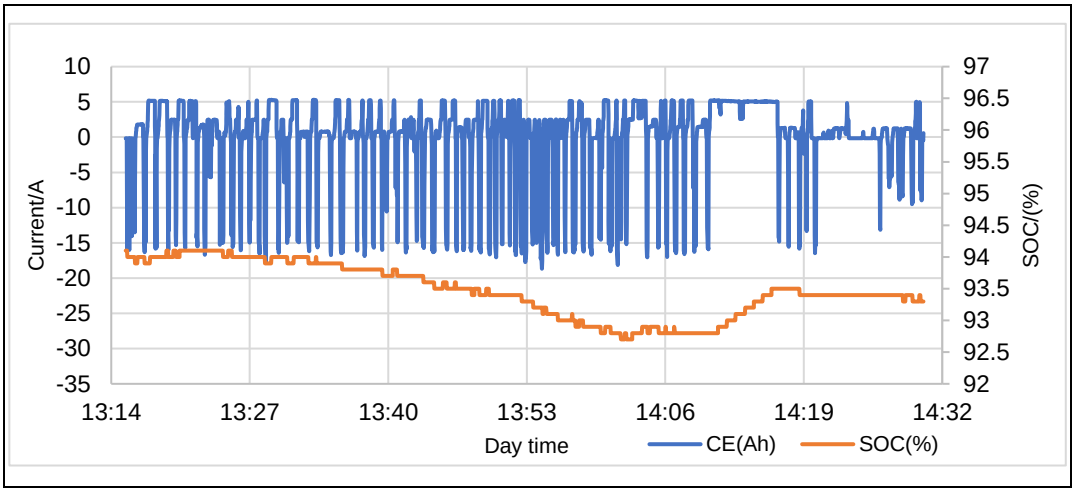

Figure 2-15: Current and SOC in traction system for HD2_WCNO Series 3 cycles.

Data in Table 2-17, Table 2-18, and Table 2-19 shows that in experiment HD2_WCNO, average harvesting time (charging mode) per cycle of 3.52 m length was 51.5 s, with an average current of 2.15 A. Average moving time per cycle was 19.8 s with and average current consumption of -7.8 A. Clearly the results show an improvement with respect to field day 1, especially in a faster harvesting pace. However, this gives less time for battery charging, which can be observed in Figure 2 15 where SOC is seen to fall. Delta SOC was 1%, which is negligible, and after a brief stop at 14:10, the energy was completely recovered, thus validating the hypothesis that the moving platform can operate solely on solar PV energy. The results of monitoring the 24 V Steering System are shown in Figure 2-16.

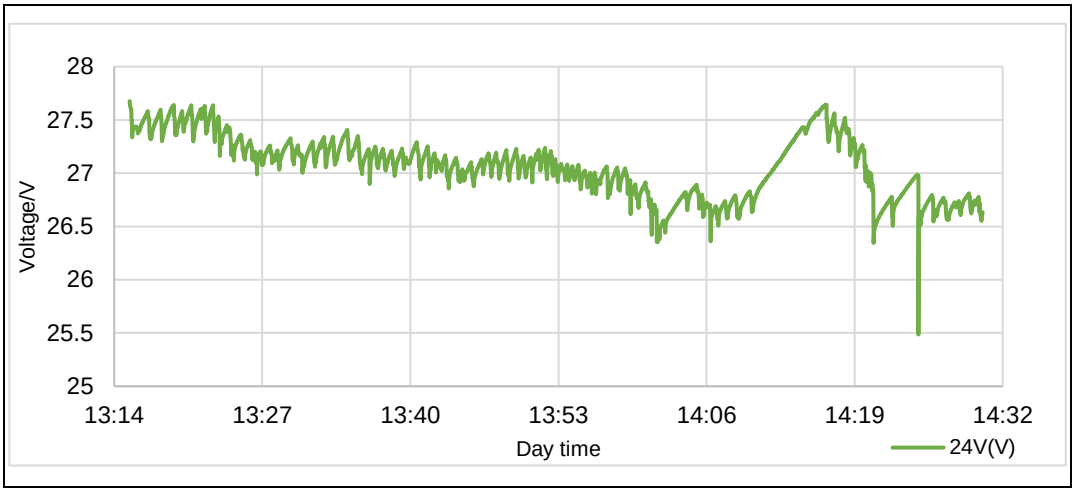

Figure 2-16: Voltage and SOC in steering system for HD2_WCNO Series3 cycles.

These batteries need to be charged at 2.47 VPC (29.6 V in 24 V systems) (“Trojan battery user’s guide,” 2012). Battery voltage began slowly decreasing during the day until 14:10 when the vehicle stopped for a few moments, and the batteries were charged at a fast rate. The down peak observed at around 14:20 was caused by a high effort from the steering and traction systems to get out of a hole.

An important factor to consider is the difference in available energy during the day, especially in the early morning. The next graph in Figure 2-17 shows battery charging data from the beginning of the test to almost mid-day.

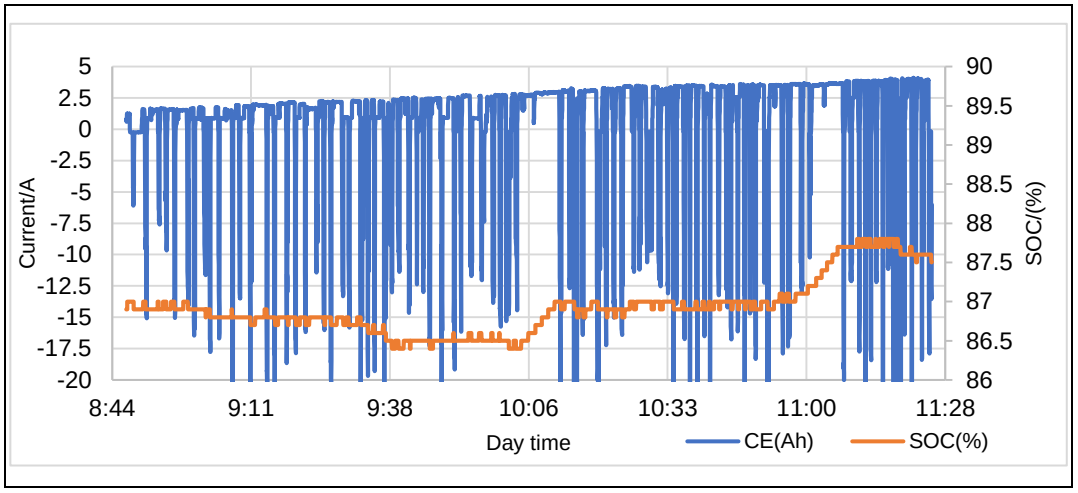

Figure 2-17: Current and SOC in traction system for HD2_WCNO Series 1 cycles.

Figure 2-17 shows that around 10:00 AM the charging current began to rise above 2.5 A. The SOC slowly diminishes at the beginning, but after 10:00AM it began recovering fast as available solar energy levels increase.

2.3.3 Harvesting Productivity

Even though the main purpose of this research was to validate the feasibility of the harvesting vehicle in terms of solar energy self-reliance, it is also important to verify that the harvesting productivity is satisfactory and not hampered. In this section, the harvesting productivity is reported.

In addition to nectarine harvest results described previously, cherry harvesting data for the vehicle from season 2015/2016 is also included, consisting in three additional days and locations. The results of all production tests are summarized in Table 2 20, Table 2 21, and Table 2 22.

Table 2-20: Vehicle harvesting log for cherries and nectarines

Field Test Days	Fruit	Location	Date
1	Cherries	Aculeo	2015-12-11
2	Cherries	Rancagua (El Porvenir)	2015-12-22
3	Cherries	Molina	2015-12-28
4 HD1	Nectarines	Coltauco	2017-01-09
5 HD2	Nectarines	Coltauco	2017-01-16

Table 2-21: Vehicle harvesting production for cherries and nectarines

Field Test	Time effective /min	Total production /kg	People on board	People by foot
1	90	216	6	0
2	166	261	8	2
3	100	108	6	0
4 HD1	167	2500	6	2
5 HD2	185	3000	6	2

Table 2-22: Harvesting production for cherries and nectarines

Field Test	Hourly productivity per person/kg	Daily productivity per person/kg	Daily typical productivity per person/kg
1	24	192	70
2	9.43	75.47	70
3	10.8	86.4	70
4 HD1	112.28	892.2	800
5 HD2	121.62	972.97	800

The results in Table 2-22 show that, although the working crew was not trained, productivity was always equal or better than in pedestrian/manual harvesting. In the case of nectarines, the productivity was higher than the traditional pedestrian process, and by the end of the second day, the team had improved continuously to reach the fastest cycle harvesting pace. As seen in Table 2-19, the average time per harvesting stop was shortened to 30 seconds for the last series of cycles (group 3).

In the case of cherries, productivity improvement was even better yet, especially in Field Test 1 (see Table 2-22) where productivity achieved with the vehicle more than doubled the conventional pedestrian way. It is worth mentioning that cherries require even more careful handling than nectarines.

2.4 Conclusions

It has been demonstrated that a fully solar-powered electric harvesting vehicle for hand-picking fresh market fruit is feasible. The developed test prototype used an array of 8 solar panels with 750W nominal capacity. It had a 1500 kg load carrying capacity, a 5 kW BLDC traction motor, and was able to carry a crew of 7 people and 2 Bins of 500 kg each. The sustainability of this vehicle was proven in several successful harvesting days in nectarines and sweet cherry orchards.

The measured autonomy was 10.16 km at 7.35 km/h in up and down paved road of 2.62% inclination. In Chilean high-density sweet cherry and nectarine orchards, the vehicle is able to operate an entire day in harvest mode consuming only 20% of its SOC without recharging batteries. Solar energy was enough to sustain a zero-emission vehicle in this heavy-duty but intermittent application, where there is enough time to recharge batteries during stops. This mode of energy recovery may be extended to other agricultural and industrial applications with similar working cycle characteristics.

In addition to energy savings and environmental advantages, the vehicle was also attractive to workers because of reduced idle times and less physical effort demanded. The reduced physical effort allowed incorporating women and elderly people to work on the vehicle, which is helpful to address labor shortage.

Productivity is affected by orchard design, and the optimal cycle timing must be defined accordingly. In nectarine harvesting, efficiency was continuously improved by adjusting the working pace and worker assigned functions, while in the sweet cherry orchard there were more limitations due to tree height and volume.

Further horticultural measurements are required to compare the effect in final fruit quality when using the solar vehicle instead of ladders. In addition, future research in the area should address other problems through robotic and computer vision techniques implemented on smart harvesting vehicles.

REFERENCES

Alcaino, M., Müller, C., Betinyani, A., & Brito, F. (2014). Exportdata Yearbook 2014. Retrieved March 10, 2017, from http://www.asoex.cl/publicaciones/expordata-yearbook/finish/26-expordata-yearbook/760-expordata-yearbook-2014.html

Azidin, F. A., & Hannan, M. A. Harvesting solar and energy management system for Light Electric Vehicles (LEVs), International Conference on Renewable Energy Research and Applications (ICRERA) § (2012). https://doi.org/10.1109/ICRERA.2012.6477268

Bechar, A., & Vigneault, C. (2016). Agricultural robots for field operations: Concepts and components. *Biosystems Engineering*, *149*, 94–111. https://doi.org/10.1016/J.BIOSYSTEMSENG.2016.06.014

Bhatti, A. R., Salam, Z., Aziz, M. J. B. A., & Yee, K. P. (2016). A critical review of electric vehicle charging using solar photovoltaic. *International Journal of Energy Research*, *40*(4), 439–461. https://doi.org/10.1002/er.3472

BOSCH. (2015). *Servolectric® Electromechanical steering system for a dynamic driving experience and highly automated functions*. Retrieved from http://www.bosch-automotive-steering.com/fileadmin/downloads/Flyer_Nkw/AS_Systemmappe_Servolectric_E_lowres_20150513.pdf

Carbon Trust. (2009). What is a carbon footprint. Retrieved from https://web.archive.org/web/20090511102744/http://www.carbontrust.co.uk/solutions/CarbonFootprinting/what_is_a_carbon_footprint.htm

Chauhan, S. (2015). Motor Torque Calculations For Electric Vehicle. *International Journal of Scientific & Technology Research*, *4*(8), 126–127. Retrieved from www.ijstr.org

CIA. (2017). People and Society of Chile. Retrieved October 16, 2017, from https://www.cia.gov/library/publications/the-world-factbook/geos/ci.html

Corsentino, B. (2017). Hurricanes Irma and Harvey may be a “wake-up call” for vulnerable cities, and local zoning laws: Expert. *CNBC*. Retrieved from https://www.cnbc.com/2017/ 09/15/hurricanes-irma-and-harvey-may-be-a-wake-up-call-for-vulnerable-cities-and-local-zoning-laws-expert.html

Dias, J. S., & Ortiz, R. (2013). Transgenic vegetables for 21st century horticulture. In M. A. Veale (Ed.), *2nd Genetically Modified Organisms in Horticulture Symposium* (pp. 15–30). White River, South Africa: INT SOC HORTICULTURAL SCIENCE.

Dixon, J. (2010). Energy storage for electric vehicles. In *2010 IEEE International Conference on Industrial Technology* (pp. 20–26). IEEE. https://doi.org/10.1109/ICIT.2010.5472647

Donnelly, G. (2017). Hurricane Irma and Harvey Damaged 1 Million Cars. *Fortune*. Retrieved from http://fortune.com/2017/09/20/hurricane-irma-harvey-damaged-cars/

Drash, W. (2017). Cimate change made Harvey and Irma worse. *CNN*.

Ehlert, A., Moreano, F., Busch, U., & Engel, K.-H. (2008). Development of a modular system for detection of genetically modified organisms in food based on ligation-dependent probe amplification. *European Food Research and Technology*, *227*(3), 805–812. https:// doi.org/10.1007/s00217-007-0790-x

Fernández, R., Salinas, C., Montes, H., & Sarria, J. (2014). Multisensory system for fruit harvesting robots. Experimental testing in natural scenarios and with different kinds of crops. *Sensors*, *14*(12), 23885–23904. https://doi.org/10.3390/s141223885

Ficha técnica de cerezo lapins. (2015). Retrieved March 20, 2017, from http://www.sna.cl/wp/wp-content/uploads/2016/04/SNA-2015.-Fichas-Cerezo.xlsx

Fundación Economía Circular. (2017). Economía Circular. Retrieved November 1, 2017, from http://economiacircular.org/

Haas, W., Krausmann, F., Wiedenhofer, D., & Heinz, M. (2015). How Circular is the Global Economy?: An Assessment of Material Flows, Waste Production, and Recycling in the European Union and the World in 2005. *Journal of Industrial Ecology*, *19*(5), 765–777. https://doi.org/10.1111/jiec.12244

Howard, T. M., & Kelly, A. (2005). Trajectory generation on rough terrain considering actuator dynamics. In *Proceedings of the 5th International Conference on Field and Service Robotics (FSR '05)*. Springer Berlin Heidelberg. https://doi.org/10.1007/978-3-540-33453-8_40

Kim, J., Baek, D., Hong, J., & Chang, N. (2014). Partially solar powered full electric vehicles. In *2014 IEEE 57th International Midwest Symposium on Circuits and Systems (MWSCAS)* (pp. 358–361). IEEE. https://doi.org/10.1109/MWSCAS.2014.6908426

Kimura, N., Seki, E., Shin, S.-C., Takahashi, S., & Makino, S. (2016). Development for 300Wh/Kg-Class High Energy Li-Ion Battery for EV. *Meeting Abstracts*, *MA2016-02*(3), 238–238. Retrieved from http://ma.ecsdl.org/content/MA2016-02/3/238.abstract

Kremer, M. (1993). Population Growth and Technological Change: One Million B.C. to 1990. *The Quarterly Journal of Economics*, *108*(3), 681–716. https://doi.org/10.2307/2118405

Larbi, P. A., & Karkee, M. (2014). Effects of orchard characteristics and operator performance on harvesting rate of a mechanical sweet cherry harvester. *GSTF Journal on Agricultural Engineering (JAE)*, *1*(1), 1–11. https://doi.org/10.5176/0000-0000

Letendre, S. (2009). Solar electricity as a fuel for light vehicles. In *Proceedings of the 2009 American Solar Energy Society Annual Conference* (pp. 1–6). Boulder. Retrieved from http://www.greenmtn.edu/letendres.aspx

Li, P., Lee, S., & Hsu, H. (2011). Review on fruit harvesting method for potential use of automatic fruit harvesting systems. *Procedia Engineering*, *23*, 351–366. https://doi.org/10.1016/j.proeng.2011.11.2514

Lippert, J., Ma, J., & Nussbaum, A. (2017). Nissan, Renault, Mitsubishi Deepen Alliance in Electric Push. Retrieved October 16, 2017, from https://www.bloomberg.com/news/articles/2017-09-15/nissan-renault-mitsubishi-deepen-alliance-with-electric-push

Lohith, K., Shankapal, S. R., & Monish Gowda, M. H. (2013). Development of four wheel steering system for a car. *Sastech Journal*, *12*(1), 90–97. Retrieved from http://www.msruas.ac.in/pdf_files/sastechJournals/May2013/13.pdf

Louie, H. M. (2015). Probabilistic modeling and statistical analysis of aggregated electric vehicle charging station load. *Electric Power Components and Systems*, *43*(20), 2311–2324. https://doi.org/10.1080/15325008.2015.1080770

Mejora el mercado laboral y crece el empleo agrícola. (2016). Retrieved March 20, 2017, from http://www.sna.cl/wp/wp-content/uploads/2016/12/Empleo-sep-nov.-2016-pdf.pdf

Ministerio de Energía. (2016). Chile lidera inersión en energias renovables. Retrieved October 16, 2017, from http://www.energia.gob.cl/tema-de-interes/chile-lidera-ranking

Ministerio de Energia, & Departamento de Geofísica Universidad de Chile. (2017). Explorador Solar. Retrieved from http://www.minenergia.cl/exploradorsolar/

Molina Monje, A., & Rondanelli Rojas, R. (2012). *Explorador del Recurso Solar en Chile*.

Motor HPM48 5000W curve of power. (2016). Retrieved August 6, 2017, from https://www.goldenmotor.com/eCar/HPM48-5000Curve.pdf

Nguyen, T.-T., Kim, H. W., Lee, G. H., & Choi, W. (2013). Design and implementation of the low cost and fast solar charger with the rooftop PV array of the vehicle. *Solar Energy*, *96*, 83–95. https://doi.org/10.1016/j.solener.2013.07.006

Param, N., & Zoffoli, J. P. (2016). Genotypic differences in sweet cherries are associated with the susceptibility to mechanical damage. *Scientia Horticulturae*, *211*, 410–419. https:// doi.org/10.1016/j.scienta.2016.09.027

Peterson, D. L., Whiting, M. D., & Wolford, S. D. (2003). Fresh-market quality tree fruit harvester part I: sweet cherry. *Applied Engineering in Agriculture*, *19*(5), 539–543.

Peterson, D. L., & Wolford, S. D. (2001). Mechanical harvester for fresh market quality stemless sweet cherries. *Transactions of the ASAE*, *44*(3), 481–485. https://doi.org/ 10.13031 /2013.6103

Precios, comercio exterior y fichas de fruta frescas exportada. (2017). Retrieved March 10, 2017, from http://www.odepa.cl/rubro/frutas-frescas/

Qingchun, F., Xiu, W., Wengang, Z., Quan, Q., & Kai, J. (2012). New strawberry harvesting robot for elevated-trough culture. *International Journal of Agricultural and Biological Engineering*, *5*(2), 1–8. https://doi.org/10.3965/j.ijabe.20120502.00?

Reimpell, J., Stoll, H., & Betzler, J. W. (2001). *The automotive chassis: engineering principles*. Butterworth-Heinemann. https://doi.org/10.1007/978-1-4020-8676-2

Reuters. (2017). Mercedes-Benz to offer 50 electrified car versions by 2022. Retrieved October 16, 2017, from https://www.autoblog.com/2017/09/11/mercedes-benz-50-electrified-car-versions-by-2022/

Rogers-Marcovitz, F., Seegmiller, N., & and A. Kelly. (2012). Continuous vehicle slip model identification on changing terrains. *RSS 2012 Workshop on Long-Term Operation of Autonomous Robotic Systems in Changing Environments*. Retrieved from https://www.ri.cmu.edu/pub_files/2012/7/contSlipModel_rssLongTerm2012.pdf

Roser, M., & Ortiz-Ospina, E. (2017). World population growth. Retrieved October 16, 2017, from https://ourworldindata.org/world-population-growth/

SalmonChile.cl. (2017). Industría del Salmón de Chile. Retrieved October 16, 2017, from http://www.salmonchile.cl/es/quienes-somos.php

Schmidt-Hebbel, K. (2015). El mundo, Chile y la agricultura: ¿Dónde estamos y adónde vamos? In *Encuentro Nacional del Agro* (pp. 1–42). Santiago: Sociedad Nacional de

Agricultura. Retrieved from http://www.sna.cl/wp/wp-content/uploads/2015/10/Enagro 2015 - Klaus Schmidt-Hebbel.pdf

Seegmiller, N., & Kelly, A. (2013). Modular dynamic simulation of wheeled mobile robots. In *Proc. Field and Service Robotics*. Springer, Cham. https://doi.org/10.1007/978-3-319-07488-7_6

Seminarsonly.com. (2016). Four-Wheel Steering System. Retrieved November 1, 2017, from http://www.seminarsonly.com/mech & auto/Four-Wheel-Steering-System.php

Shepardson, E. S., Markwardt, E. D., Millier, W. F., & Rehkugler, G. E. (1970). Mechanical harvesting of fruits and vegetables. *New York's Food and Life Sciences Bulletin*, *5*(1).

Shiigi, T., Kondo, N., Kurita, M., Ninomiya, K., Rajendra, P., Kamata, J., … Kohno, Y. (2008). Strawberry harvesting robot for fruits grown on table top culture. *American Society of Agricultural and Biological Engineers Annual International Meeting 2008*, *5*(8), 3139–3148. https://doi.org/10.13031/2013.24754

Smith, E., & Whiting, M. (2007). New developments toward mechanizing sweet cherry harvest. *Hortscience: A Publication of the American Society for Horticultural Science*, *42*(4), 880.

Snell, L. D. (2008). *Force and moment analysis of stacked counter rotating eccentric mass tree shaker energy-wheel system* (Master Thesis, Ames). Iowa State University. Retrieved from http://lib.dr.iastate.edu/cgi/viewcontent.cgi?article=16402&context=rtd

Sun, Y., Zhong, Z., Li, T., Yi, L., Hu, Y., Wan, H., … Li, Q. (2017). Impact of Ocean Warming on Tropical Cyclone Size and Its Destructiveness. *Scientific Reports*, *7*(1), 8154. https://doi.org/10.1038/s41598-017-08533-6

Trojan battery user's guide. (2012). Retrieved September 7, 2017, from http://www. trojanbattery.com/pdf/TrojanBattery_UsersGuide.pdf

Wally Rippel. (2007). Induction Versus DC Brushless Motors. Retrieved November 4, 2017, from https://www.tesla.com/blog/induction-versus-dc-brushless-motors

World Bank. (2017). Agriculture, value added percentage of GDP. Retrieved March 13, 2017, from http://data.worldbank.org/indicator/NV.AGR.TOTL.ZS

A P P E N D I C E S

APPENDIX A: CHASSIS

Figure A-1: Cherokee in junkyard La Pintana

Figure A-2: Cherokee front chassis acquisition

Figure A-3: Cherokee chassis cut process

Figure A-4: Cherokee chassis after clean & cut process.

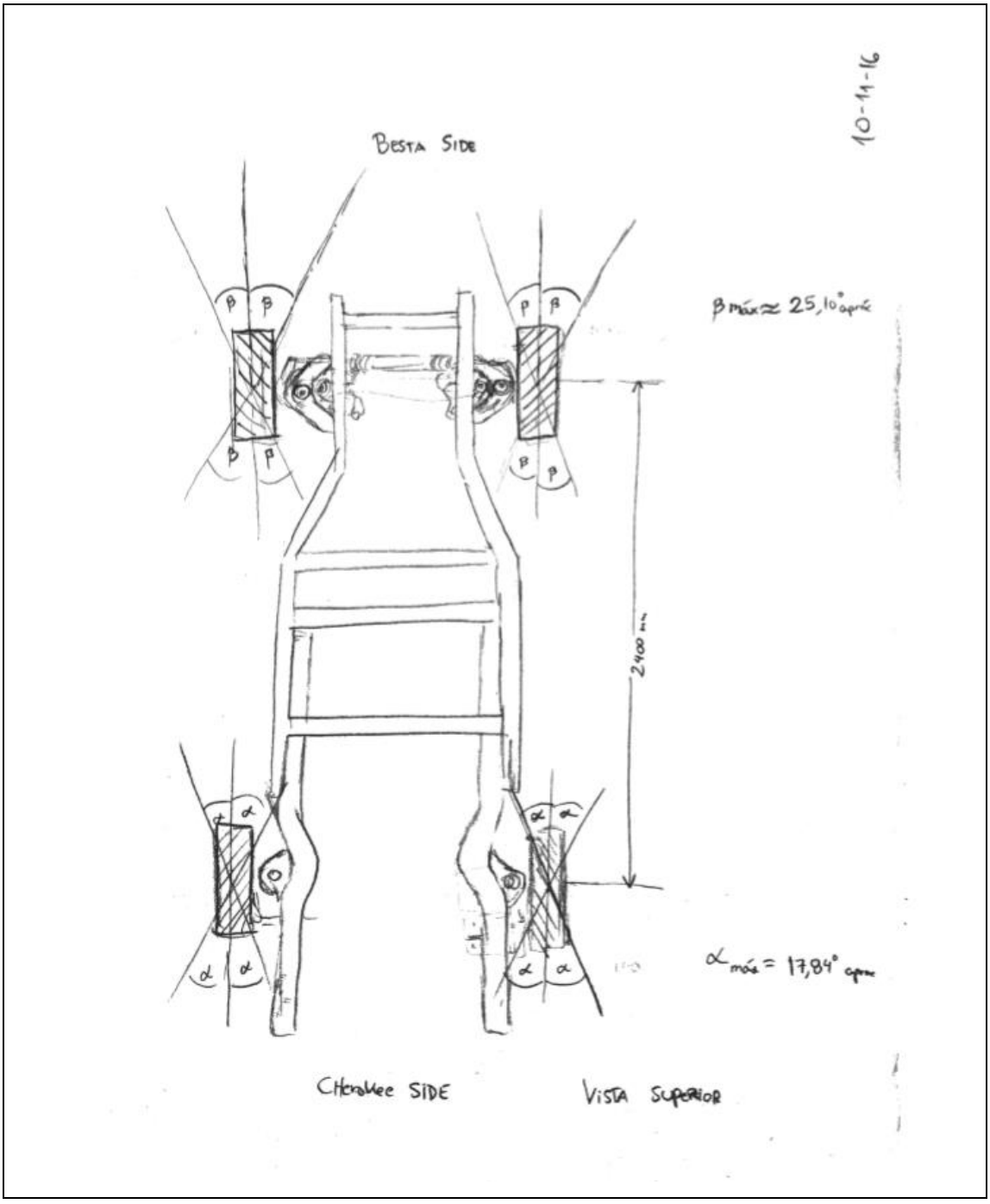

Figure A-5: Chassis drawing with steering angle measure.

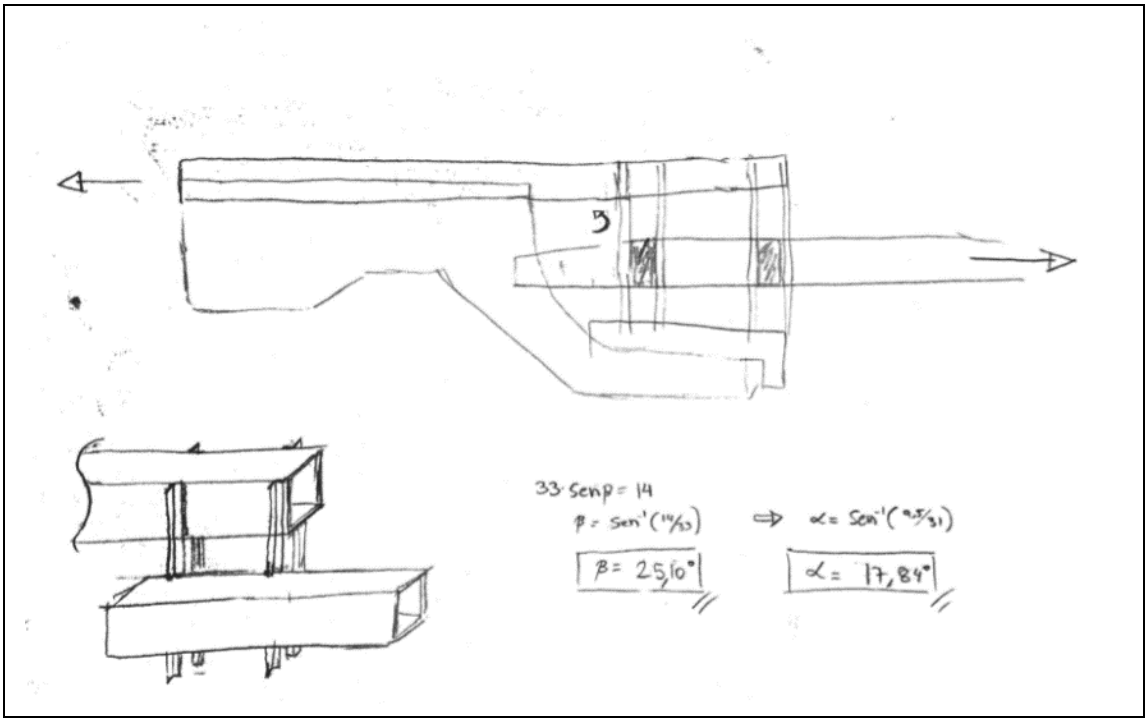

Figure A-6: Joint structure drawn with steering angle calculation.

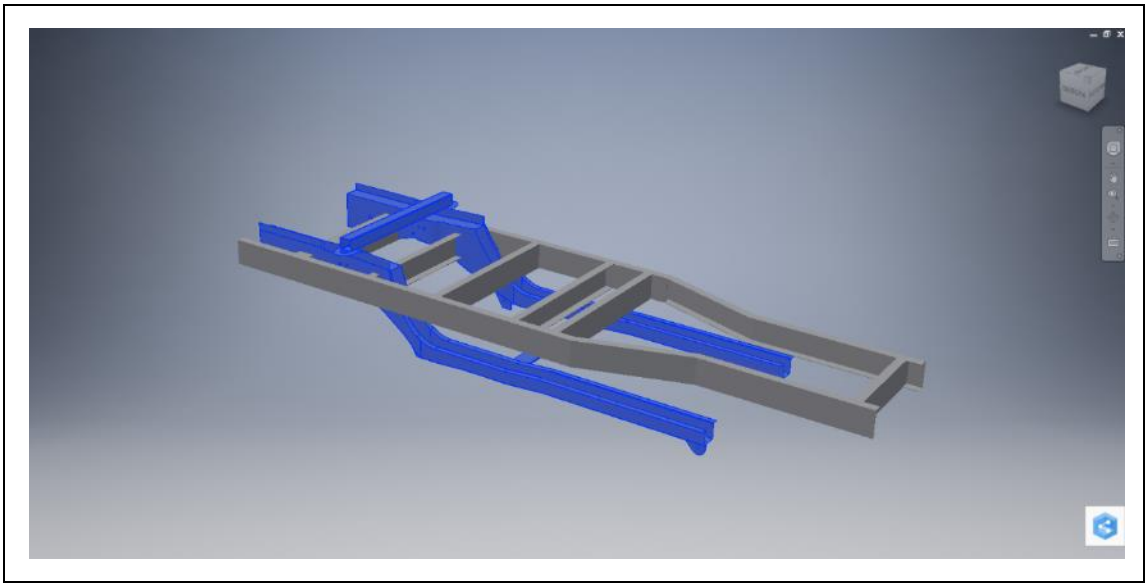

Figure A-7: CAD modeling of Cherokee's and Kia Besta chassis.

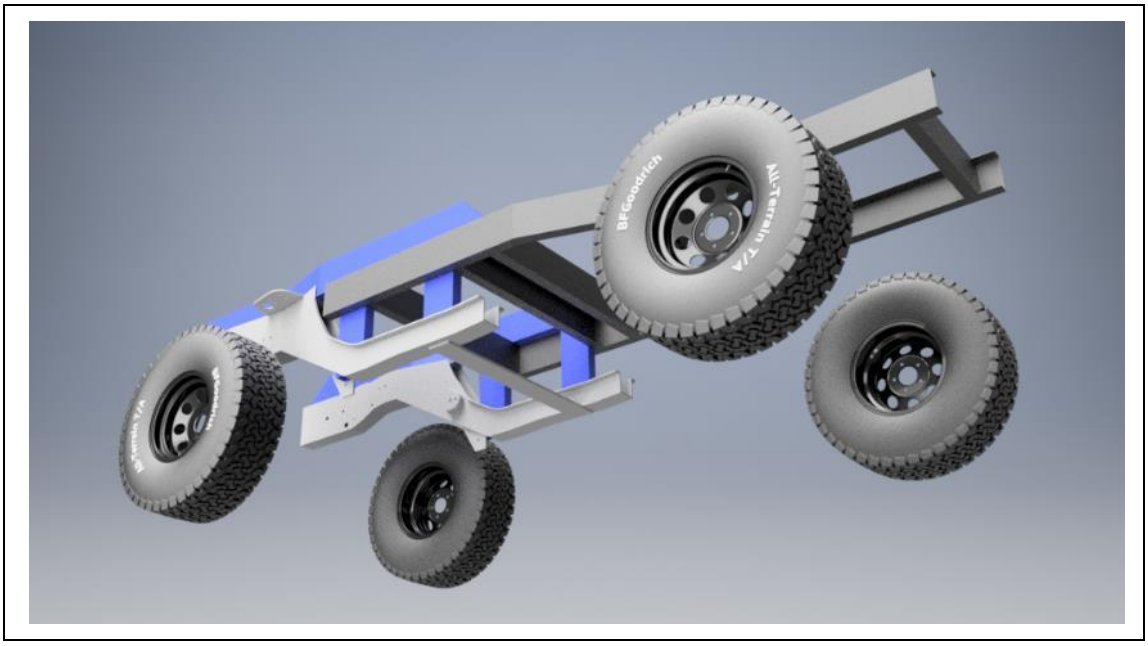

Figure A-8: CAD design of the complete chassis.

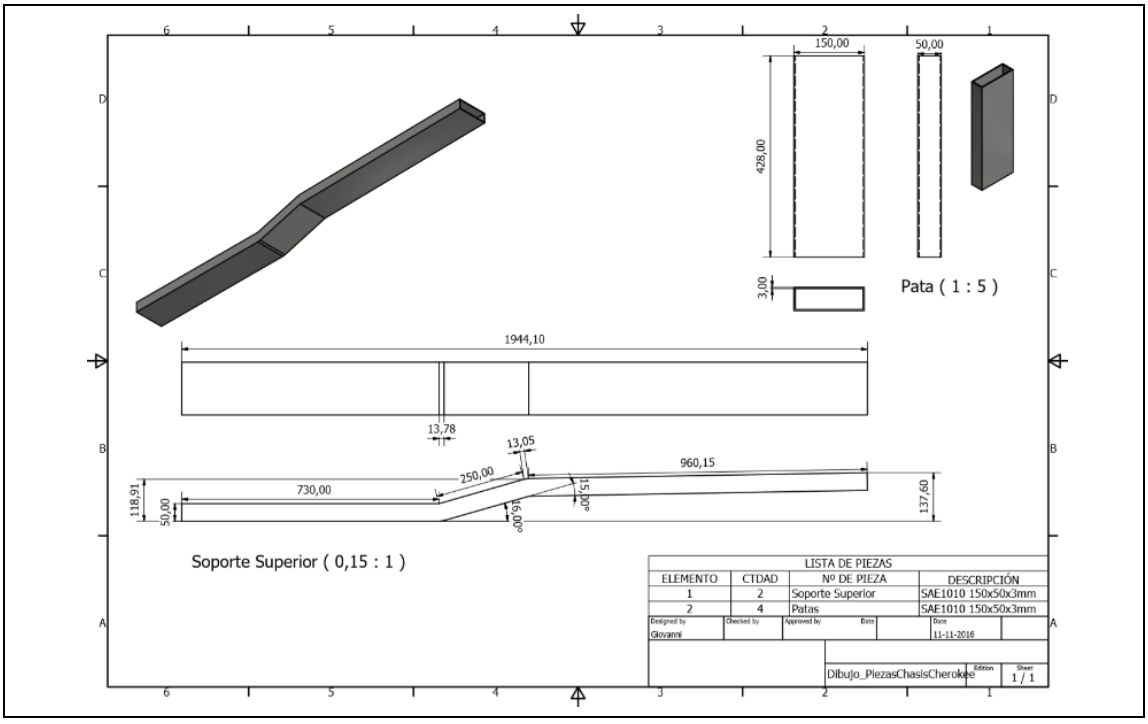

Figure A-9: Fabrication drawing of joint structure

Figure A-10: Join structure assembly

Figure A-11: Chassis complete.

APPENDIX B: STEERING SYSTEM

Table B-1: List of pieces, size, quantity (N°), and length for platform

Piece	Name	Size	N°	Length
PLateral	Perfil_PLateral_Borde	40x20x2	4	970
	Perfil_PLateral_Back	40x20x2	2	3960
	Perfil_PLateral_Frontis	70x30x2	2	4000
	Perfil_PLateral_Guía	15x35x1,5	18	950
Pcentral_FrameU	Perfil_PCentral_FrontisSuperior	40x40x2	2	4070
	Perfil_PCentral_CostillaSuperior	40x40x2	4	1220
	Perfil_PCentral_BordeSuperior	40x40x2	2	1300
Pcentral_FrameM	Perfil_PCentral_FrontisInferior	40x80x3	1	4070
	Perfil_PCentral_CostillaInferior	40x40x2	3	1180
	Perfil_PCentral_BordeSuperior	40x40x2	2	1300
	Perfil_PCentral_FrontisSuperior	40x40x2	1	4070
Pcentral_FrameD	Perfil_PCentral_FrontisInferior	40x80x3	1	4070
	Perfil_PCentral_CostillaInferior	40x40x2	4	1180
	Perfil_PCentral_BordeMedio	40x40x2	2	1300
	Perfil_PCentral_FrontisSuperior	40x40x2	1	4070
Base	Perfil_Base_Largeros	50x50x2	2	4150
	Perfil_Base_Centrales	50x50x2	2	670
	Perfil_Base_Patas	50x50x2	4	200
	Perfil_Base_Angulos	50x50x2	8	300

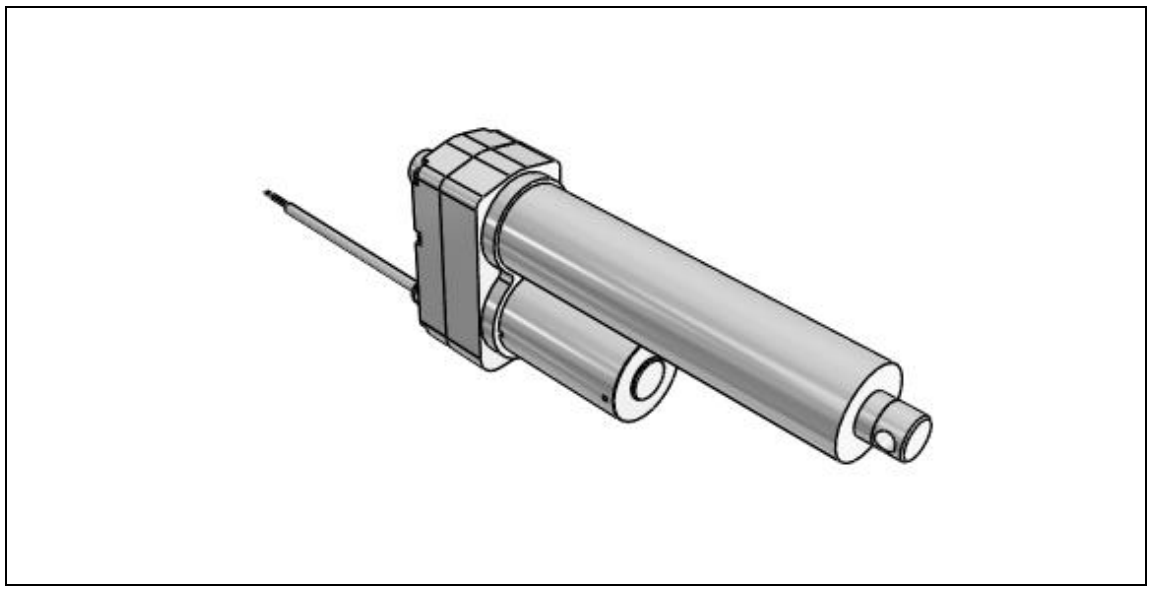

Figure B-1: 3D model of the linear actuator SKF CAHB-21 from the manufacturer.[11]

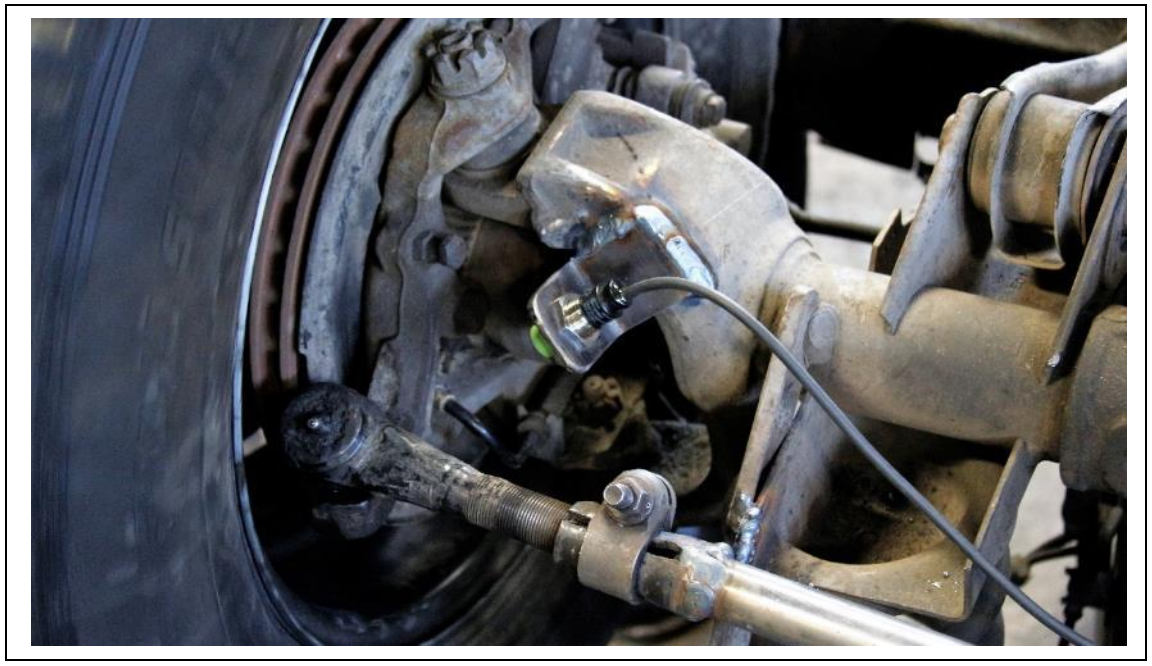

Figure B-2: Limit sensor over the linked bar in the Cherokee axis.

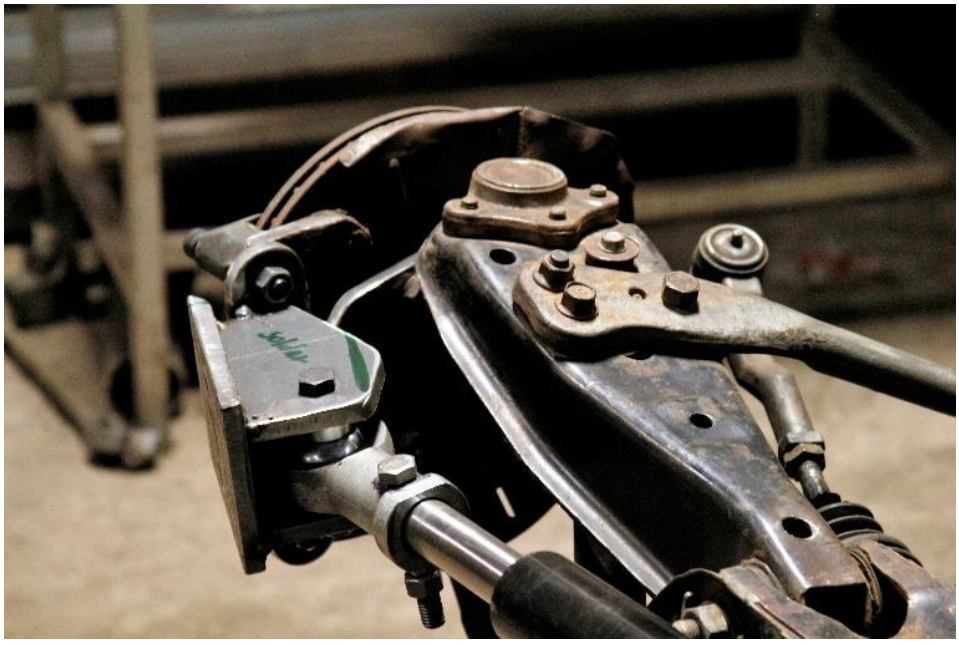

Figure B-3: Arm actuator ball mount in the caliper space

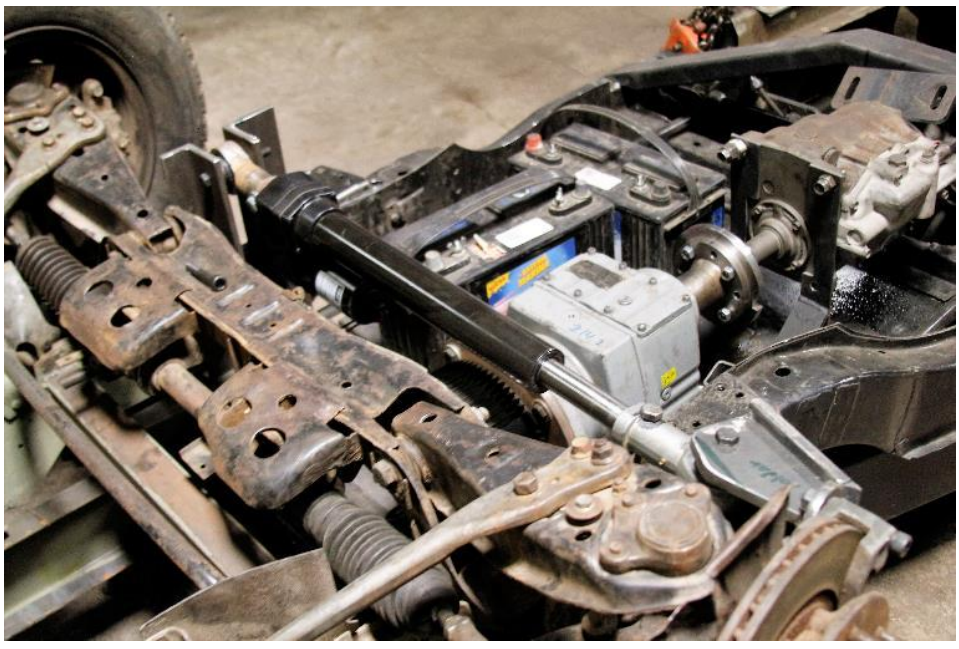

Figure B-4: Linear actuator installed

Figure B-5: Testing crab steering state

Figure B-6: Testing the joysticks with the PLC

APPENDIX C: TRACTION SYSTEM

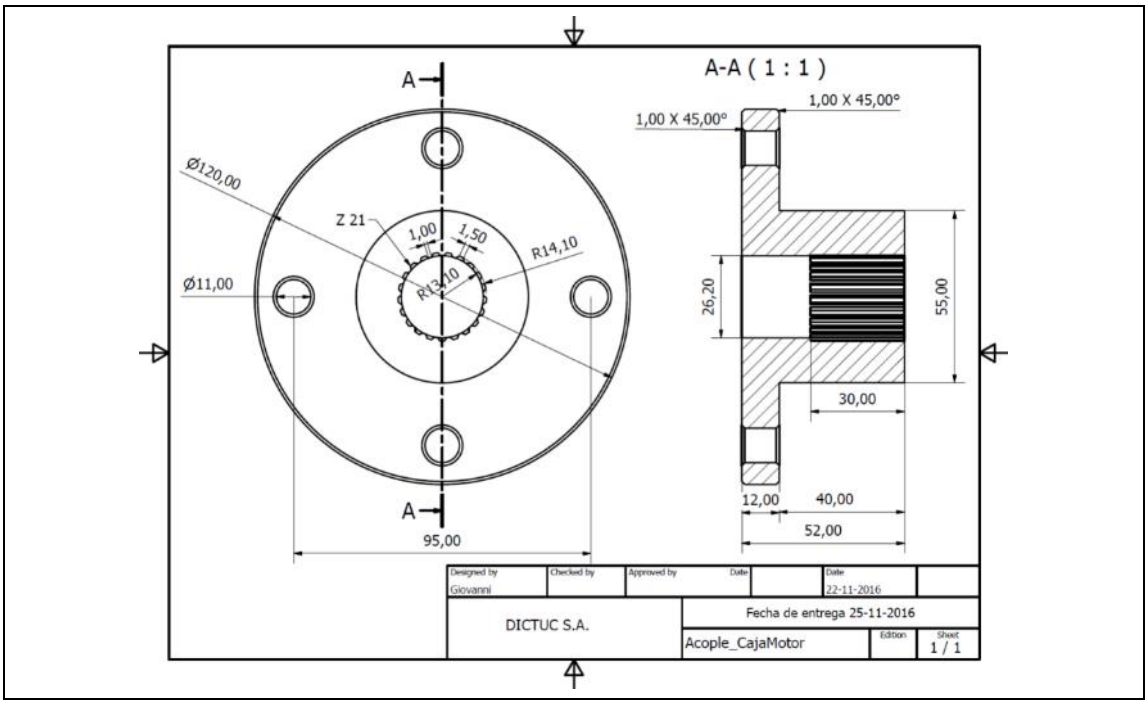

Figure C-1: Fabrication drawing of joint torque piece.

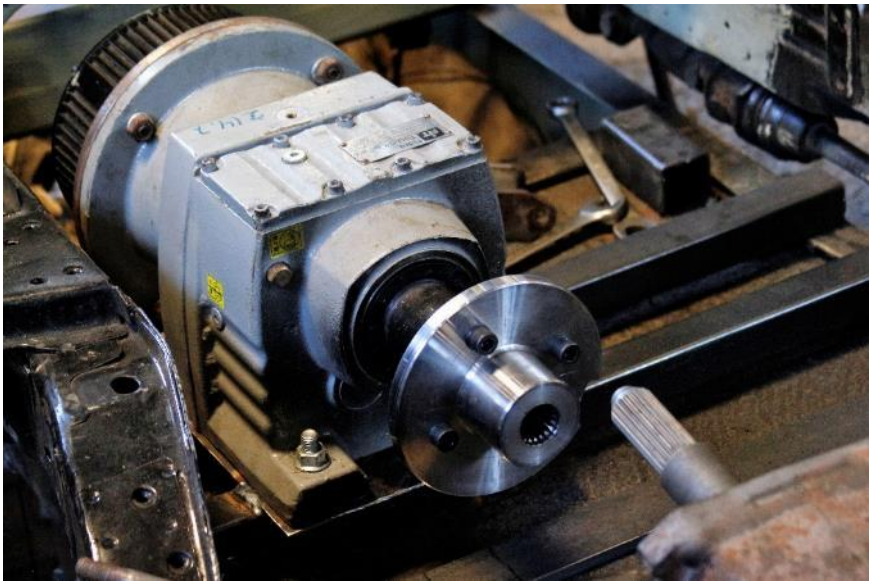

Figure C-2: Joint torque piece connected to the reduction box.

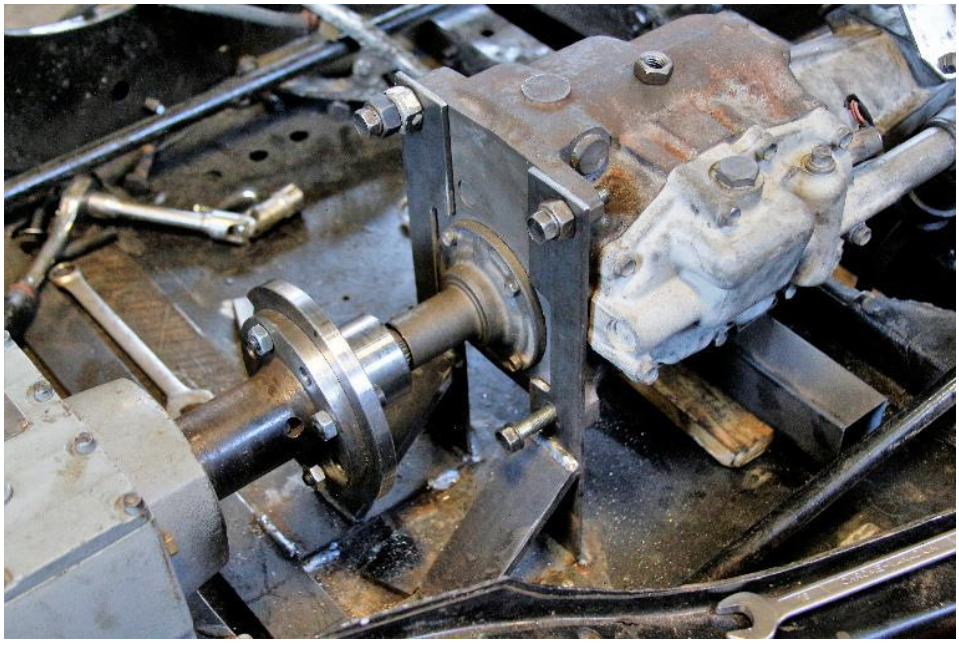

Figure C-3: Joint torque piece in serie with the gearbox

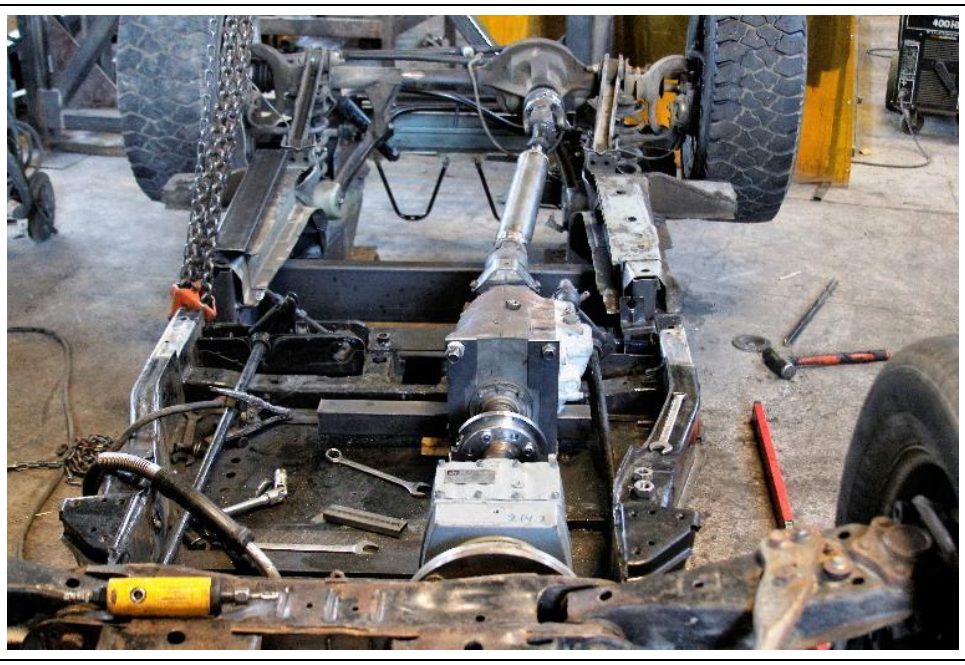

Figure C-4: Assembly of the traction system

APPENDIX D: PLATFORM SYSTEM

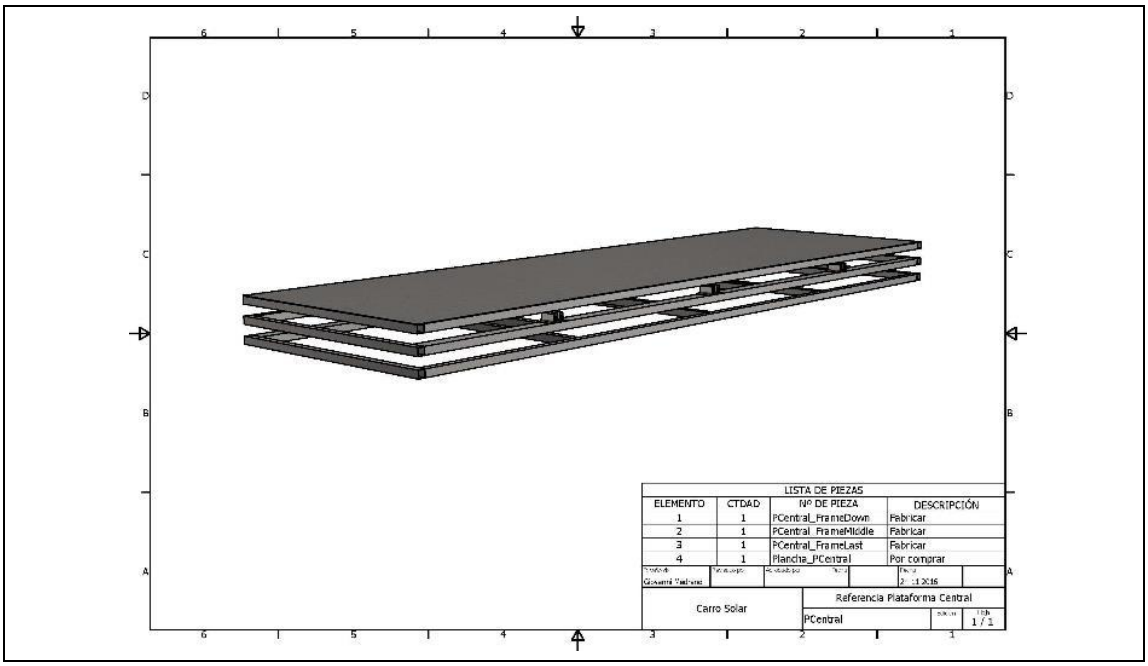

Figure D-1: Drawing of central platform.

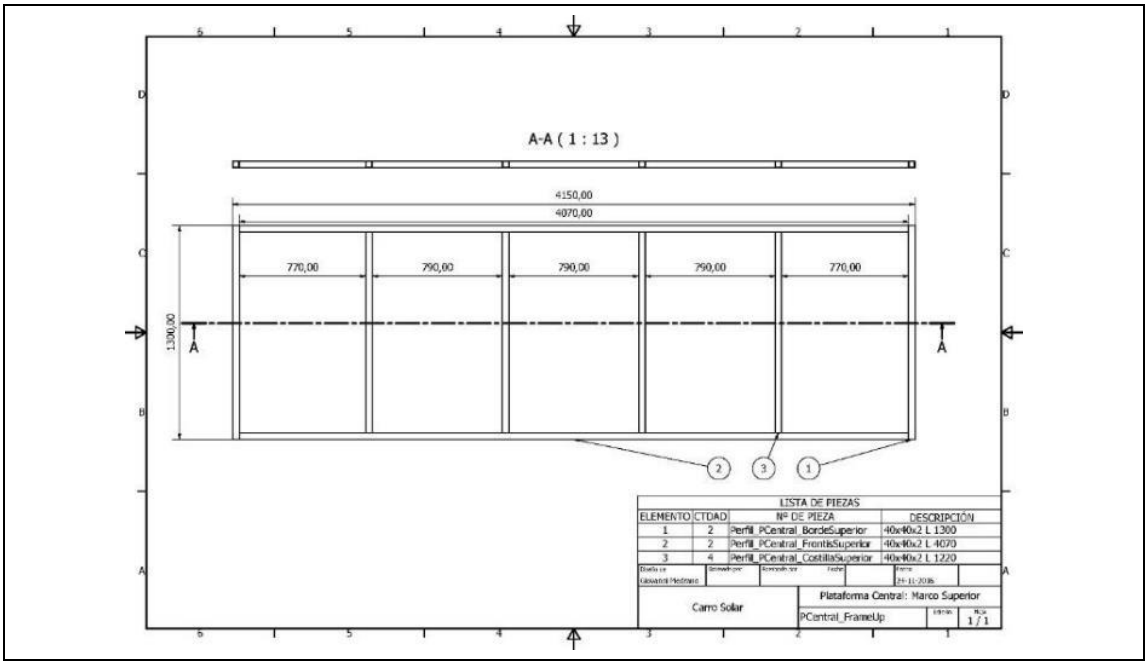

Figure D-2: Fabrication drawing of central platform frame up.

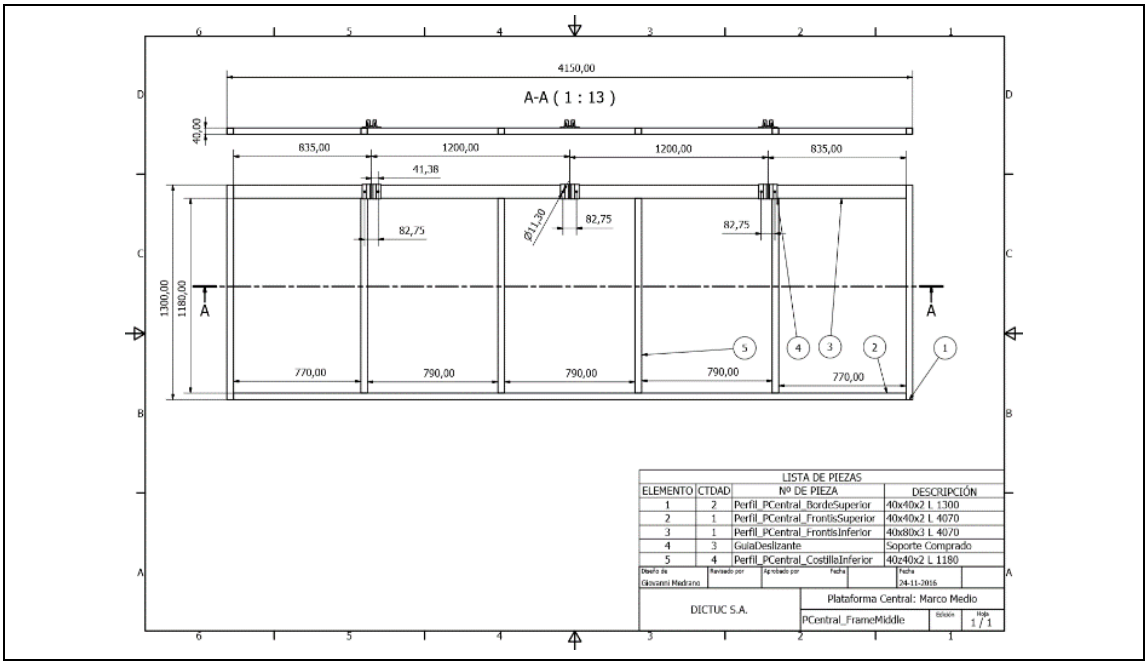

Figure D-3: Fabrication drawing of central platform frame middle.

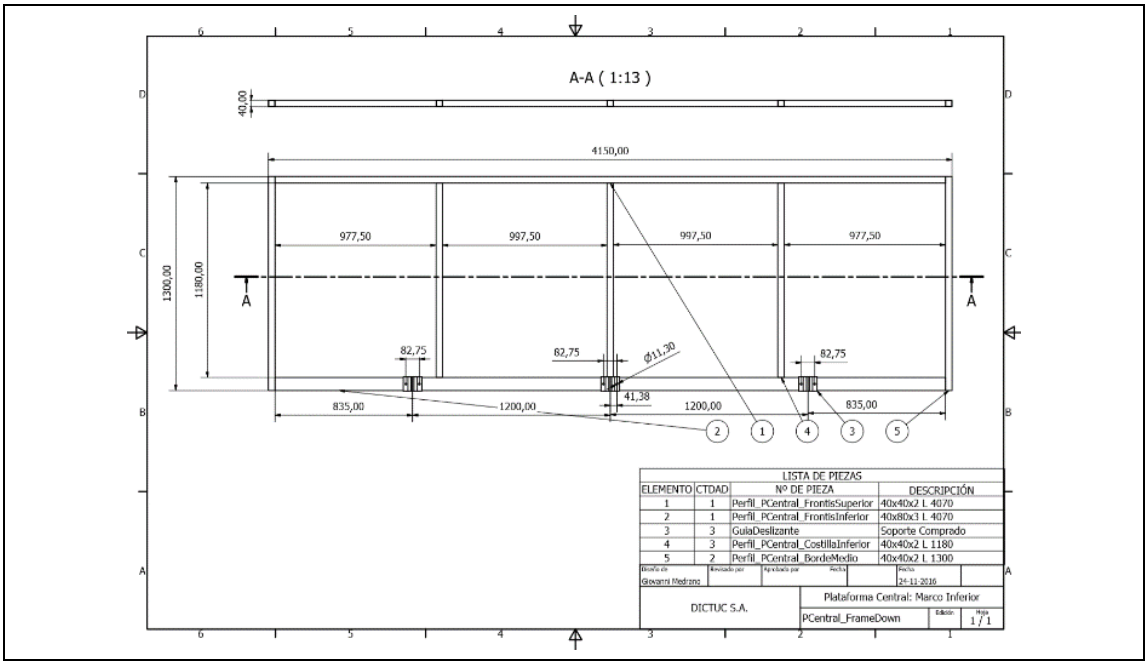

Figure D-4: Fabrication drawing of central platform frame down.

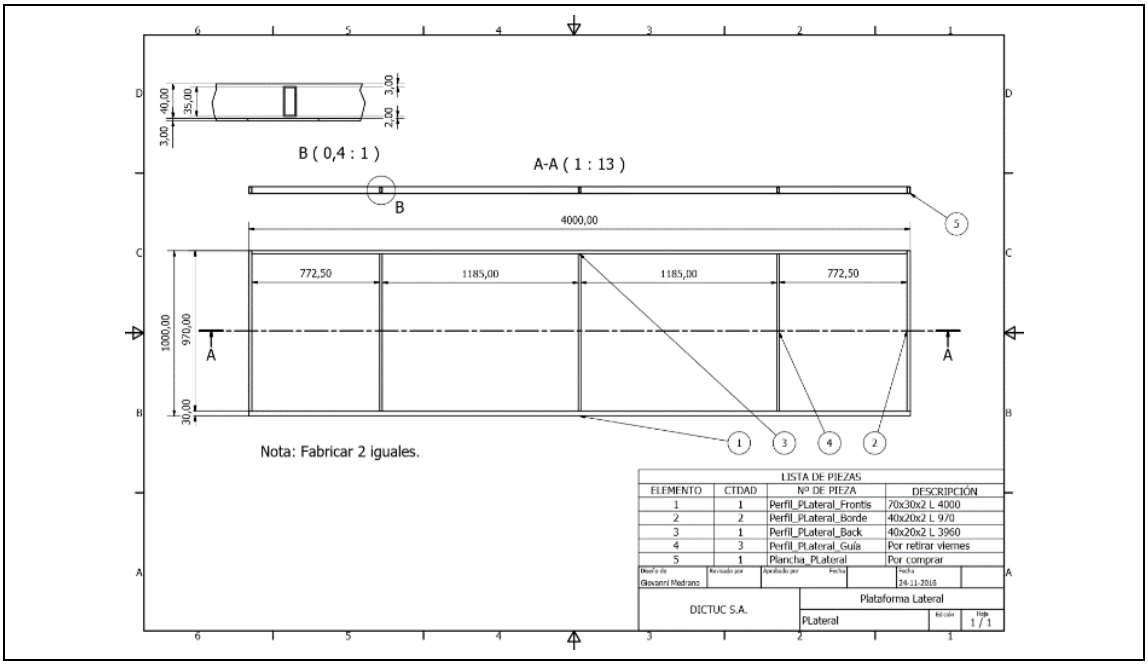

Figure D-5: Fabrication drawing of lateral platform.

APPENDIX E: MEASUREMENTS

a) Excel VBA macros for Split series in individual samples.

```
Sub LogSeries()
'Almacena Punto de Inicio y Fin de las series en la hoja "Series"
'NOTA: La hoja LogSerie debe estar creada y con los encabezados de tabla respectivos
'NOTA: Verificar largo de los datos
Dim serie, contador, fila, rev As Integer
Dim mov As Boolean
contador = 2
serie = 2
fila = 1
rev = 1
mov = False 'Estado [MOV=True,CHARGE=False] depende de si los datos comienzan con el carro mov o
charging

Workbooks("Test1.xlsm").Worksheets("Data").Activate
Range("J1").value = 0

Do While IsEmpty(Range("H" & contador).value) = False
    If Range("H" & contador) = True Then
        Range("J" & contador).value = 0
        If mov Then 'El carro esta en modo MOV
            Workbooks("Test1.xlsm").Worksheets("Series").Range("K" & serie).value = serie - 1 'Log No de
                Serie CHARGE
            fila = Range("H" & contador).Row 'Copia valor de la fila del cambio de estado [MOV,CHARGE]
                Workbooks("Test1.xlsm").Worksheets("Series").Range("L" & serie).value = fila 'Log Inicio
                CHARGE
            Workbooks("Test1.xlsm").Worksheets("Series").Range("C" & serie).value = fila - 1 'Log Fin
MOV
            serie = serie + 1
            mov = False
        Else
            Workbooks("Test1.xlsm").Worksheets("Series").Range("A" & serie).value = serie - 1 'Log No de
                Serie MOV
            fila = Range("H" & contador).Row
            Workbooks("Test1.xlsm").Worksheets("Series").Range("B" & serie).value = fila 'Log Inicio
MOV
            Workbooks("Test1.xlsm").Worksheets("Series").Range("M" & serie - 1).value = fila - 1 'Log Fin
                CHARGE anterior
            mov = True
        End If
    Else
        Range("J" & contador).value = Range("J" & contador - 1).value + Range("I" & contador).value
    End If
    contador = contador + 1
Loop
Workbooks("Test1.xlsm").Worksheets("Series").Range("M" & 1).value = "Fin"
Workbooks("Test1.xlsm").Worksheets("Series").Range("M" & serie - 1).value = contador - 1
Range("J1").value = "TIME"
End Sub
```

```
Sub GetInfoSeries()
'Obtiene la información de las series: [Duración, I_prom, DeltaCE]
'NOTA: Verificar largo de los datos
```

```
Dim contador, inicio, fin  As Integer
contador = 2
Workbooks("Test1.xlsm").Worksheets("Series").Activate
Do While IsEmpty(Range("A" & contador).value) = False
      inicio = Range("B" & contador).value
      fin = Range("C" & contador).value
      Range("D" & contador).value = Workbooks("Test1.xlsm").Worksheets("Data").Range("J" & fin).value
            'Duracion
      Range("E" & contador).value =
Application.WorksheetFunction.Average(getArray(Workbooks("Test1.xlsm").
            Worksheets("Data").Range("C" & inicio & ":C" & fin)))
      Range("F" & contador).value = Application.WorksheetFunction.Min(getArray(Workbooks("Test1.xlsm").
            Worksheets("Data").Range("C" & inicio & ":C" & fin)))
      Range("G" & contador).value = Workbooks("Test1.xlsm").Worksheets("Data").Range("D" & fin).value –
            Workbooks("Test1.xlsm").Worksheets("Data").Range("D" & inicio).value
      inicio = Range("L" & contador).value
      fin = Range("M" & contador).value
      Range("N" & contador).value = Workbooks("Test1.xlsm").Worksheets("Data").Range("J" & fin).value
            'Duracion
      Range("O" & contador).value =
Application.WorksheetFunction.Average(getArray(Workbooks("Test1.xlsm").
            Worksheets("Data").Range("C" & inicio & ":C" & fin)))
      Range("P" & contador).value = Application.WorksheetFunction.Max(getArray(Workbooks("Test1.xlsm").
            Worksheets("Data").Range("C" & inicio & ":C" & fin)))
      Range("Q" & contador).value = Workbooks("Test1.xlsm").Worksheets("Data").Range("D" & fin).value –
            Workbooks("Test1.xlsm").Worksheets("Data").Range("D" & inicio).value

      contador = contador + 1
Loop
End Sub
```

```
Function getArray(dataRange As Range) As Variant()
      Dim arr As Variant
      ReDim arr(dataRange.Rows.Count, dataRange.Columns.Count)
      Dim i As Integer, j As Integer
      For i = 1 To dataRange.Rows.Count
            For j = 1 To dataRange.Columns.Count
                  arr(i, j) = dataRange(i, j)
            Next
      Next
      getArray = arr
End Function
```

```
'SERIES DE CONSUMO DE CORRIENTE
Sub ConsumoCorriente()
   Dim serie, fila, grupo, inicio, fin As Integer
   Dim SerieIni, SerieFin As Integer
   Dim Title, xAxis, yAxis As String

   Workbooks("Test1.xlsm").Worksheets("Series").Activate
   grupo = Range("U1").value
   Range("U5").value = Workbooks("Test1.xlsm").Worksheets("Processing").Range("D" & 4 + grupo).value
   Range("U6").value = Workbooks("Test1.xlsm").Worksheets("Processing").Range("E" & 4 + grupo).value

   Title = "Current Consumption series" & grupo
   xAxis = "Time (s)"
```

```
    yAxis = "Current (A)"

    SerieIni = Range("U5").value
    SerieFin = Range("U6").value

    Workbooks("Test1.xlsm").Worksheets("Data").Activate
    Range("L3").Select

    ActiveSheet.Shapes.AddChart2(240, xlXYScatterLinesNoMarkers).Select

    serie = 1
    For fila = SerieIni + 1 To SerieFin + 1
       inicio = Workbooks("Test1.xlsm").Worksheets("Series").Range("B" & fila).value
       fin = Workbooks("Test1.xlsm").Worksheets("Series").Range("C" & fila).value

       ActiveChart.SeriesCollection.NewSeries
       ActiveChart.FullSeriesCollection(serie).Values = "='Data'!$C$" & inicio & ":$C$" & fin
       ActiveChart.FullSeriesCollection(serie).XValues = "='Data'!$J$" & inicio & ":$J$" & fin
       ActiveChart.FullSeriesCollection(serie).Format.Line.Weight = 0.5
       serie = serie + 1
    Next fila

    ActiveChart.ChartTitle.Text = Title
    ActiveChart.Axes(xlCategory, xlPrimary).HasTitle = True
    ActiveChart.Axes(xlCategory, xlPrimary).AxisTitle.Characters.Text = xAxis
    ActiveChart.Axes(xlValue, xlPrimary).HasTitle = True
    ActiveChart.Axes(xlValue, xlPrimary).AxisTitle.Characters.Text = yAxis

    ActiveChart.Axes(xlValue).Crosses = xlMinimum
    ActiveChart.Axes(xlCategory).Crosses = xlMinimum
End Sub
```

```
'SERIES CARGA DE CORRIENTE
Sub CargaCorriente()

    Dim serie, fila, grupo, inicio, fin As Integer
    Dim SerieIni, SerieFin As Integer
    Dim Title, xAxis, yAxis As String

    Workbooks("Test1.xlsm").Worksheets("Series").Activate
    grupo = Range("U1").value
    Range("U11").value = Workbooks("Test1.xlsm").Worksheets("Processing").Range("D" & 4 + grupo).value
    Range("U12").value = Workbooks("Test1.xlsm").Worksheets("Processing").Range("E" & 4 + grupo).value

    Title = "Current Charge series" & grupo
    xAxis = "Time (s)"
    yAxis = "Current (A)"

    SerieIni = Range("U11").value
    SerieFin = Range("U12").value

    Workbooks("Test1.xlsm").Worksheets("Data").Activate
    Range("L5").Select

    ActiveSheet.Shapes.AddChart2(240, xlXYScatterLinesNoMarkers).Select

    serie = 1
```

```
  For fila = SerieIni + 1 To SerieFin + 1
    inicio = Workbooks("Test1.xlsm").Worksheets("Series").Range("L" & fila).value
    fin = Workbooks("Test1.xlsm").Worksheets("Series").Range("M" & fila).value

    ActiveChart.SeriesCollection.NewSeries
    ActiveChart.FullSeriesCollection(serie).Values = "='Data'!$C$" & inicio & ":$C$" & fin
    ActiveChart.FullSeriesCollection(serie).XValues = "='Data'!$J$" & inicio & ":$J$" & fin
    ActiveChart.FullSeriesCollection(serie).Format.Line.Weight = 0.5
    serie = serie + 1
  Next fila

  ActiveChart.ChartTitle.Text = Title
  ActiveChart.Axes(xlCategory, xlPrimary).HasTitle = True
  ActiveChart.Axes(xlCategory, xlPrimary).AxisTitle.Characters.Text = xAxis
  ActiveChart.Axes(xlValue, xlPrimary).HasTitle = True
  ActiveChart.Axes(xlValue, xlPrimary).AxisTitle.Characters.Text = yAxis

  ActiveChart.Axes(xlValue).Crosses = xlMinimum
  ActiveChart.Axes(xlCategory).Crosses = xlMaximum

End Sub
```

```
'SERIES CAMBIO DE CARGA BATERIAS EN MOVIMIENTO
Sub ConsumoEnergia()

  Dim serie, fila, grupo, inicio, fin As Integer
  Dim SerieIni, SerieFin As Integer
  Dim Title, xAxis, yAxis As String

  Workbooks("Test1.xlsm").Worksheets("Series").Activate
  grupo = Range("U1").value
  Range("U17").value = Workbooks("Test1.xlsm").Worksheets("Processing").Range("D" & 4 + grupo).value
  Range("U18").value = Workbooks("Test1.xlsm").Worksheets("Processing").Range("E" & 4 + grupo).value

  Title = "Energy Consumption series" & grupo
  xAxis = "Time (s)"
  yAxis = "Energy (Ah)"

  SerieIni = Range("U17").value
  SerieFin = Range("U18").value

  Workbooks("Test1.xlsm").Worksheets("Data").Activate
  Range("L7").Select

  ActiveSheet.Shapes.AddChart2(240, xlXYScatterLinesNoMarkers).Select

  serie = 1
  For fila = SerieIni + 1 To SerieFin + 1
    inicio = Workbooks("Test1.xlsm").Worksheets("Series").Range("B" & fila).value
    fin = Workbooks("Test1.xlsm").Worksheets("Series").Range("C" & fila).value

    ActiveChart.SeriesCollection.NewSeries
    ActiveChart.FullSeriesCollection(serie).Values = "='Data'!$D$" & inicio & ":$D$" & fin
    ActiveChart.FullSeriesCollection(serie).XValues = "='Data'!$J$" & inicio & ":$J$" & fin
    ActiveChart.FullSeriesCollection(serie).Format.Line.Weight = 0.5
    serie = serie + 1
  Next fila
```

```
    ActiveChart.ChartTitle.Text = Title
    ActiveChart.Axes(xlCategory, xlPrimary).HasTitle = True
    ActiveChart.Axes(xlCategory, xlPrimary).AxisTitle.Characters.Text = xAxis
    ActiveChart.Axes(xlValue, xlPrimary).HasTitle = True
    ActiveChart.Axes(xlValue, xlPrimary).AxisTitle.Characters.Text = yAxis

    ActiveChart.Axes(xlValue).Crosses = xlMinimum
    ActiveChart.Axes(xlCategory).Crosses = xlMinimum

End Sub
```

```
'SERIES CAMBIO DE CARGA BATERIAS EN CARGA
Sub CargaEnergia()

    Dim serie, fila, grupo, inicio, fin As Integer
    Dim SerieIni, SerieFin As Integer
    Dim Title, xAxis, yAxis As String

    Workbooks("Test1.xlsm").Worksheets("Series").Activate
    grupo = Range("U1").value
    Range("U23").value = Workbooks("Test1.xlsm").Worksheets("Processing").Range("D" & 4 + grupo).value
    Range("U24").value = Workbooks("Test1.xlsm").Worksheets("Processing").Range("E" & 4 + grupo).value

    Title = "Energy Recharge series" & grupo
    xAxis = "Time (s)"
    yAxis = "Energy (Ah)"

    SerieIni = Range("U23").value
    SerieFin = Range("U24").value

    Workbooks("Test1.xlsm").Worksheets("Data").Activate
    Range("L9").Select
    ActiveSheet.Shapes.AddChart2(240, xlXYScatterLinesNoMarkers).Select
    serie = 1
    For fila = SerieIni + 1 To SerieFin + 1
        inicio = Workbooks("Test1.xlsm").Worksheets("Series").Range("L" & fila).value
        fin = Workbooks("Test1.xlsm").Worksheets("Series").Range("M" & fila).value
        ActiveChart.SeriesCollection.NewSeries
        ActiveChart.FullSeriesCollection(serie).Values = "='Data'!$D$" & inicio & ":$D$" & fin
        ActiveChart.FullSeriesCollection(serie).XValues = "='Data'!$J$" & inicio & ":$J$" & fin
        ActiveChart.FullSeriesCollection(serie).Format.Line.Weight = 0.5
        serie = serie + 1
    Next fila
    ActiveChart.ChartTitle.Text = Title
    ActiveChart.Axes(xlCategory, xlPrimary).HasTitle = True
    ActiveChart.Axes(xlCategory, xlPrimary).AxisTitle.Characters.Text = xAxis
    ActiveChart.Axes(xlValue, xlPrimary).HasTitle = True
    ActiveChart.Axes(xlValue, xlPrimary).AxisTitle.Characters.Text = yAxis
    ActiveChart.Axes(xlValue).Crosses = xlMinimum
    ActiveChart.Axes(xlCategory).Crosses = xlMaximum

End Sub
```

```
Sub RunSeries()
    Workbooks("Test1.xlsm").Worksheets("Processing").Activate
```

```
    Dim serie, inicio, fin As Integer
    serie = Range("O2").value
    inicio = Range("D" & 4 + serie).value
    fin = Range("E" & 4 + serie).value
    Workbooks("Test1.xlsm").Worksheets("Series").Activate
    Range("U1").value = serie
    Range("U5").value = inicio
    Range("U11").value = inicio
    Range("U17").value = inicio
    Range("U23").value = inicio
    Range("U6").value = fin
    Range("U12").value = fin
    Range("U18").value = fin
    Range("U24").value = fin
    Call ConsumoCorriente
    Call CargaCorriente
    Call ConsumoEnergia
    Call CargaEnergia
End Sub
```

APPENDIX F: GENERALS

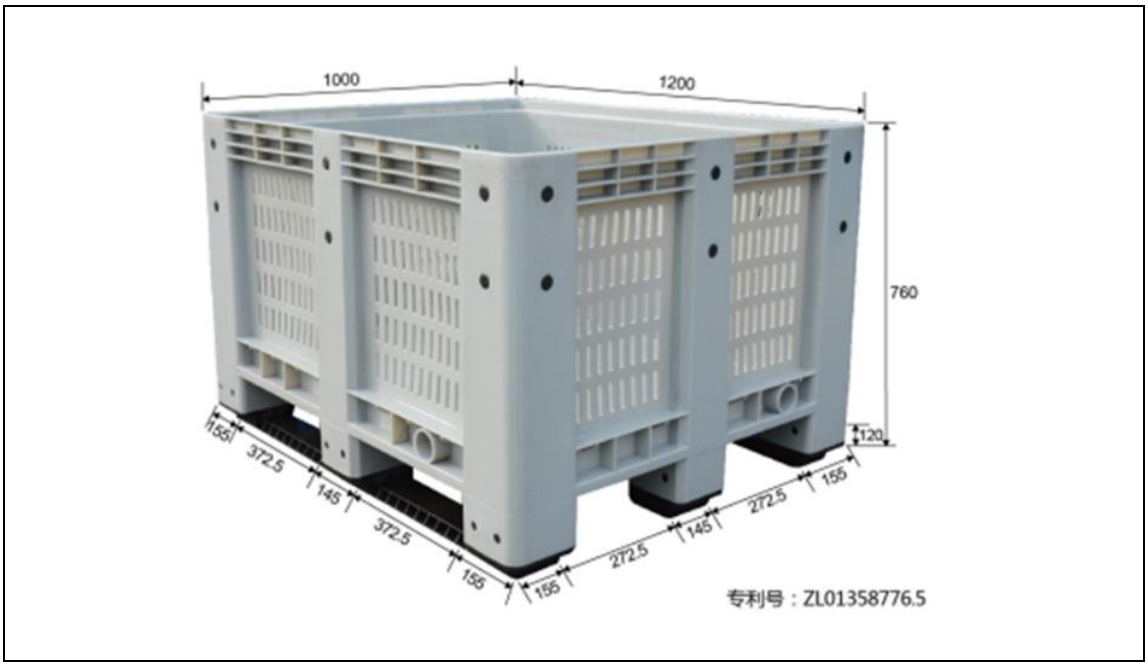

Figure F-1: Bin measurements in mm.

Figure F-2 Transportation of the vehicle in low loader

Figure F-3 Driving test previous harvest with ladders in the background

Figure F-4 Harvesting lunch break